Natural variation in *TBP-ASSOCIATED FACTOR 4b* controls meiotic crossover and germline transcription in Arabidopsis

Emma J. Lawrence[1], Hongbo Gao[2], Andrew J. Tock[1], Christophe Lambing[1], Alexander R. Blackwell[1], Xiaoqi Feng[2]* and Ian R. Henderson[1]*

[1] Department of Plant Sciences, Downing Street, University of Cambridge, Cambridge, CB2 3EA, United Kingdom
[2] Department of Cell and Developmental Biology, John Innes Centre, Norwich, NR4 7UH, United Kingdom

* Correspondence: xiaoqi.feng@jic.ac.uk and irh25@cam.ac.uk

Summary:

Meiotic crossover frequency varies within genomes, which influences genetic diversity and adaptation. In turn, genetic variation within populations can act to modify crossover frequency in *cis* and *trans*. To identify genetic variation that controls meiotic crossover frequency we screened Arabidopsis accessions using fluorescent recombination reporters. We mapped a genetic modifier of crossover frequency in Col×Bur populations of Arabidopsis to a premature stop codon within *TBP-ASSOCIATED FACTOR 4b* (*TAF4b*), which encodes a subunit of the RNA polymerase II general transcription factor TFIID. The Arabidopsis *taf4b* mutation is a rare variant found in the British Isles, originating in South-West Ireland. Using genetics, genomics and immunocytology we demonstrate a genome-wide decrease in *taf4b* crossovers, with strongest reduction in the sub-telomeric regions. Using RNA-seq from purified meiocytes, we show that *TAF4b* expression is meiocyte-enriched, whereas its paralog *TAF4* is broadly expressed. Consistent with the role of TFIID in promoting gene expression, RNA-seq of wild type and *taf4b* meiocytes identified widespread transcriptional changes, including in genes that regulate the meiotic cell cycle and recombination. Therefore, *TAF4b* duplication is associated with acquisition of meiocyte-specific expression and promotion of germline transcription, which acts directly or indirectly to elevate crossovers. This identifies a novel mode of meiotic recombination control via a general transcription factor.

Keywords:

Meiosis, recombination, crossover, *rQTL*, TAF4b, transcription.

Introduction:

Meiosis is a specialized eukaryotic cell division that produces haploid spores from diploid mother cells, via one round of DNA replication and two rounds of chromosome segregation [1]. During prophase of meiosis I, chromosomes undergo DNA double strand breaks (DSBs) that are repaired using a homolog to form reciprocal crossovers or gene conversions [1]. Independent chromosome segregation during meiosis and homologous recombination create new patterns of genetic diversity [1, 2]. Although the core meiotic recombination pathway is highly conserved [1, 3], the number and distribution of crossovers varies between species [4, 5]. At least one ‘obligate’ crossover is generally required per chromosome pair to ensure balanced segregation at anaphase I [1]. However higher numbers of crossovers are rare in natural species, with ~1-3 crossovers typically observed per chromosome pair, irrespective of genome size [1, 4]. Hence, genetic variation that controls recombination within and between species has the potential to influence adaptation [2, 4], although the extent that sequence polymorphism controls crossover remains to be fully understood.

In plants, *cis*- and *trans*-acting genetic variation influence meiotic recombination frequency [4, 5]. Examples of *cis*-acting variation include structural genetic changes, such as inversions and translocations, which can suppress crossover formation at large physical scales (kilobase-megabase) [5, 6]. Inhibitory *cis* effects acting at the local scale (nucleotide-kilobase) may also occur following interhomolog strand invasion, where heterozygosity causes base pair mismatches [3]. *Trans*-acting variation that modifies recombination has also been observed in the *Arabidopsis thaliana HEI10* gene [7], which encodes a meiosis-specific E3 ligase that promotes crossover formation. In mammals, *HEI10* is related to *RNF212*, and natural variation in both genes modifies crossover frequency [3, 4]. Hence, the effects of genetic polymorphism on crossover are varied and scale-dependent.

In this work, we sought to further explore natural genetic variation in Arabidopsis that influences meiotic crossover frequency. *Arabidopsis thaliana* predominantly self-fertilizes, but is estimated to outcross at a rate between 0.3-2.5% [8]. Signatures of outcrossing are evident in Arabidopsis, as (i) linkage disequilibrium decays rapidly over kilobase distances, (ii) historical crossover hotspots are detected, and (iii) outcrossing and heterozygosity in natural stands have been directly observed [8–12]. Hence, genetic variation that controls crossover recombination has the potential to influence adaptation in this species. Using this approach we have identified the TAF4b TFIID subunit as a novel *trans* regulator of crossover frequency, which we also show promotes germline gene expression.

Results:

Multiple recombination QTLs (*rQTL*s) control meiotic crossover frequency between the Arabidopsis Col-0 and Bur-0 accessions

Crossover frequency can be measured in Arabidopsis using Fluorescent Tagged Lines (FTLs) that comprise linked transgenes expressing different colors of fluorescent protein in the seed (*NapA* promoter), or pollen (*LAT52* promoter) [13–16]. Crossovers occurring between hemizygous FTL T-DNAs linked on the same chromosome can be detected via analysis of color inheritance through meiosis [13–16]. FTL T-DNAs typically define megabase intervals and have predominantly been generated in the Col-0 (Col) background [13, 16, 17]. We have previously crossed several FTLs to diverse accessions [7, 15], and these data showed that the Irish accession Bur-0 (Bur) shows overall high crossover frequency in Col/Bur F_1 hybrids, relative to other hybrids [15]. However, specific FTL intervals showed either higher (*I1fg*, *I2f*, *CEN3*) or lower (*I1b*, *420*) crossovers in Col/Bur F_1 hybrids compared to Col/Col inbreds, indicating region-specific effects of polymorphism [15]. Therefore, we sought to further screen Bur for *cis* and *trans*-acting loci that modify crossover frequency.

To explore the contribution of *cis* and *trans* modifiers of recombination that are polymorphic between Col and Bur, we used the *420* FTL, which is 5.11 Mb and located sub-telomerically on chromosome 3 (Figure 1A) [17]. We measured crossovers in this interval in 151 Col-*420*×Bur *RG*/++ F_2 individuals, in order to perform a quantitative trait loci (QTL) scan for regions associating with recombination rate (Figure 1B–1C and Data S1). The variation in F_2 *420* crossover frequency was significantly greater than observed in replicate Col-*420*/Bur F_1 individuals (Brown-Forsythe test, $P=9.76\times10^{-6}$) (Figure 1D and Data S1), consistent with the presence of Col/Bur *trans* modifiers influencing recombination. Col-*420*×Bur F_2 individuals were genotyped using simple sequence length polymorphism (SSLP) PCR markers throughout the genome (Figure 1E), and a QTL scan was performed to test for associations with *420* crossover frequency (Figure 1F). This approach identified 4 significant recombination QTLs (*rQTL*s) (α=0.05, 1,000 permutations), which in a joint additive model explained 64.4% of the variation in crossover frequency, with a total LOD score of 33.8 (Figure 1F and Table 1).

Two strong *rQTL* peaks were detected on chromosome one that displayed distinct genetic behaviours. Bur alleles of *rQTL1a* and *rQTL1b* act recessively and semi-dominantly to reduce crossover frequency, respectively (Figure 1F, Figure S1A–1B and Table 1). *rQTL1b* maps in proximity to *HEI10*, which has previously been shown to act semi-dominantly [7] (Figure S1B and Table 1). Furthermore, Bur and L*er* share the putative causal non-synonymous *HEI10* R264G substitution [7], which is consistent with *rQTL1b* representing variation in *HEI10*. We also detected a weak *rQTL* on chromosome 2 caused by a dominant Bur allele, in addition to a previously observed *cis* effect caused by juxtaposition of heterozygosity and homozygosity on chromosome 3, where *420* is located (Figure S1C–1E and Table 1) [15].

Fine mapping of *rQTL1a* identifies variation in the TFIID complex subunit TAF4b

As *trans* recombination modifiers have not previously been observed in vicinity to *rQTL1a*, and due to the strength of its effect on recombination, we sought to fine map this locus (Figure 2 and Figure S2). We generated lines where the *rQTL1a* region was Col/Bur heterozygous and the rest of the genome was Col/Col, in order to remove the effects of the other *rQTL*s (Figure S2). Using these lines we produced a large BC_2F_2 population (*n*=501) (Figure S2). BC_2F_2 individuals with a crossover within *rQTL1a* (*n*=152) were used to refine the causal region to a 30 kb interval (Figure 2A–2B and Data S1). Further genetic mapping narrowed *rQTL1a* to a 14.4 kb interval containing five genes, of which At1g27720 carried a SNP in Bur causing a premature stop codon (L481*) (Figure 2C–2D). This mutation was absent in other accessions where *rQTL1a* was not previously detected (Ct-1, Cvi-0, Mt-0, L*er*-0 and Can-0 [7, 15]), identifying At1g27720 as the strongest candidate gene underlying *rQTL1a.*

To confirm the identity of *rQTL1a* as At1g27720, we performed transformation experiments using a *rQTL1a* introgression line that carried the *420* FTL. This introgression, denoted as $rQTL1a^{Bur}$, contains a 1.6 Mb region from Bur, but is Col homozygous throughout the rest of genome. The $rQTL1a^{Bur}$ introgression was transformed with genomic clones of the five genes within the *rQTL1a* credible interval, or an empty vector, and *420* crossover frequency in the resulting transformants compared to untransformed wild type and the $rQTL1a^{Bur}$ introgression (Figure 2F, Figure S3A–3C and Data S1). These experiments demonstrated that At1g27720, which encodes TAF4b, specifically complemented the $rQTL1a^{Bur}$ crossover defect (Figure 2F, Figure S3A–3C and Data S1). The $rQTL1a^{Bur}$ introgression is herein defined as *taf4b-1*. We also obtained an independent T-DNA insertion allele in At1g27720 (*taf4b-2*), which significantly reduced *420* crossover frequency compared to wild type and *taf4b-2*/+ heterozygotes (generalised linear model [GLM], $P<2\times10^{-16}$) (Figure 2G, Figure S3D-3F and Data S1). Together this provides genetic proof that mutation of *TAF4b* reduces crossover frequency within the *420* interval and occurs as a natural modifier of recombination in Arabidopsis.

TAF4b encodes TATA Binding Protein (TBP)-Associated Factor 4b, which is a subunit of the TFIID complex [18]. TFIID is a general transcription factor composed of TBP and several TAFs that forms part of the pre-initiation complex which recruits RNA polymerase II to gene promoters [19, 20]. There are 18 TAFs in Arabidopsis, including two *TAF4* paralogs; *TAF4* and *TAF4b*, which share 43.7% amino acid identity [18] (Figure S4). Both TAF4 and TAF4b possess a RCD1-SRO-TAF4 (RST) domain, histone-fold domain (HFD) and a conserved C-terminal domain (CCTD) (Figure S4B). In yeast, the TAF4 HFD heterodimerises with TAF12 within the TFIID complex to form a histone-like pair [21]. The Bur *taf4b-1* polymorphism produces a stop codon at amino acid 481, upstream of the HFD (Figure 2D). Therefore, *taf4b-1* is predicted to produce a truncated protein lacking the HFD required for interactions within TFIID [21].

Bur was collected from the Burren, a region of karstified limestone in South-West Ireland. Within the 1,001 Genomes Project, the Bur *taf4b-1* polymorphism was identified in two further accessions, Cal-0 and Cal-2, that were collected in the United Kingdom [22]. Cal-0, Cal-2 and Bur have highly similar haplotypes genome-wide, suggesting they are related via recent migration [22]. To further investigate the geographic distribution of *taf4b-1*, we genotyped an additional set of accessions collected from the British Isles [23]. This identified a small number of accessions (9 of 116) from South-West Ireland, collected in proximity to the Burren, and one from Scotland, that carry *taf4b-1* (Figure 2E and Table S1). This shows that *taf4b-1* is a rare mutation that likely arose in South-West Ireland. In contrast, the *HEI10* R264G polymorphism is globally distributed in 11.4% of the 1,001 Genomes Project accessions [7]. We investigated whether fertility was changed in *taf4b* by counting seeds per silique in Col, *taf4b-1* and *taf4b-2*, and observed no significant differences between genotypes (Student's *t* test, P=0.718 and P=0.234) (Table S2). Hence, although crossovers are reduced in *taf4b-1*, this does not associate with significantly decreased fertility.

Sub-telomeric crossover frequency is reduced in *taf4b*

We further investigated the effect of *taf4b-1* on crossover frequency using an additional 8 FTL intervals located throughout the genome and representing 40.4 Mb in total (Figure 3A–3C) [16]. Crossover frequency significantly decreased in *taf4b-1* in all FTL intervals tested compared to wild type siblings, with decreases ranging from 9.0% to 27.1% (Figure 3B–3C and Data S1). Interestingly, the magnitude of *taf4b-1* crossover decrease correlated negatively with distance from the telomere (Spearman's ρ=-0.7, P=0.04) (Figure 3B), indicating that distal sub-telomeric recombination is most strongly reduced in *taf4b-1*. We also analysed crossovers via MLH1 immunostaining on diakinesis-stage male meiocytes (Figure 3D–3E and Table S3). MLH1 foci associated with meiotic chromatin (stained with DAPI) can be used to measure Class I crossover numbers [7]. We counted MLH1 foci in both *taf4b-1* and Bur, which displayed mean reductions of between 2 and 3 MLH1 foci, relative to Col (Mann-Whitney-Wilcoxon tests, $P=3.17\times10^{-6}$ and $P=1.36\times10^{-5}$) (Figure 3D–3E and Table S3). We generated a meiotic atlas via DAPI-staining of spread male meiocytes in Col and Bur (*taf4b-1*) (Figure 3F). Meiotic progression showed normal homologous pairing at pachytene and five bivalents at diakinesis and metaphase I in both genotypes (Figure 3F). No univalents were detected in 40 Col and 44 Bur metaphase I cells, or 21 Col and 34 Bur cells at diakinesis (Figure 3F). Taken together, these data confirm crossover reduction in *taf4b-1* throughout the genome, although the obligate crossover is maintained. As these experiments measure recombination in inbred backgrounds, we next sought to map crossovers in *taf4b-1* mutants that were genetically hybrid.

To generate *taf4b-1* hybrids, Bur was crossed to the *taf4b-1* introgression, producing Col/Bur F_1 hybrids that are *taf4b-1* homozygous. Col/Bur F_1 hybrids were generated as a control, which are *taf4b-1* heterozygous. *420* was maintained in these lines and used to confirm that *taf4b-1*/Bur F_1 display significantly reduced crossover frequency compared to Col/Bur F_1 (GLM, $P<2.0\times10^{-6}$) (Figure 4A and Data S1). F_2 populations were generated and 180 and 186 individuals from the Col/Bur and *taf4b*-1/Bur populations were sequenced, respectively. These data were used to identify crossover locations in each F_2, using a set of 446,361 Col/Bur SNPs (Figure 4B–4D). It was necessary to mask the ~0.6 Mb *taf4b-1* introgressed region on chromosome 1 from analysis (Figure 4D), which is Bur homozygous in the *taf4b-1* population, meaning crossovers cannot be detected here.

The Col/Bur control F_2 population contained on average 7.72 crossovers per F_2, whereas the *taf4b-1*/Bur F_2 contained significantly fewer (6.81 crossovers per F_2) (Mann-Whitney-Wilcoxon test, $P=4.06\times10^{-5}$) (Figure 4B and Table S4). Consistent with the previous FTL analysis, we observed that *taf4b-1* crossovers were most strongly reduced in the distal sub-telomeric regions (Figure 4D). To statistically assess this, a Poisson model was used to compare the crossover counts in 10 scaled chromosome windows along the telomere to

centromere axis, summed across all chromosome arms, between Col/Bur and *taf4b-1*/Bur populations (Figure S5). Crossovers within the 1st and 2nd sub-telomeric windows were significantly reduced in *taf4b-1*/Bur compared to Col/Bur (Benjamini-Hochberg (BH) multiple-testing-corrected $P=1.30\times10^{-2}$ and $P=9.88\times10^{-3}$) (Figure S5). Together, these data confirm crossover decrease in *taf4b-1* in both inbred and hybrid contexts, with greatest reduction in the sub-telomeric regions.

TAF4b expression is germline-enriched compared to *TAF4*

As noted, two *TAF4* paralogs exist in the *A. thaliana* genome (Figure S4). Several plant and animal *TBP* and *TAF* genes are duplicated and exhibit cell type-specific expression and functions, including in the germline [19, 24]. Phylogenetic analysis of eukaryotic TAF4 proteins resolved monophyletic animal, fungal and plant clades (Figure S4A). Fungal genomes encode a single *TAF4* gene, whereas independent *TAF4* duplications have occurred within vertebrates and plants (Figure S4). Vertebrate sequences divide into two conserved *TAF4* and *TAF4b* clades, whereas within land plants, basal species possess a single *TAF4* gene and multiple duplications have occurred within flowering plants, including within the Brassicaceae (Figure S4A). Hence, *TAF4* has undergone repeated duplications across the eukaryotic phylogeny, associated with functional specialisation.

Due to the role of *TAF4b* in promoting crossovers, we investigated *TAF4* and *TAF4b* gene expression using RNA-seq data generated from purified male meiocytes and leaf tissue [25] (Figure 5A). As expected, genes with known roles in meiotic recombination exhibit strongly elevated expression in meiocytes and low expression in leaf tissue, whilst photosynthetic genes display the opposite pattern (Figure 5A). Consistent with a role in meiotic recombination, *TAF4b* showed high expression in meiocytes and low expression in leaf, whereas *TAF4* was constitutively expressed between leaf and meiocyte samples (Figure 5A). We confirmed these expression patterns for *TAF4* and *TAF4b* using semi-quantitative RT-PCR from floral buds and leaf tissue (Figure S6A–6B). These data demonstrate that *TAF4b* expression is enriched in the germline and during meiosis, whereas *TAF4* adopts a broader, constitutive expression pattern.

TAF4b promotes germline expression of regulators of meiosis

As TAF4b is predicted to interact within TFIID and promote transcription, we sought to compare gene expression in *taf4b-1*, Bur and Col, using RNA-seq of purified meiocytes [25]. Approximately 2,000 male meiocytes were dissected from each genotype and RNA was extracted and sequenced. DESeq2 was used to identify differentially expressed genes in *taf4b-1* and Bur, relative to Col. We observed down-regulation of 1,271 genes and up-regulation of 279 genes in *taf4b-1* (BH-adjusted $P<0.01$), which significantly overlapped those identified in Bur (91.7% overlap of down-regulated genes) (Figure 5C and Figure S7A–S7B). As *TAF4b* has germline-enriched expression, we predicted that its target genes would also show germline-enriched expression compared to leaf. Indeed, the *taf4b-1* down-regulated genes are significantly enriched for genes that are up-regulated in wild type meiocytes compared to leaves (hypergeometric test, $P=1.6\times10^{-185}$) (Figure 5D). This shows that TAF4b promotes germline gene transcription, with functional relevance for meiotic recombination.

Gene ontology (GO) tests were performed on the genes that are down-regulated in *taf4b-1* and up-regulated in wild type meiocytes compared to leaves (Figure S7C and Table S5). Over-represented GO terms include ‘protein ubiquitination’, ‘regulation of transcription’, ‘meiotic sister chromatid cohesion’, ‘male meiosis chromosome segregation’ and ‘chromosome condensation’ (Figure S7 and Table S5). This included genes with known meiotic functions, including (i) *WAPL2* and *PATRONUS1,* which are involved in the removal and protection of cohesin during meiosis, respectively [26, 27], (ii) *DUET/MMD1,* which is a

transcriptional regulator of male meiosis [28], (iii) *JASON* that is essential for spindle orientation in meiosis II [29], (iv) *OSD1,* which controls meiotic cell cycle progression [30] and (v) *H2A.Z/HTA11* which encodes a histone variant associated with crossover sites in Arabidopsis [12]. TAF4b-dependent transcription of one, or a combination, of these genes could promote meiotic recombination in wild type.

A smaller group of 279 genes were significantly up-regulated in *taf4b-1*, which may represent indirect targets. 42.7% of these genes are also up-regulated in wild type meiocytes compared to leaves, which represents a significant overlap (hypergeometric test, $P=4.05\times10^{-25}$). Over-represented GO terms within these genes include 'meiotic DNA DSB formation', 'chiasma assembly', 'meiotic sister chromatid cohesion' and 'meiotic chromosome condensation' (Figure S7D and Table S5). Known genes with a role in meiosis include, (i) *PRD1*, which encodes a SPO11-1 accessory factor required for DSB formation [31], (ii) *MSH5*, which is required for wild type levels of Class I crossovers [32], (iii) *REC8*, which encodes a cohesin component of the meiotic axis [33], (iv) *SWI1,* which is required for formation of the axis and sister chromatid cohesion [34] and (v) *ATM*, which is required for DNA damage signalling [35]. Hence, transcriptional changes in these genes in *taf4b-1* may also contribute to decreased crossover frequency.

Discussion:

Through genetic mapping and immunocytology, we demonstrate a novel role for TAF4b in promoting meiotic crossover in Arabidopsis. TFIID was initially thought to adopt an essential and ubiquitous role in RNA polymerase II transcription. However, *TAF* gene duplications have occurred in plants and animals that are associated with acquisition of specialised expression patterns and functions [19, 24, 36]. Here we show that Arabidopsis *TAF4b* is expressed in the germline, whereas its paralog *TAF4* is broadly and constitutively expressed. This parallels gonad-specific *TAF4b* expression versus global *TAF4* expression observed in mice, *Xenopus* and *Drosophila* [37–41]. This is interesting considering that *TAF4* duplication occurred independently in animal and plant lineages [42]. In mice, loss of *TAF4b* leads to sterility in males and females, indicating a strict requirement during gametogenesis [37, 43], whereas the Arabidopsis *taf4b* mutant does not significantly reduce fertility. Therefore, in comparison to mice, the Arabidopsis *taf4b* germline phenotype more specifically influences crossover levels, without causing meiotic arrest or sterility.

The effect of TAF4b on crossover number and distribution may occur indirectly via its effects on transcription of target genes that regulate meiotic recombination (Figure 6A). The enrichment of GO terms associated with ubiquitin in the *TAF4b* target genes could relate to the role of this post-translational modification in controlling progression of meiosis and recombination [44–47]. Notably, the previously identified *rQTL HEI10* encodes a conserved putative ubiquitin or SUMO E3 ligase that promotes crossovers in diverse eukaryotes [7]. *WAPL2* and *PATRONUS1* have roles in the removal and protection of cohesin, respectively [26, 48]. Notably, the *taf4b-1* up-regulated genes include *REC8*, which encodes a meiosis-specific kleisin subunit of cohesin [49], and *SWI1,* which is required for formation of the meiotic axis and sister chromatid cohesion [34, 50]. It is possible that altered expression of any of these genes could act independently, or in combination, to reduce crossovers in *taf4b*, with greatest effect in the sub-telomeres (Figure 6A).

It is also possible that TAF4b binding directly regulates crossover formation (Figure 6B-6C). For example, variant TAF complexes may impart unique chromatin structure at gene promoters, which could have a direct impact on recombination. It is notable that gene promoters are endogenous sites for meiotic DSB and crossover hotspots in Arabidopsis and other plants [11, 12, 51–54]. Hence, TAF4b-TFIID binding, or the act of transcription itself, may modify chromatin and influence the accessibility of gene promoters to recombination proteins (Figure 6B-6C). Notably, cohesin occupancy on chromosomes is also influenced by

transcription in several species [55–57]. Although cohesin is required for organisation of meiotic chromosomes and recombination, it is also associated with suppression of recombination at the local scale [58, 59]. Hence, the effect of TAF4b on meiotic transcription could modify cohesin accumulation and thereby influence recombination. It is also possible that TAF4b may directly recruit recombination proteins to gene promoters and promote meiotic DSB formation or crossover repair (Figure 6C).

We demonstrate crossover reduction within the euchromatic chromosome arms in *taf4b* and most strongly in distal sub-telomeric regions. As the *420* FTL interval we used to test for recombination modifiers is sub-telomeric, this may have sensitized our screen towards detection of *TAF4b*. Interestingly, several other genetic backgrounds show greatest increases in sub-telomeric crossover frequency, including (i) *HEI10* overexpression lines [7, 60], (ii) the anti-crossover mutants *fancm*, *figl1* and *recq4a recq4b* [60, 61], (iii) the CG DNA methylation maintenance mutant *met1* [62] and (iv) *cdka;1* cell division kinase mutants [63]. Arabidopsis chromosomes show gradients of sequence polymorphism and chromatin modifications along the telomere to centromere axis [60, 61]. Regional differences in genetic and epigenetic information may contribute to relative increases in sub-telomeric crossover frequency in these genetic backgrounds, when the recombination pathways are changed. Notably Arabidopsis male meiosis produces more crossovers than female, with additional events occurring in the sub-telomeres, which are derived from the Class I repair pathway [61, 64]. Further work will be required to understand what connects distalization of crossovers observed in these diverse backgrounds. It may also be interesting to screen for natural modifiers of crossover frequency specifically in the pericentromeric or interstitial regions of the chromosomes.

Recombination modifier loci, such as *TAF4b*, have the potential to modulate the response of a population to selection [65, 66]. The Col-*420*×Bur *trans* modifier *rQTL*s identified here exhibit opposing genetic effects on crossover frequency. This is consistent with the results of *rQTL* mapping in Col×L*er* populations, where the identified *rQTL*s also displayed opposite effects on crossover frequency [7]. Although our sampling is limited, it appears that recombination rate in natural populations of Arabidopsis is controlled by multiple *trans* modifiers, indicating a complex genetic architecture. Overall recombination levels are maintained at low levels across eukaryotes, with typically one or two crossovers occurring per chromosome per meiosis [1]. This may indicate that high levels of meiotic crossover are unfavourable and consequently selected against. Therefore, antagonistic recombination modifiers may act to balance recombination in natural Arabidopsis populations, at levels sufficient to ensure balanced chromosome segregation and fertility, whilst avoiding excessive disruption of beneficial linked variation.

Acknowledgements:

We thank Gregory Copenhaver (University of North Carolina), Avraham Levy (The Weizmann Institute) and Scott Poethig (University of Pennsylvania, USA) for FTLs, Piotr Ziolkowski for Col-*420*/Bur seed, Sureshkumar Balasubramanian (Monash University) for providing British and Irish Arabidopsis accessions, Mathilde Grelon (INRA, Versailles) for providing the MLH1 antibody, and the Gurdon Institute for access to microscopes. This work was supported by a BBSRC DTP studentship (EJL), European Research Area Network for Coodinating Action in Plant Sciences/BBSRC **“**DeCOP**”** (BB/M004937/1) (CAL), a BBSRC David Phillips Fellowship (BB/L025043/1) (HG, XF), the European Research Council (CoG ‘SynthHotspot’) (AJT, CAL, IRH) and (StG ‘SexMeth’) (XF) and a Sainsbury Charitable Foundation Studentship (ARB).

Author Contributions:

E.L., H.G., C.L. and A.B. conducted the experiments. E.L., H.G., C.L., A.T., A.B., X.F. and I.H. analysed the data and wrote the paper.

Declaration of Interests:

The authors declare no competing interests.

Main-text Figure and Table Legends:

Figure 1. Recombination QTL (*rQTL*) mapping in Arabidopsis Col×Bur populations. (A) Physical map of chromosome 3 showing the positions of *420* FTL T-DNA markers (red and green triangles). (B) Diagram illustrating the pedigree used for *rQTL* mapping. (C) Fluorescent micrographs showing *420* (*RG*/++) seed using red or green fluorescent filters. (D) Histogram of *420* cM phenotypes in F_1 (dark blue) and F_2 (light blue) Col/Bur individuals. Mean values are shown by the dashed lines. (E) Representative ethidium bromide stained gel showing an SSLP marker amplified from Bur, Col and Col/Bur F_1 plants. (F) Col-*420*×Bur F_2 multiple (two-dimensional) QTL scan showing logarithm of the odds ratio (LOD) scores on chromosomes 1, 2 and 3. Positions of genetic markers (cM) are denoted by ticks on the *x*-axis. The horizontal red line indicates the LOD significance threshold (α=0.05). *See also Figures S1 and S2, Data S1 and Table S6.*

Figure 2. Genetic polymorphism in *TAF4b* underlies *rQTL1a*. (A) LOD scores for markers associated with *420* crossover frequency (cM) using QTL mapping in a BC_2F_2 population, over a 3.5 Mb region containing *rQTL1a*. Physical markers are denoted by *x*-axis ticks (red line=LOD significance threshold, α=0.05). (B) *420* cM for BC_2F_2 individuals Col/Col, Col/Bur or Bur/Bur at the *rQTL1a* peak marker. Error bars represent mean and standard error. (C) Genotypes (Bur/Bur=blue, Col/Bur=purple) of four BC_2F_2 individuals in a 30 kb region around *rQTL1a* with *420* cM. Gene models are shown beneath. (D) *TAF4b* gene structure (blue rectangles=exons) and domain positions. The *taf4b-1* premature stop codon, *taf4b-2* T-DNA insertion, and *TAF4b* genomic region used for complementation, are shown. (E) Locations of Arabidopsis accessions collected in the British Isles with Col/Col (red), Col/Bur (purple) or Bur/Bur (blue) *TAF4b* genotypes (*taf4b-1* dCAPS marker=triangles or 1,001 Genomes Project=circles). The Burren is shown beneath at higher resolution. (F) *420* cM in $rQTL1a^{Bur}$, $rQTL1a^{Bur}$ transformed with empty vector, $rQTL1a^{Bur}$ transformed with *TAF4b*, or wild-type Col-*420*. Significance was assessed by Mann-Whitney-Wilcoxon tests (***=P≤0.001). (G) As for F, but showing *420* cM in *taf4b-2*, wild type or *taf4b-2*/+ heterozygous siblings. *See also Figures S2, S3 and S4, Data S1 and Tables S1 and S6.*

Figure 3. *TAF4b* promotes crossover frequency genome-wide in inbreds. (A) The Arabidopsis genome showing the position of FTL T-DNAs (red and green triangles) used to measure crossovers. Scale bar=5 Mb. (B) Correlation between the % decrease in crossover frequency between wild type and *taf4b-1* siblings in FTL intervals shown in A, in addition to *420*, and the interval midpoint as a proportion of chromosome arm length, where the telomere (*TEL*) is 0 and the centromere (*CEN*) is 1. (C) Crossover frequency (cM) in the FTL intervals in wild type +/+ (red), *taf4b-1*/+ (purple) and *taf4b-1* (blue) F_2 siblings. Error bars represent the standard deviation. Significance was assessed by GLM tests (**=P≤0.01 and ***=P≤0.001). (D) Representative micrographs showing Col, *taf4b-1* and Bur male diakinesis-stage meiocytes stained for DAPI (blue) and immunostained for MLH1 (red). Scale bar=10 µm. (E) Quantification of MLH1 count data from Col, *taf4b-1* and Bur. Error bars represent the mean and the standard deviation. Significance was assessed by Mann-Whitney-Wilcoxon tests (***=P≤0.001). (F) DAPI-stained spreads of Col (wild type) and Bur (*taf4b-1*) male meiocytes at the labeled stages of meiosis. All scale bars=10 µm. *See also Data S1 and Tables S2 and S3.*

Figure 4. *TAF4b* promotes crossover frequency most strongly in distal sub-telomeric regions. (A) *420* crossover frequency (cM) in Col/Bur and *taf4b-1*/Bur F_1 hybrids. Mean crossover frequency for each genotype is denoted by a red circle. F_1 individuals used as parents for Col/Bur and *taf4b-1*/Bur GBS F_2 populations are highlighted in purple and blue, respectively. Significance was assessed by GLM tests (***=$P \leq 0.001$). (B) Histograms displaying the number of crossovers per individual in Col/Bur (purple) and *taf4b-1*/Bur (blue) F_2 GBS populations. Mean crossover number of each population is denoted by a vertical dashed line. (C) Crossover frequency along the proportional (scaled) length of all chromosome arms from telomeres (*TEL*) to centromeres (*CEN*) in Col/Bur (purple) and *taf4b-1*/Bur (blue) F_2 populations. Mean values are denoted by the horizontal dashed lines. (D) Crossover frequency over the five chromosomes in Col/Bur (purple) and *taf4b-1*/Bur (blue) F_2 populations. Crossovers were tallied in 300 kb windows, divided by the number of F_2 individuals, and a rolling mean plotted along the five chromosomes. Centromere (*CEN*) positions are denoted by vertical dashed lines and telomere (*TEL*) positions by vertical solid lines. The location of the *taf4b-1* introgressed region is represented by grey shading. *See also Figure S5, Data S1 and Table S4.*

Figure 5. TAF4b drives a germline transcriptional program associated with promotion of crossovers. (A) Expression level (transcripts per million, TPM) of genes with known roles in meiosis or photosynthesis, and *TAF4* and *TAF4b*, from meiocyte and leaf replicate RNA-seq libraries [25]. A relative colour scale applies within each panel, where green and red denote high and low TPM values, respectively. (B) As for A, but showing genes significantly down-regulated in *taf4b-1* compared to Col meiocytes and up-regulated in Col meiocytes compared to Col leaf tissue, ordered according to fold-change in *taf4b-1*. Expression in Col, *taf4b-1* and Bur meiocyte RNA-seq libraries, and Col leaf and meiocyte libraries [25], is shown. Genes with known roles in meiosis are highlighted. (C) Venn diagram displaying the overlap between genes that are significantly down-regulated in Bur (false discovery rate [FDR]<0.01), and genes that are significantly down-regulated in *taf4b-1* (FDR<0.01), compared to Col. (D) Venn diagram displaying the overlap between genes significantly down-regulated in *taf4b-1* relative to Col (FDR<0.01), and genes significantly up-regulated in Col meiocytes relative to Col leaf tissue [25] (FDR<0.01). *See also Figures S6 and S7, and Tables S5 and S6.*

Figure 6. Direct and indirect models for TAF4b in promotion of crossovers. (A) Model for TAF4b acting within the TFIID complex to promote expression of meiotic regulatory genes. The putative direct TAF4b targets are those genes which are down-regulated in *taf4b-1* (red), while genes that are up-regulated (green) are likely indirect targets. Known regulators of meiotic recombination present in these groups are listed. (B) Direct model showing TAF4b interacting directly with a protein that influences DSB formation or crossover progression (X). (C) An alternative direct model showing a TAF4b-containing variant TFIID complex influencing DNA accessibility at the promoter/transcriptional start site region, promoting DSB formation by SPO11-1.

Table 1. Location and effect size of *rQTL*s identified in the Col-*420*×Bur F_2 population. *See also Figure S1.*

Chr	*rQTL*	Position (cM)	Proximal marker (bp)	+/- 1.5 LOD units (cM)	+/- 1.5 LOD markers (kb)	420 cM			Mode of action	LOD	Variance (%)
						Col/ Col	Col/ Bur	Bur/ Bur			
1	*rQTL1a*	34.1	9,567,731	31…37	8,547…10,655	16.6	15.6	10.9	Recessive Bur	15	20.7
1	*rQTL1b*	77.5	18,237,140	69…94	16,161…25,036	17.8	15.3	12.3	Semi-dominant	9.4	11.8
2	*rQTL2*	2.0	132,652	0…26	132…14,407	13.4	15.3	15.1	Dominant Bur	5.5	6.6
3	*rQTL3*	22.0	10,695,968	9…34	4,049…17,088	16.0	13.7	17.0	*Cis* effect	7.8	9.5

STAR Methods:

EXPERIMENTAL MODEL AND SUBJECT DETAILS

Plant material

Arabidopsis thaliana accessions were obtained from the Nottingham Arabidopsis Stock Centre (NASC) or kindly donated by Sureshkumar Balasubramanian (Monash University). Fluorescent Tagged Lines (FTLs) were kindly provided by Avraham Levy (Weizmann Institute) and Scott Poethig (University of Pennsylvania). The *taf4b-2* T-DNA insertion (SALK_025468) was obtained from NASC. Plants were cultivated on commercial F2 compost and grown in controlled environment chambers at 20°C with long day 16/8 hour light/dark photoperiods, 60% humidity and 150 µmol light intensity. Prior to germination seeds were kept for two days in the dark at 4°C to stratify germination.

METHOD DETAILS

Measurement of crossovers using FTLs

Three pictures of FTL seed were acquired at minimum magnification using a charge coupled device (CCD) camera; (i) brightfield, (ii) UV through a dsRed filter and (iii) UV through a GFP filter. The CellProfiler program was used to identify seed boundaries in micrographs and to assign a RFP and GFP fluorescence intensity value to each seed object [15, 67]. Histograms of seed fluorescence can be used to classify fluorescent and non-fluorescent seed for each colour. When plants have been self-fertilized, genetic distance is calculated using the formula: $cM = 100\times(1–[1-2(N_G+N_R)/N_T]^{½})$, where N_G is a number of green-alone fluorescent seeds, N_R is a number of red-alone fluorescent seed and N_T is the total number of seeds counted.

Complementation of rQTL1a^{Bur} via transformation

rQTL1a candidate genes were PCR amplified from Col genomic DNA using Phusion High-Fidelity DNA Polymerase (New England Biolabs), and cloned into binary vector pGREEN0029 using restriction digestion. Binary vectors were transformed into *Agrobacterium tumefaciens* GV3101, which were used to transform Arabidopsis via floral dipping.

MLH1 immunostaining of diakinesis-stage meiocytes

Inflorescences were collected from 5 week-old *A. thaliana* plants and placed in fixative (3:1 absolute ethanol:glacial acetic acid) at 4°C, followed by three fixative washes. Flower buds at floral stages 8-10 were dissected from the inflorescences under a dissecting microscope in a solution of fresh fixative solution. Buds were washed (3×2 minutes) in citrate buffer (4.45 mM trisodium citrate, 5.55 mM citric acid) before being transferred to an enzyme solution (0.3% w/v cellulase (Sigma), 0.3% w/v pectolyase (Sigma)) in a moist chamber at 37°C for 1.5 hours. Cell wall digestion was stopped by replacing the enzyme solution with citrate buffer. Buds were then individually transferred into a drop of water on a polysine slide (Thermo Scientific) and gently disrupted by tapping with a brass rod to release the meiocytes. 5 µl of 60% acetic acid were added twice and mixed with the meiocytes and placed on a heated block at 48°C for one minute. 100 µl of ice-cold fixative solution was added to the slides, followed by drying while inverted using a hairdryer. Slides were stained with a solution of DAPI (10 µg/ml) in Vectashield antifade mounting medium. Immunostaining of MLH1 was performed on acetic acid chromosome spreads from the fixed floral buds. The following antibodies were used: α-ASY1 (rabbit, 1/500 dilution) (gift from Chris Franklin, University of Birmingham) and α-MLH1 (rabbit, 1/200 dilution) (gift from

Mathilde Grelon, INRA, Versailles). Microscopy was conducted using a DeltaVision Personal DV microscope (Applied Precision/GE Healthcare) equipped with a CDD CoolSNAP HQ2 camera (Photometrics). Image capture was performed using softWoRx software version 5.5 (Applied Precision/GE Healthcare).

Genotyping-by-sequencing

DNA was extracted and used to prepare sequencing libraries from 180 Col/Bur and 186 *taf4b-1*/Bur F_2 individuals. DNA was digested with 0.3 units of dsDNA Shearase (Zymo Research) in a final volume of 15 µL. The resulting DNA fragments were end-repaired with 3 units of T4 DNA polymerase (New England Biolabs), 10 units of T4 polynucleotide kinase (Thermo Fisher Scientific) and 1.25 units of Klenow fragment (New England Biolabs), in the presence of 0.4 mM dNTPs in a reaction volume of 30 µL for 30 min at 20°C. DNA fragments were cleaned as described [68], and the protocol was followed until the DNA fragment size selection step. To size-select DNA following barcoded Illumina adaptor ligation, 30 µL of a mixture of eight concentrated DNA libraries were combined in a tube containing 48 µL of a 1:1 mix of AMPure XP magnetic SPRI beads (Beckman-Coulter) in water. After 5 minutes incubation at room temperature, the samples were placed on a magnetic rack and allowed to clear before supernatant was transferred to a fresh tube and mixed with 0.12 volumes of undiluted SPRI beads. After 5 min of incubation at room temperature, the tubes were placed on a magnetic rack and allowed to clear. The supernatants were discarded, and the beads washed twice with 80% ethanol. DNA was eluted in 20 µL of 10 mM Tris (pH 8.0). 12 µL of the eluate was used for PCR amplification in a reaction volume of 50 µL using KAPA HiFi Hot-Start ReadyMix PCR kit (Kapabiosystems) and the reported DNA oligonucleotides [68]. Twelve cycles of PCR amplification were performed, and PCR products were then purified using SPRI beads and quantified using a Bioanalyzer. The resulting libraries were subjected to paired-end 150 bp sequencing on an Illumina NextSeq instrument, with 96 barcoded libraries sequenced per lane.

Meiocyte purification and RNA-seq

Stage 9 flower buds were collected and squeezed between a glass slide and coverslip to release meiocytes in prophase I [25]. Meiocytes were cleaned and transferred to a new slide with a glass capillary pipette and washed with 1×PBS buffer three times. Approximately 2,000 meiocytes were collected per replicate. RNA-seq libraries were generated and sequenced using an Illumina NextSeq500 instrument and a 75 bp single-end sequencing (Illumina).

QUANTIFICATION AND STATISTICAL ANALYSIS

Recombination quantitative trait loci mapping

Simple sequence length polymorphism (SSLP) PCR primers were designed using the 1,001 Genomes Bur-0 sequence [22], and used to collect genotype data in Col-*420*/Bur populations. Two-dimensional QTL mapping was performed using Haley-Knott regression with a 2 cM step size in R/qtl version 1.40-8 [69]. Significant loci were combined into an additive model using the *fitqtl* function, after performing *addint* to test for significant interactions between loci. *refineqtl* was used to refine the positions of the *rQTL*s in the context of the final model and derive the percentage of phenotypic variation explained by each locus. For fine mapping, one-dimensional mapping was performed using a 0.1 cM step size. LOD thresholds for genome-wide significance (α=0.05) were established from 1,000 permutation replicates.

Genotyping-by-sequencing data analysis

Sequencing reads derived from one lane of Col/Bur F_2 genomic DNA were aligned to the TAIR10 genome assembly using Bowtie2 [60, 70]. Col/Bur variant sites were called using SAMtools and BCFtools [71]. Sites were filtered to remove those with qualities <100 and >2.5× mean coverage and repeat masked. A set of 446,361 SNPs were selected for analysis. Sequencing data from barcoded libraries was then aligned to TAIR10 and analysed for genotype at the 446,361 SNPs previously identified. These data were then used to identity crossover sites using the TIGER pipeline [68]. To evaluate differences between crossovers in Col/Bur and *taf4b-1*/Bur F_2 populations, crossovers were counted in proportionally scaled windows (10^{ths}) between each telomere and centromere. For each population, windowed crossover frequencies were summed across all F_2 individuals and chromosome arms. For each 10^{th} of the combined chromosome arms, crossovers were modeled by Poisson regression with the log link function using the *glm* function in R, with population included as the predictor variable. Model goodness-of-fit was evaluated using chi-squared tests based on the residual deviance and degrees of freedom ($P>0.05$), by comparison of observed and model-predicted means and standard errors, and by comparison of Bayesian Information Criterion values for Poisson and alternative regression models.

Bioinformatics analysis of RNA-seq data

For each library, transcript abundances were quantified by mapping reads to the TAIR10 reference transcriptome using Salmon version 0.9.1 in "quasi-mapping-based mode" with default parameters [72]. Transcript-level estimates were summed to derive a single expression estimate for each parent gene identifier [73], and the regularized logarithm (rlog) transformation was applied, yielding approximately equal variances across mean expression estimates. Euclidean distances between samples were calculated using the rlog-transformed data. Sample-to-sample distances were visualized with principal component analysis and multi-dimensional scaling plots using the rlog transformed data. For heat map analysis, gene-level transcripts per million (TPM) expression values were derived by summing transcript-level TPM values estimated by Salmon.

Differentially expressed genes were identified using DESeq2 version 1.16.1 [74], using untransformed expression. Genes with more than one read across all samples within a contrast were retained. Additional filtering of genes with low mean read counts was automatically applied by DESeq2. For each contrast, differentially expressed genes with BH-adjusted *P*-values <0.01 were identified. Log_2 fold change in gene expression was plotted against the mean of read counts normalized by library size for each gene in MA plots. A Bayesian method implemented in DESeq2 was used to moderate the log_2 fold changes obtained for genes with low or variable expression levels. Up-regulated and down-regulated genes in *taf4b-1* were evaluated for enrichment of genes up-regulated in wild type meiocytes compared to leaves (BH-adjusted $P<0.01$) using the hypergeometric distribution. Genes representing the intersection of those down-regulated, or up-regulated, in *taf4b-1* (BH-adjusted $P<0.01$) and up-regulated in meiocytes (BH-adjusted $P<0.01$), were analyzed for gene ontology (GO) term enrichment. Gene sets were analyzed for over-representation of "biological process" GO terms relative to their representation among all genes in the TAIR10 annotation, using topGO (version 2.26.0) [75]. Significantly enriched terms were identified by applying the default topGO algorithm coupled with the Fisher's exact test statistic ($P\leq0.05$).

DATA AND CODE AVAILABILITY

Data and Code Availability Statement

The sequencing data files generated during this study are available at Annotare (EMBL-EBI) accessions E-MTAB-XXXX (GBS) and E-MTAB-7870 (RNA-seq). Downstream code, files and analysis are available from the corresponding authors on request.

Lead Contact and Materials Availability Statement

Further information and requests for resources and reagents should be directed to and will be fulfilled by the Lead Contact Ian Henderson (irh25@cam.ac.uk). Sequencing data files generated in this study have been deposited in ArrayExpress accessions E-MTAB-XXXX and E-MTAB-7870.

Legends for supplemental Excel tables, videos or dataset files:

Data S1. FTL fluorescent seed count data. *Related to Figures 1, 2, 3 and 4*. Data is subdivided to indicate the specific experiment the data is associated with; (A) Col-*420*×Bur F_2 mapping population, (B) Col-*420*/Bur F_1 hybrids, (C) Col-*420*×Bur BC_2F_2 mapping population, (D) Transformation of *rQTL1a*^{Bur} with candidate genes, (E) *taf4b-2*×Col-*420* F_2, (F) *taf4b-1*×Col-FTL F_2 and (G) Col/Bur and *taf4b-1*/Bur F_1 hybrids. Genetic distance is calculated as $cM=100\times(1-[1-2(N_G+N_R)/N_T]^{½})$, where N_G is the number of green alone seeds, N_R is the number of red alone seeds and N_T is the total number of seeds analysed.

Table S6. SSLP, CAPS and dCAPS genotyping and additional oligonucleotides. *Related to Figures 1, 2 and 5*. For SSLP oligonucleotides, expected amplicon size from Col and Bur sequence, chromosome, and coordinates (base pairs, bp) of the first nucleotide of the deletion according to the TAIR10 reference assembly, are displayed. For CAPS and dCAPS oligonucleotides, the restriction enzyme used, expected amplicon size(s) from Col and Bur sequence, chromosome, and coordinates (bp) of the polymorphism according to the TAIR10 reference assembly are displayed. The d-*taf4b-1*-F and d-*taf4b-1*-R primers were used for genotyping the *taf4b-1* mutation.

References:

1. Mercier, R., Mézard, C., Jenczewski, E., Macaisne, N., and Grelon, M. (2015). The molecular biology of meiosis in plants. Annu. Rev. Plant Biol. *66*, 297–327.
2. Barton, N. H., and Charlesworth, B. (1998). Why sex and recombination? Cold Spring Harb. Symp. Quant. Biol. *281*, 187–95.
3. Hunter, N. (2015). Meiotic Recombination: The Essence of Heredity. Cold Spring Harb. Perspect. Biol. *7*, a016618.
4. Stapley, J., Feulner, P. G. D., Johnston, S. E., Santure, A. W., and Smadja, C. M. (2017). Variation in recombination frequency and distribution across eukaryotes: patterns and processes. Philos. Trans. R. Soc. B Biol. Sci. *372*, 20160455.
5. Lawrence, E. J., Griffin, C. H., and Henderson, I. R. (2017). Modification of meiotic recombination by natural variation in plants. J. Exp. Bot. *68*, 5471–5483.
6. Fransz, P., Linc, G., Lee, C.-R., Aflitos, S. A., Lasky, J. R., Toomajian, C., Hoda, A., Peters, J., van Dam, P., Ji, X., et al. (2016). Molecular, genetic and evolutionary analysis of a paracentric inversion in Arabidopsis thaliana. Plant J. *88*, 159–178.
7. Ziolkowski, P. A., Underwood, C. J., Lambing, C., Martinez-Garcia, M., Lawrence, E. J., Ziolkowska, L., Griffin, C., Choi, K., Franklin, F. C. H., Martienssen, R. A., et al. (2017). Natural variation and dosage of the HEI10 meiotic E3 ligase control Arabidopsis crossover recombination. Genes Dev. *31*, 306–317.
8. Bomblies, K., Yant, L., Laitinen, R. A., Kim, S.-T., Hollister, J. D., Warthmann, N., Fitz, J., and Weigel, D. (2010). Local-scale patterns of genetic variability, outcrossing, and spatial structure in natural stands of Arabidopsis thaliana. PLoS Genet. *6*, e1000890.
9. Cao, J., Schneeberger, K., Ossowski, S., Günther, T., Bender, S., Fitz, J., Koenig, D., Lanz, C., Stegle, O., Lippert, C., et al. (2011). Whole-genome sequencing of multiple Arabidopsis thaliana populations. Nat. Genet. *43*, 956–63.
10. Kim, S., Plagnol, V., Hu, T. T., Toomajian, C., Clark, R. M., Ossowski, S., Ecker, J. R., Weigel, D., and Nordborg, M. (2007). Recombination and linkage disequilibrium in Arabidopsis thaliana. Nat. Genet. *39*, 1151–1155.

11. Horton, M. W., Hancock, A. M., Huang, Y. S., Toomajian, C., Atwell, S., Auton, A., Muliyati, N. W., Platt, A., Sperone, F. G., Vilhjálmsson, B. J., et al. (2012). Genome-wide patterns of genetic variation in worldwide Arabidopsis thaliana accessions from the RegMap panel. Nat. Genet. *44*, 212–6.
12. Choi, K., Zhao, X., Kelly, K. A., Venn, O., Higgins, J. D., Yelina, N. E., Hardcastle, T. J., Ziolkowski, P. A., Copenhaver, G. P., Franklin, F. C. H., et al. (2013). Arabidopsis meiotic crossover hot spots overlap with H2A.Z nucleosomes at gene promoters. Nat. Genet. *45*, 1327–36.
13. Berchowitz, L. E., and Copenhaver, G. P. (2008). Fluorescent Arabidopsis tetrads: a visual assay for quickly developing large crossover and crossover interference data sets. Nat. Protoc. *3*, 41–50.
14. Yelina, N. E., Ziolkowski, P. A., Miller, N., Zhao, X., Kelly, K. A., Muñoz, D. F., Mann, D. J., Copenhaver, G. P., and Henderson, I. R. (2013). High-throughput analysis of meiotic crossover frequency and interference via flow cytometry of fluorescent pollen in Arabidopsis thaliana. Nat. Protoc. *8*, 2119–2134.
15. Ziolkowski, P. A., Berchowitz, L. E., Lambing, C., Yelina, N. E., Zhao, X., Kelly, K. A., Choi, K., Ziolkowska, L., June, V., Sanchez-Moran, E., et al. (2015). Juxtaposition of heterozygosity and homozygosity during meiosis causes reciprocal crossover remodeling via interference. Elife *4*, e03708.
16. Wu, G., Rossidivito, G., Hu, T., Berlyand, Y., and Poethig, R. S. (2015). Traffic lines: new tools for genetic analysis in Arabidopsis thaliana. Genetics *200*, 35–45.
17. Melamed-Bessudo, C., Yehuda, E., Stuitje, A. R., and Levy, A. A. (2005). A new seed-based assay for meiotic recombination in Arabidopsis thaliana. Plant J. *43*, 458–66.
18. Lago, C., Clerici, E., Mizzi, L., Colombo, L., and Kater, M. M. (2004). TBP-associated factors in Arabidopsis. Gene *342*, 231–241.
19. Goodrich, J. A., and Tjian, R. (2010). Unexpected roles for core promoter recognition factors in cell-type-specific transcription and gene regulation. Nat. Rev. Genet. *11*, 549–558.
20. Louder, R. K., He, Y., López-Blanco, J. R., Fang, J., Chacón, P., and Nogales, E. (2016). Structure of promoter-bound TFIID and model of human pre-initiation complex assembly. Nature *531*, 604–609.
21. Gangloff, Y.-G., Romier, C., Thuault, S., Werten, S., and Davidson, I. (2001). The histone fold is a key structural motif of transcription factor TFIID. Trends Biochem. Sci. *26*, 250–257.
22. The 1001 Genomes Consortium, Alonso-Blanco, C., Andrade, J., Becker, C., Bemm, F., Bergelson, J., Borgwardt, K. M. M., Cao, J., Chae, E., Dezwaan, T. M. M., et al. (2016). 1,135 Genomes Reveal the Global Pattern of Polymorphism in Arabidopsis thaliana. Cell *166*, 481–491.
23. Tabib, A., Vishwanathan, S., Seleznev, A., McKeown, P. C., Downing, T., Dent, C., Sanchez-Bermejo, E., Colling, L., Spillane, C., and Balasubramanian, S. (2016). A Polynucleotide Repeat Expansion Causing Temperature-Sensitivity Persists in Wild Irish Accessions of Arabidopsis thaliana. Front. Plant Sci. *7*, 1311.
24. Freiman, R. N. (2009). Specific variants of general transcription factors regulate germ cell development in diverse organisms. Biochim. Biophys. Acta *1789*, 161–6.
25. Walker, J., Gao, H., Zhang, J., Aldridge, B., Vickers, M., Higgins, J. D., and Feng, X. (2018). Sexual-lineage-specific DNA methylation regulates meiosis in Arabidopsis. Nat. Genet. *50*, 130–137.
26. De, K., Sterle, L., Krueger, L., Yang, X., and Makaroff, C. A. (2014). Arabidopsis thaliana WAPL Is Essential for the Prophase Removal of Cohesin during Meiosis. PLoS Genet. *10*, e1004497.
27. Cromer, L., Jolivet, S., Horlow, C., Chelysheva, L., Heyman, J., De Jaeger, G., Koncz, C., De Veylder, L., and Mercier, R. (2013). Centromeric cohesion is protected twice at meiosis, by SHUGOSHINs at anaphase I and by PATRONUS at interkinesis. Curr. Biol. *23*, 2090–9.

28. Andreuzza, S., Nishal, B., Singh, A., and Siddiqi, I. (2015). The Chromatin Protein DUET/MMD1 Controls Expression of the Meiotic Gene TDM1 during Male Meiosis in Arabidopsis. PLoS Genet. *11*, e1005396.
29. De Storme, N., and Geelen, D. (2011). The Arabidopsis Mutant jason Produces Unreduced First Division Restitution Male Gametes through a Parallel/Fused Spindle Mechanism in Meiosis II. PLANT Physiol. *155*, 1403–1415.
30. Cromer, L., Heyman, J., Touati, S., Harashima, H., Araou, E., Girard, C., Horlow, C., Wassmann, K., Schnittger, A., De Veylder, L., et al. (2012). OSD1 Promotes Meiotic Progression via APC/C Inhibition and Forms a Regulatory Network with TDM and CYCA1;2/TAM. PLoS Genet. *8*, e1002865.
31. De Muyt, A., Vezon, D., Gendrot, G., Gallois, J.-L., Stevens, R., and Grelon, M. (2007). AtPRD1 is required for meiotic double strand break formation in Arabidopsis thaliana. EMBO J. *26*, 4126–37.
32. Higgins, J. D., Vignard, J., Mercier, R., Pugh, A. G., Franklin, F. C. H., and Jones, G. H. (2008). AtMSH5 partners AtMSH4 in the class I meiotic crossover pathway in Arabidopsis thaliana, but is not required for synapsis. Plant J. *55*, 28–39.
33. Chelysheva, L., Diallo, S., Vezon, D., Gendrot, G., Vrielynck, N., Belcram, K., Rocques, N., Márquez-Lema, A., Bhatt, A. M., Horlow, C., et al. (2005). AtREC8 and AtSCC3 are essential to the monopolar orientation of the kinetochores during meiosis. J. Cell Sci. *118*, 4621–32.
34. Mercier, R., Vezon, D., Bullier, E., Motamayor, J. C., Sellier, A., Lefèvre, F., Pelletier, G., and Horlow, C. (2001). SWITCH1 (SWI1): a novel protein required for the establishment of sister chromatid cohesion and for bivalent formation at meiosis. Genes Dev. *15*, 1859–71.
35. Garcia, V., Bruchet, H., Camescasse, D., Granier, F., Bouchez, D., and Tissier, A. (2003). AtATM is essential for meiosis and the somatic response to DNA damage in plants. Plant Cell *15*, 119–32.
36. Hochheimer, A., and Tjian, R. (2003). Diversified transcription initiation complexes expand promoter selectivity and tissue-specific gene expression. Genes Dev. *17*, 1309–20.
37. Falender, A. E., Freiman, R. N., Geles, K. G., Lo, K. C., Hwang, K., Lamb, D. J., Morris, P. L., Tjian, R., and Richards, J. S. (2005). Maintenance of spermatogenesis requires TAF4b, a gonad-specific subunit of TFIID. Genes Dev. *19*, 794–803.
38. Xiao, L., Kim, M., and DeJong, J. (2006). Developmental and cell type-specific regulation of core promoter transcription factors in germ cells of frogs and mice. Gene Expr. Patterns *6*, 409–419.
39. Grive, K. J., Gustafson, E. A., Seymour, K. A., Baddoo, M., Schorl, C., Golnoski, K., Rajkovic, A., Brodsky, A. S., and Freiman, R. N. (2016). TAF4b Regulates Oocyte-Specific Genes Essential for Meiosis. PLOS Genet. *12*, e1006128.
40. Hiller, M., Chen, X., Pringle, M. J., Suchorolski, M., Sancak, Y., Viswanathan, S., Bolival, B., Lin, T.-Y., Marino, S., and Fuller, M. T. (2004). Testis-specific TAF homologs collaborate to control a tissue-specific transcription program. Development *131*, 5297–5308.
41. Freiman, R. N., Albright, S. R., Zheng, S., Sha, W. C., Hammer, R. E., and Tjian, R. (2001). Requirement of Tissue-Selective TBP-Associated Factor TAFII105 in Ovarian Development. Science (80-.). *293*, 2084–2087.
42. Antonova, S. V., Boeren, J., Timmers, H. T. M., and Snel, B. (2019). Epigenetics and transcription regulation during eukaryotic diversification: the saga of TFIID. Genes Dev. doi: 10.1101/gad.3000475.117.
43. Falender, A. E., Shimada, M., Lo, Y. K., and Richards, J. S. (2005). TAF4b, a TBP associated factor, is required for oocyte development and function. Dev. Biol. *288*, 405–419.
44. Reynolds, A., Qiao, H., Yang, Y., Chen, J. K., Jackson, N., Biswas, K., Holloway, J. K., Baudat, F., De Massy, B., Wang, J., et al. (2013). RNF212 is a dosage-sensitive regulator of crossing-over during mammalian meiosis. Nat. Genet. *45*, 269–78.

45. Rao, H. B. D. P., Qiao, H., Bhatt, S. K., Bailey, L. R. J., Tran, H. D., Bourne, S. L., Qiu, W., Deshpande, A., Sharma, A. N., Beebout, C. J., et al. (2017). A SUMO-ubiquitin relay recruits proteasomes to chromosome axes to regulate meiotic recombination. Science *355*, 403–407.
46. Qiao, H., Prasada Rao, H. B. D., Yang, Y., Fong, J. H., Cloutier, J. M., Deacon, D. C., Nagel, K. E., Swartz, R. K., Strong, E., Holloway, J. K., et al. (2014). Antagonistic roles of ubiquitin ligase HEI10 and SUMO ligase RNF212 regulate meiotic recombination. Nat. Genet. *46*, 194–9.
47. Chelysheva, L., Vezon, D., Chambon, A., Gendrot, G., Pereira, L., Lemhemdi, A., Vrielynck, N., Le Guin, S., Novatchkova, M., and Grelon, M. (2012). The Arabidopsis HEI10 is a new ZMM protein related to Zip3. PLoS Genet. *8*, e1002799.
48. Zamariola, L., De Storme, N., Vannerum, K., Vandepoele, K., Armstrong, S. J., Franklin, F. C. H., and Geelen, D. (2014). SHUGOSHINs and PATRONUS protect meiotic centromere cohesion in *Arabidopsis thaliana*. Plant J. *77*, 782–794.
49. Cai, X., Dong, F., Edelmann, R. E., and Makaroff, C. A. (2003). The Arabidopsis SYN1 cohesin protein is required for sister chromatid arm cohesion and homologous chromosome pairing. J. Cell Sci. *116*, 2999–3007.
50. Mercier, R. (2003). The meiotic protein SWI1 is required for axial element formation and recombination initiation in Arabidopsis. Development *130*, 3309–3318.
51. Choi, K., Reinhard, C., Serra, H., Ziolkowski, P.A., Underwood, C. J., Zhao, X., Hardcastle, T. J. T., Yelina, N. N. E., Griffin, C., Jackson, M., et al. (2016). Recombination Rate Heterogeneity within Arabidopsis Disease Resistance Genes. PLoS Genet. *12*, e1006179.
52. Choi, K., Zhao, X., Tock, A. J., Lambing, C., Underwood, C. J., Hardcastle, T. J., Serra, H., Kim, J., Cho, H. S., Kim, J., et al. (2018). Nucleosomes and DNA methylation shape meiotic DSB frequency in Arabidopsis thaliana transposons and gene regulatory regions. Genome Res., *28*, 532–546.
53. Shilo, S., Melamed-Bessudo, C., Dorone, Y., Barkai, N., and Levy, A. A. (2015). DNA Crossover Motifs Associated with Epigenetic Modifications Delineate Open Chromatin Regions in Arabidopsis. Plant Cell *27*, 2427–2436.
54. Wijnker, E., Velikkakam James, G., Ding, J., Becker, F., Klasen, J. R., Rawat, V., Rowan, B. A., de Jong, D. F., de Snoo, C. B., Zapata, L., et al. (2013). The genomic landscape of meiotic crossovers and gene conversions in Arabidopsis thaliana. Elife *2*, e01426.
55. Busslinger, G. A., Stocsits, R. R., van der Lelij, P., Axelsson, E., Tedeschi, A., Galjart, N., and Peters, J.-M. (2017). Cohesin is positioned in mammalian genomes by transcription, CTCF and Wapl. Nature *544*, 503–507.
56. Lengronne, A., Katou, Y., Mori, S., Yokobayashi, S., Kelly, G. P., Itoh, T., Watanabe, Y., Shirahige, K., and Uhlmann, F. (2004). Cohesin relocation from sites of chromosomal loading to places of convergent transcription. Nature *430*, 573–578.
57. Sun, X., Huang, L., Markowitz, T. E., Blitzblau, H. G., Chen, D., Klein, F., and Hochwagen, A. (2015). Transcription dynamically patterns the meiotic chromosome-axis interface. Elife *4*. doi: 10.7554/eLife.07424
58. Kugou, K., Fukuda, T., Yamada, S., Ito, M., Sasanuma, H., Mori, S., Katou, Y., Itoh, T., Matsumoto, K., Shibata, T., et al. (2009). Rec8 guides canonical Spo11 distribution along yeast meiotic chromosomes. Mol. Biol. Cell *20*, 3064–76.
59. Kim, K. P., Weiner, B. M., Zhang, L., Jordan, A., Dekker, J., and Kleckner, N. (2010). Sister cohesion and structural axis components mediate homolog bias of meiotic recombination. Cell *143*, 924–37.
60. Serra, H., Lambing, C., Griffin, C. H., Topp, S. D., Seguela-Arnaud, M., Fernandes, J., Mercier, R., and Henderson, I. R. (2018). Massive crossover elevation via combination of HEI10 and recq4a recq4b during Arabidopsis meiosis. Proc. Natl. Acad. Sci. U. S. A., 2437–2442.
61. Fernandes, J. B., Seguela-Arnaud, M., Larcheveque, C., Lloyd, A. H., and Mercier, R. (2017). Unleashing meiotic crossovers in hybrid plants. Proc. Natl. Acad. Sci. U. S. A.

115, 2431–2436.
62. Yelina, N. E., Lambing, C., Hardcastle, T. J., Zhao, X., Santos, B., and Henderson, I. R. (2015). DNA methylation epigenetically silences crossover hot spots and controls chromosomal domains of meiotic recombination in Arabidopsis. Genes Dev. *29*, 2183–202.
63. Wijnker, E., Harashima, H., Müller, K., Parra-Nuñez, P., de Snoo, C. B., van de Belt, J., Dissmeyer, N., Bayer, M., Pradillo, M., and Schnittger, A. (2019). The Cdk1/Cdk2 homolog CDKA;1 controls the recombination landscape in Arabidopsis. Proc. Natl. Acad. Sci. U. S. A., *116*, 12534–12539.
64. Giraut, L., Falque, M., Drouaud, J., Pereira, L., Martin, O. C., and Mézard, C. (2011). Genome-wide crossover distribution in Arabidopsis thaliana meiosis reveals sex-specific patterns along chromosomes. PLoS Genet. *7*, e1002354.
65. Coop, G., and Przeworski, M. (2006). An evolutionary view of human recombination. Nat. Rev. Genet. *8*, 23–34.
66. Feldman, M. W., Otto, S. P., and Christiansen, F. B. (1996). POPULATION GENETIC PERSPECTIVES ON THE EVOLUTION OF RECOMBINATION. Annu. Rev. Genet. *30*, 261–295.
67. Carpenter, A. E., Jones, T. R., Lamprecht, M. R., Clarke, C., Kang, I. H., Friman, O., Guertin, D. A., Chang, J. H., Lindquist, R. A., Moffat, J., et al. (2006). CellProfiler: image analysis software for identifying and quantifying cell phenotypes. Genome Biol. *7*, R100.
68. Rowan, B. A., Patel, V., Weigel, D., and Schneeberger, K. (2015). Rapid and Inexpensive Whole-Genome Genotyping-by-Sequencing for Crossover Localization and Fine-Scale Genetic Mapping. G3 (Bethesda). *5*, 385–98.
69. Arends, D., Prins, P., Jansen, R. C., and Broman, K. W. (2010). R/qtl: high-throughput multiple QTL mapping. Bioinformatics *26*, 2990–2.
70. Langmead, B., and Salzberg, S. L. (2012). Fast gapped-read alignment with Bowtie 2. Nat. Methods *9*, 357–9.
71. Li, H., Handsaker, B., Wysoker, A., Fennell, T., Ruan, J., Homer, N., Marth, G., Abecasis, G., and Durbin, R. (2009). The Sequence Alignment/Map format and SAMtools. Bioinformatics *25*, 2078–9.
72. Patro, R., Duggal, G., Love, M. I., Irizarry, R. A., and Kingsford, C. (2017). Salmon provides fast and bias-aware quantification of transcript expression. Nat. Methods *14*, 417–419.
73. Soneson, C., Love, M. I., and Robinson, M. D. (2016). Differential analyses for RNA-seq: transcript-level estimates improve gene-level inferences. F1000Research *4*, 1521.
74. Love, M. I., Huber, W., and Anders, S. (2014). Moderated estimation of fold change and dispersion for RNA-seq data with DESeq2. Genome Biol. *15*, 550.
75. Alexa, A., and Rahnenfuhrer, J. (2016). topGO: Enrichment Analysis for Gene Ontology. R Package. version 2.26.0.

KEY RESOURCES TABLE

REAGENT or RESOURCE	SOURCE	IDENTIFIER
Deposited Data		
Genotyping-by-sequencing sequencing read fastq files	This manuscript	E-MTAB-XXXX
RNA-sequencing read fastq files	This manuscript	E-MTAB-7870
Experimental Models: Organisms/Strains		
A. thaliana Bur-0	NASC	N22679
A. thaliana Col-0	NASC	N22681
A. thaliana taf4b-1 introgression and recombinant Col/Bur lines	This manuscript	N/A
A. thaliana taf4b-2 T-DNA line	NASC	SALK_025468 (N525468)
A. thaliana Col-*420* FTL	Avraham Levy Laboratory	[17]
A. thaliana 1.18, 1.13, 2.2, 3.15, 5.1, 5.2, 5.1 and 5.18 FTLs in Col background	Scott Poethig Laboratory	[16]
A. thaliana Irish and Scottish accessions	Sureshkumar Balasubramanian Laboratory	[23]
Oligonucleotides		
See Table S6	This manuscript	N/A
Software and Algorithms		
R/qtl version 1.40-8	[69]	http://www.rqtl.org/
Bowtie2	[70]	https://github.com/BenLangmead/bowtie2
SAMtools	[71]	https://github.com/samtools
TIGER	[68]	N/A
Salmon	[72]	https://github.com/COMBINE-lab/salmon
DESeq2	[74]	https://bioconductor.org/packages/release/bioc/html/DESeq2.html

topGO	[75]	https://bioconductor.org/packages/release/bioc/html/topGO.html

Figure 1

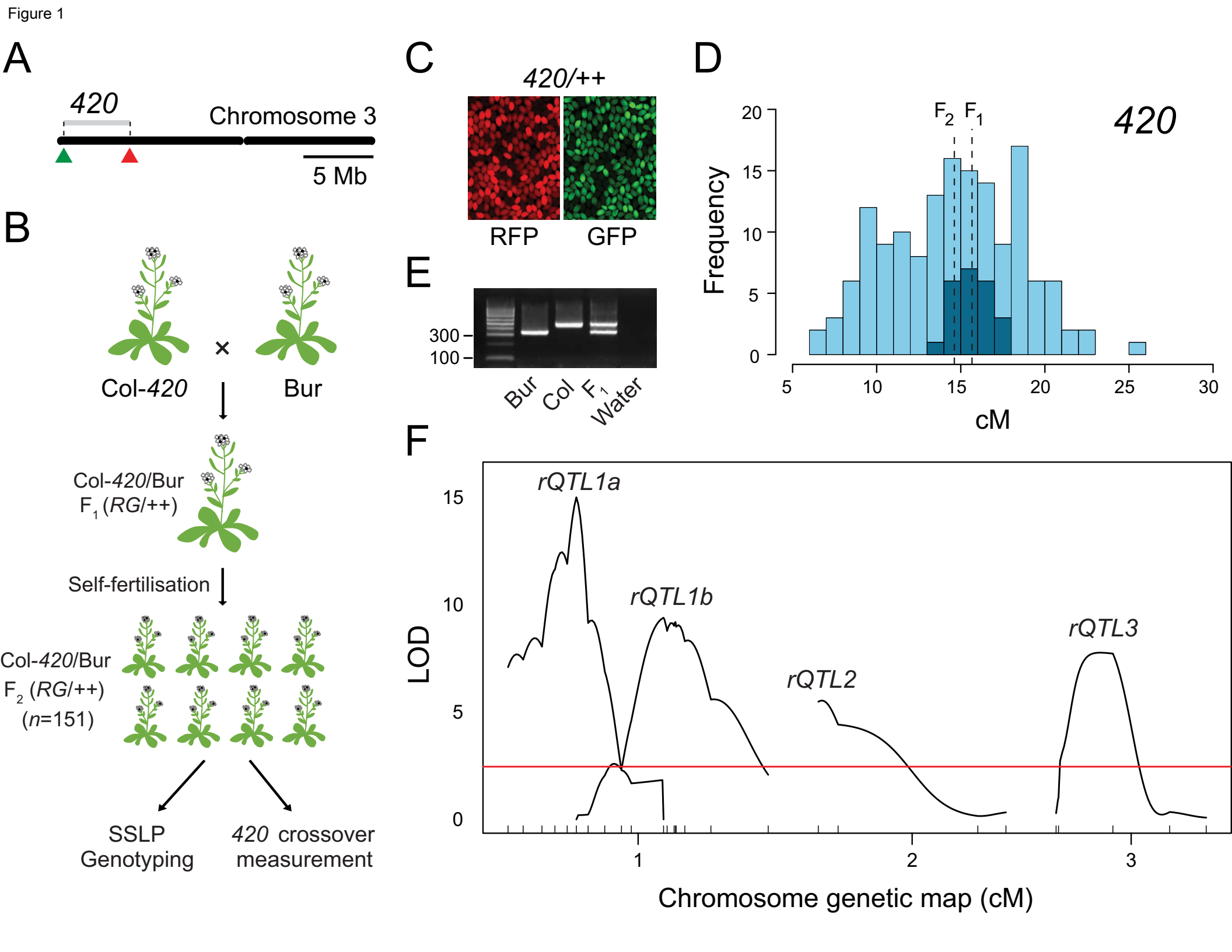
A
420
Chromosome 3
5 Mb
B
Col-420
×
Bur
Col-420/Bur
F1 (RG/++)
Self-fertilisation
Col-420/Bur
F2 (RG/++)
(n=151)
SSLP
Genotyping
420 crossover
measurement
C
420/++
RFP
GFP
D
420
F2
F1
Frequency
cM
E
300
100
Bur
Col
F1
Water
F
rQTL1a
rQTL1b
rQTL2
rQTL3
LOD
Chromosome genetic map (cM)

Figure 2

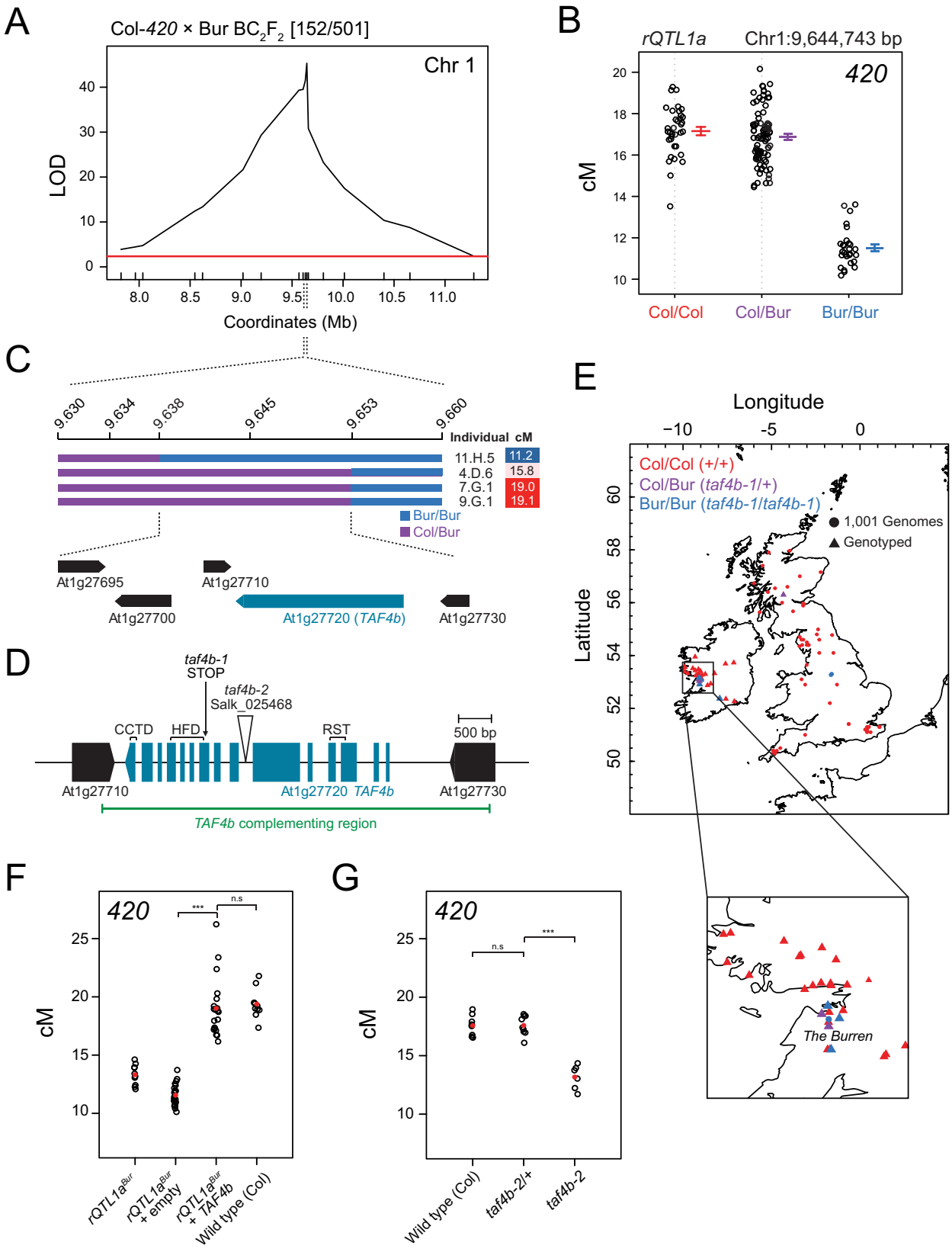
A
Col-420 × Bur BC2F2 [152/501]
Chr 1
LOD
Coordinates (Mb)
B
rQTL1a
Chr1:9,644,743 bp
420
cM
Col/Col
Col/Bur
Bur/Bur
C
Individual cM
11.H.5 11.2
4.D.6 15.8
7.G.1 19.0
9.G.1 19.1
Bur/Bur
Col/Bur
At1g27695
At1g27710
At1g27700
At1g27720 (TAF4b)
At1g27730
D
taf4b-1 STOP
taf4b-2 Salk_025468
CCTD
HFD
RST
500 bp
At1g27710
At1g27720 TAF4b
At1g27730
TAF4b complementing region
E
Longitude
Latitude
Col/Col (+/+)
Col/Bur (taf4b-1/+)
Bur/Bur (taf4b-1/taf4b-1)
1,001 Genomes
Genotyped
The Burren
F
420
cM
rQTL1aBur
rQTL1aBur + empty
rQTL1aBur + TAF4b
Wild type (Col)
G
420
cM
Wild type (Col)
taf4b-2/+
taf4b-2

Figure 3

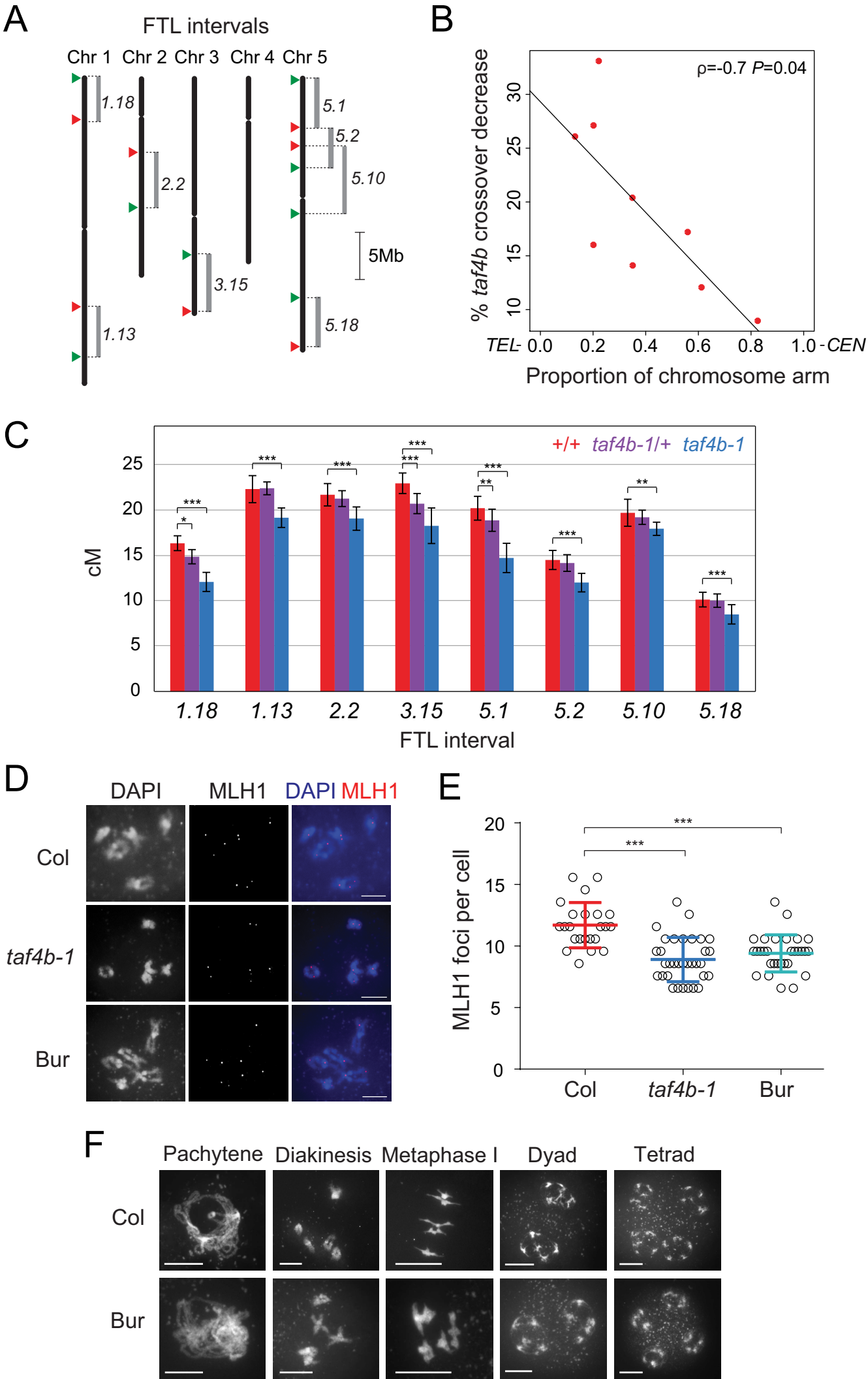
A
FTL intervals
Chr 1
Chr 2
Chr 3
Chr 4
Chr 5
1.18
2.2
3.15
1.13
5.1
5.2
5.10
5.18
5Mb
B
ρ=-0.7 P=0.04
% taf4b crossover decrease
TEL-
-CEN
Proportion of chromosome arm
C
+/+
taf4b-1/+
taf4b-1
cM
FTL interval
1.18
1.13
2.2
3.15
5.1
5.2
5.10
5.18
D
DAPI
MLH1
DAPI MLH1
Col
taf4b-1
Bur
E
MLH1 foci per cell
Col
taf4b-1
Bur
F
Pachytene
Diakinesis
Metaphase I
Dyad
Tetrad
Col
Bur

Figure 4

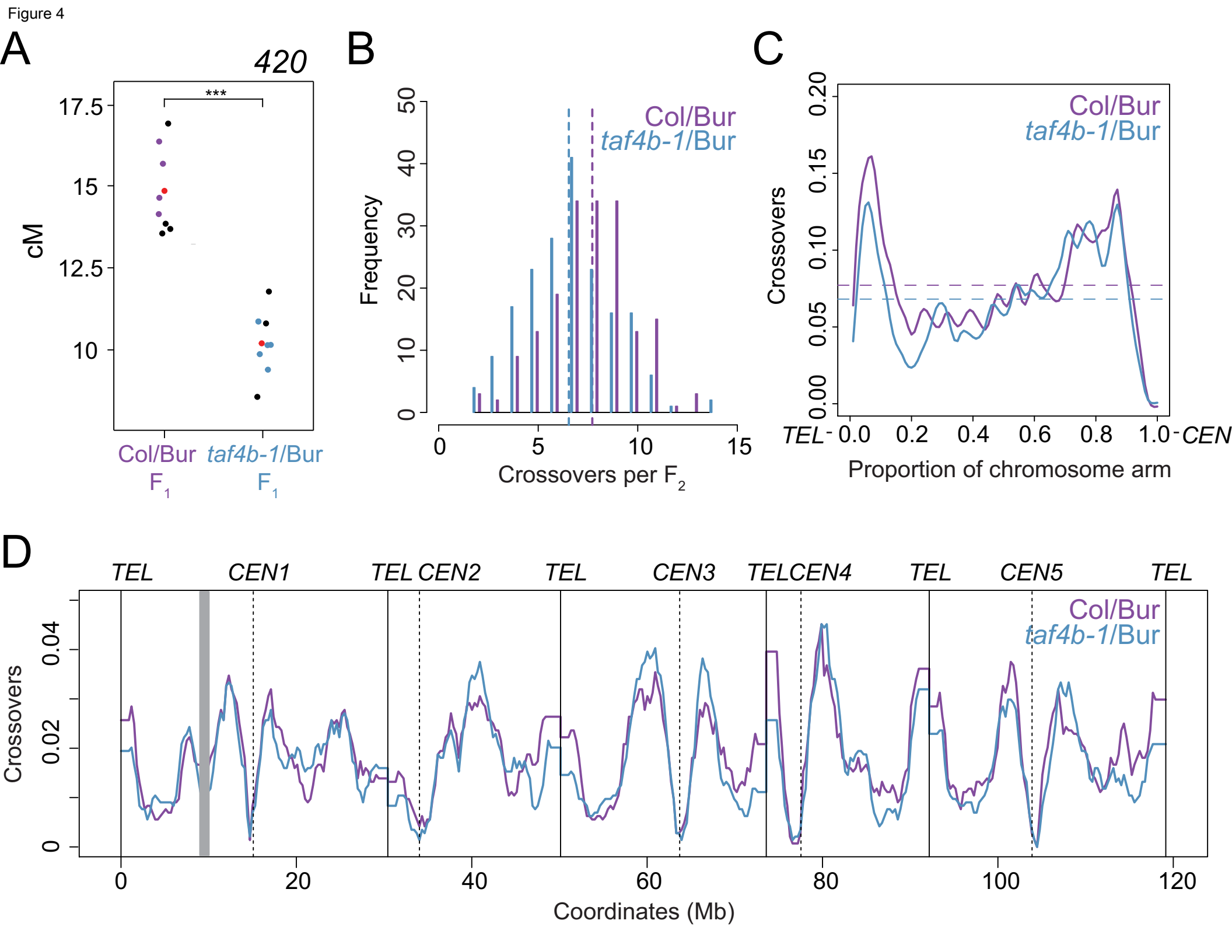
A
420
***
17.5
15
12.5
10
cM
Col/Bur F1
taf4b-1/Bur F1
B
Col/Bur
taf4b-1/Bur
Frequency
0
10
20
30
40
50
0
5
10
15
Crossovers per F2
C
Col/Bur
taf4b-1/Bur
Crossovers
0.00
0.05
0.10
0.15
0.20
TEL
0.0
0.2
0.4
0.6
0.8
1.0
CEN
Proportion of chromosome arm
D
TEL
CEN1
TEL
CEN2
TEL
CEN3
TEL
CEN4
TEL
CEN5
TEL
Col/Bur
taf4b-1/Bur
Crossovers
0
0.02
0.04
0
20
40
60
80
100
120
Coordinates (Mb)

Figure 5

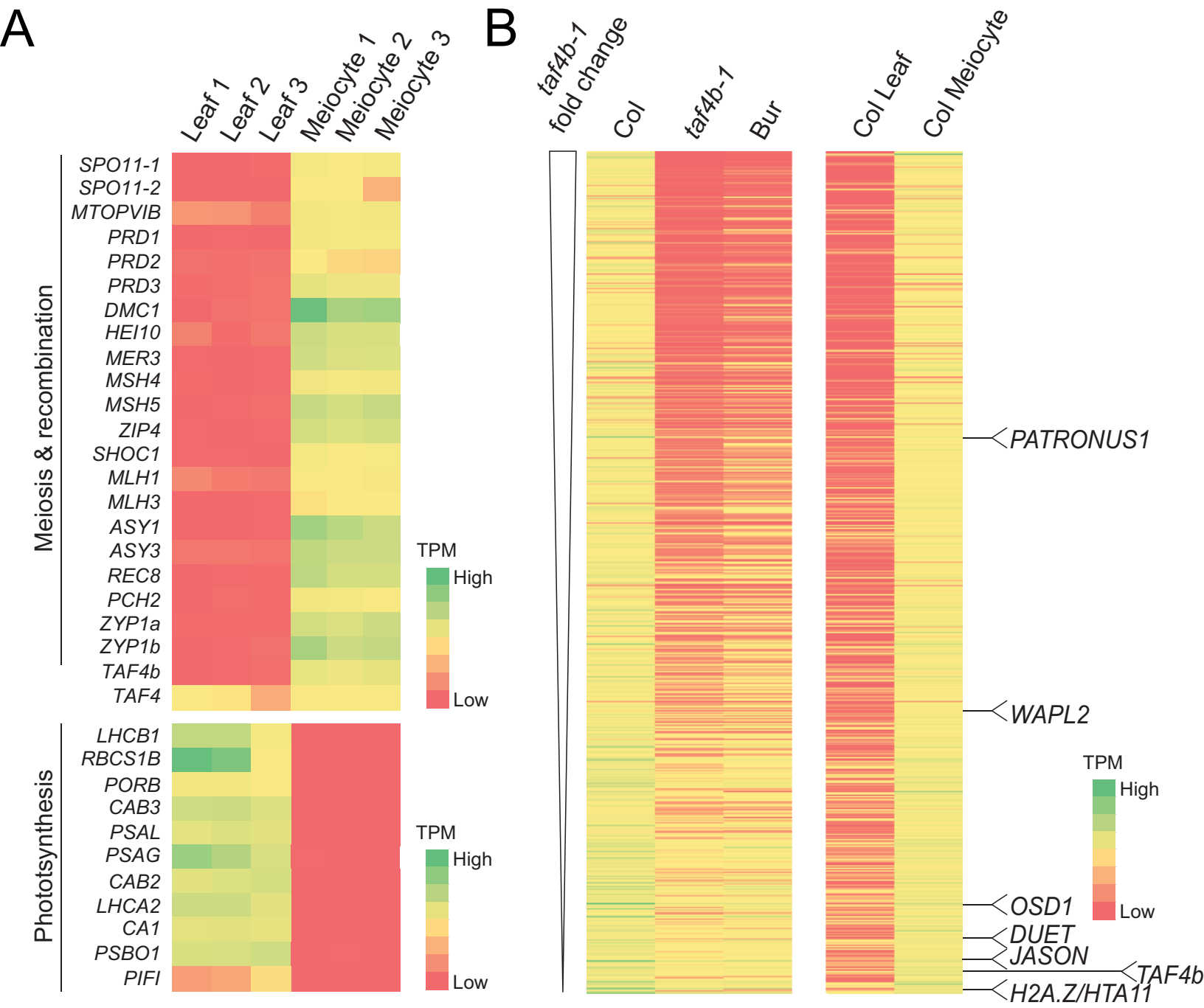
A
Leaf 1
Leaf 2
Leaf 3
Meiocyte 1
Meiocyte 2
Meiocyte 3
Meiosis & recombination
SPO11-1
SPO11-2
MTOPVIB
PRD1
PRD2
PRD3
DMC1
HEI10
MER3
MSH4
MSH5
ZIP4
SHOC1
MLH1
MLH3
ASY1
ASY3
REC8
PCH2
ZYP1a
ZYP1b
TAF4b
TAF4
TPM
High
Low
Photosynthesis
LHCB1
RBCS1B
PORB
CAB3
PSAL
PSAG
CAB2
LHCA2
CA1
PSBO1
PIFI
TPM
High
Low
B
taf4b-1 fold change
Col
taf4b-1
Bur
Col Leaf
Col Meiocyte
PATRONUS1
WAPL2
TPM
High
Low
OSD1
DUET
JASON
TAF4b
H2A.Z/HTA11

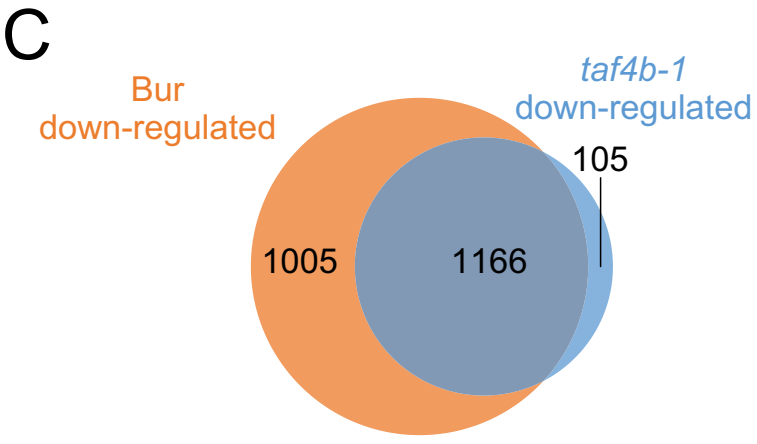
C
Bur
down-regulated
taf4b-1
down-regulated
105
1005
1166

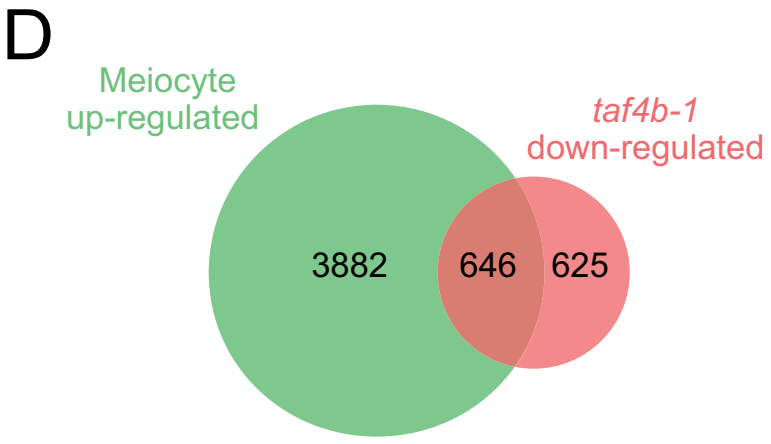
D
Meiocyte
up-regulated
taf4b-1
down-regulated
3882
646
625

Figure 6

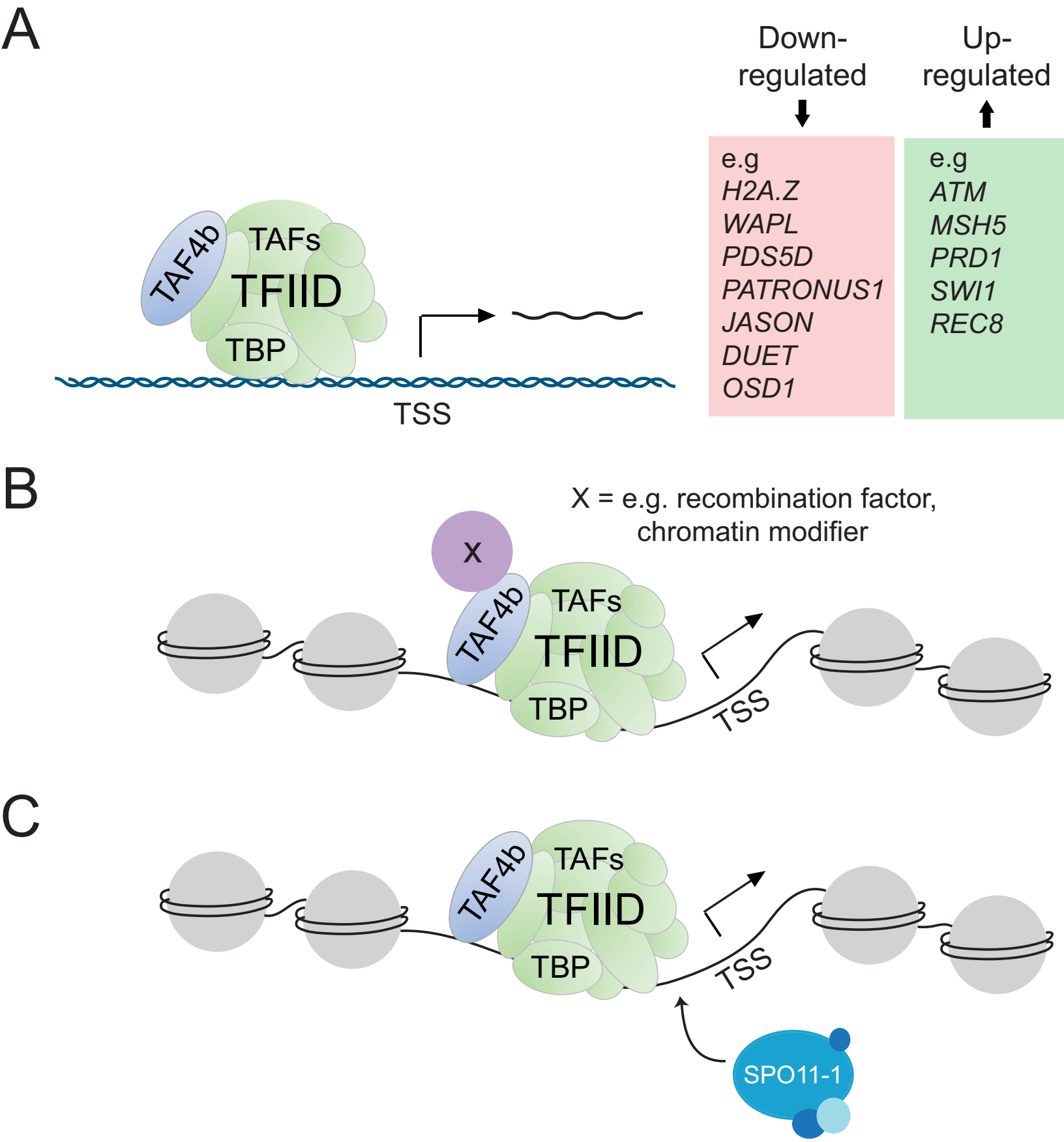
A
Down-regulated
Up-regulated
e.g
H2A.Z
WAPL
PDS5D
PATRONUS1
JASON
DUET
OSD1
e.g
ATM
MSH5
PRD1
SWI1
REC8
TAF4b
TAFs
TFIID
TBP
TSS
B
X = e.g. recombination factor, chromatin modifier
X
TAF4b
TAFs
TFIID
TBP
TSS
C
TAF4b
TAFs
TFIID
TBP
TSS
SPO11-1

Supplemental Figures S1 to S7

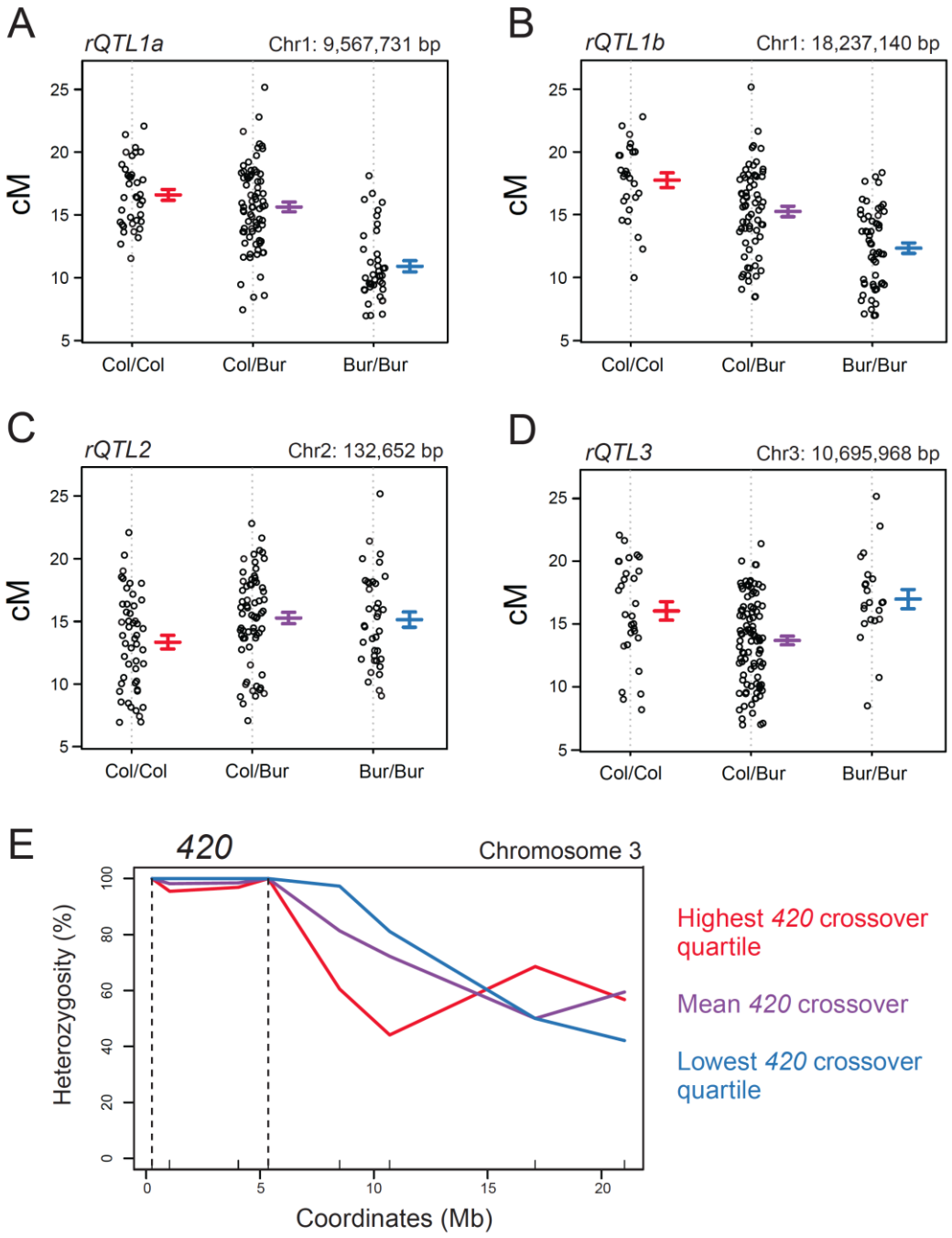

Figure S1. *420* crossover phenotypes according to *rQTL* genotype in Col/Bur F_2 individuals. *Related to Figure 1 and Table 1.* (A) *420* crossover frequency (cM) for F_2 individuals with Col/Col, Col/Bur or Bur/Bur genotype at the *rQTL1a* peak marker. Error bars represent the mean and the standard error. (B) As for A, but for the *rQTL1b* peak marker. (C) As for A, but for the *rQTL2* peak marker. (D) As for A, but for the *rQTL3* peak marker. (E) Heterozygosity (%) on chromosome 3 for all F_2 individuals in the highest crossover frequency quartile (red), lowest crossover frequency quartile (blue), and the population mean (purple). *X*-axis ticks denote the physical locations of genotyping markers. Locations of fluorescent reporter T-DNAs are indicated by vertical dashed lines.

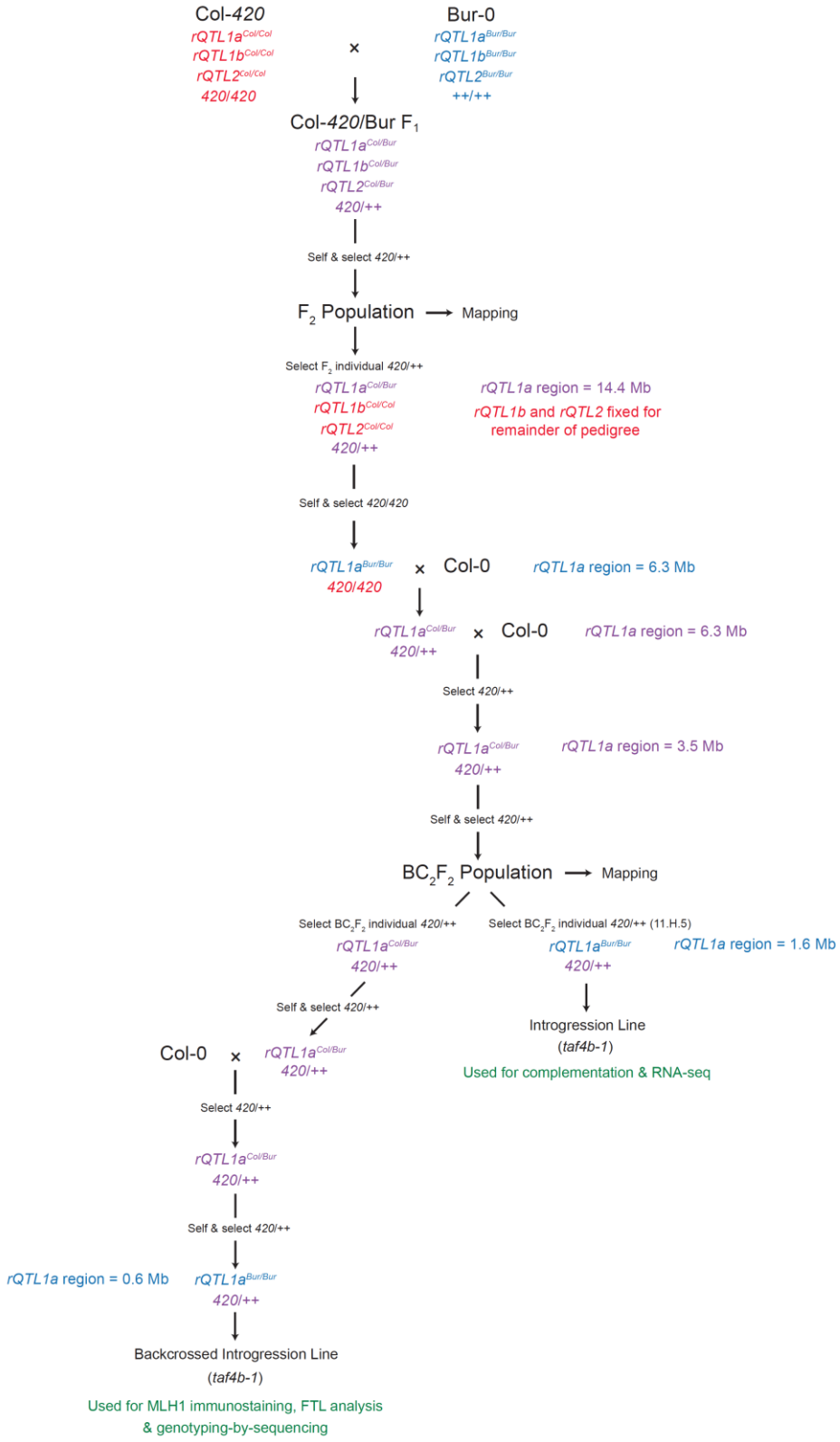

Figure S2. Crossing schematic for generation of Col-*420*×Bur genetic mapping populations. *Related to Figures 1 and 2*. Crossing schematic for generation of Col-*420*×Bur F_2 and BC_2F_2 mapping populations, and *taf4b-1* introgression lines. Col/Col genotypes are indicated in red, Col/Bur genotypes in purple, and Bur/Bur genotypes in blue. The size of *rQTL1a* segregating/fixed regions in different lines is indicated.

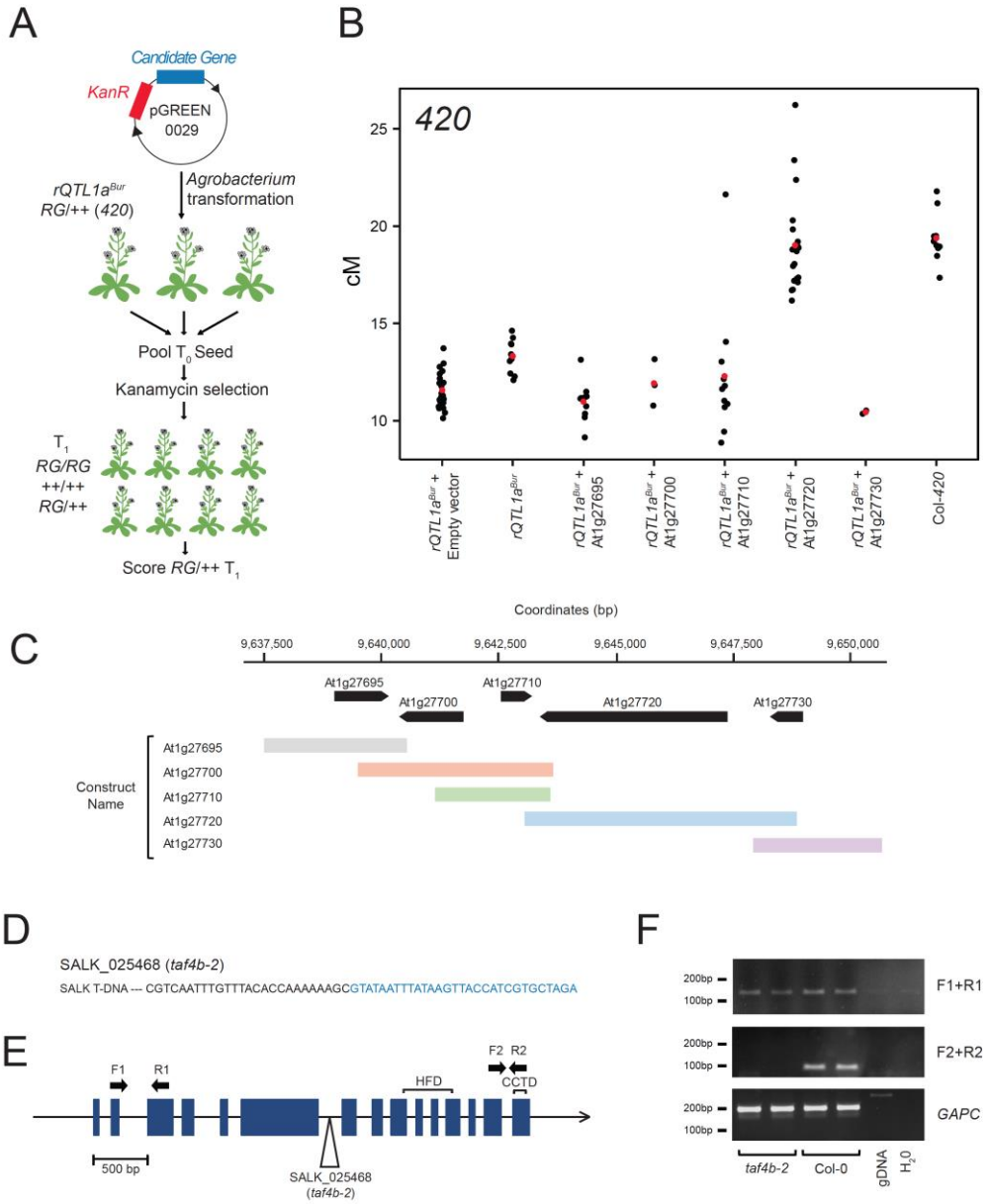

Figure S3. Transformation of *rQTL1a* candidate genes to test for complementation of the crossover phenotype and analysis of the *taf4b-2* T-DNA insertion allele. *Related to Figure 2.* (A) Diagram illustrating T-DNA constructs containing the Col amplicon of each candidate gene and *KanR* (kanamycin resistance gene), between left and right T-DNA borders that are represented by black arrows. *rQTL1a*^{Bur} denotes the *rQTL1a* introgression line containing *420* in *cis* (*RG/++*). (B) *420* crossover frequencies (cM) of individual *rQTL1a*^{Bur} T_1 following transformation with empty vector or the *rQTL1a* candidate genes (At1g27695^{Col}, At1g27700^{Col}, At1g27710^{Col}, At1g27720^{Col} and At1g27730^{Col}). The untransformed *rQTL1a*^{Bur} introgression line and Col-*420* controls are displayed for comparison. Individual T_1 are denoted as black circles and population means as red circles. (C) Regions amplified for restriction cloning of the five *rQTL1a* candidate genes. Genomic positions of each gene are denoted by black arrows, and shaded bars represent the regions amplified for each construct. (D) Sequencing reads displaying the boundary between genomic sequence (blue) and T-DNA insertion sequence (black) in SALK_025468 (*taf4b-2*). (E) Genomic location of *taf4b-2* T-DNA insertion identified in A, indicated on a schematic of *TAF4b*, where blue rectangles denote exons. (F) RT-PCR using *taf4b-2* and Col floral bud cDNA, and genomic DNA and water controls, using the primer pairs indicated in E (F1+R1, F2+R2). A *GAPC* control amplification on the same samples is also shown.

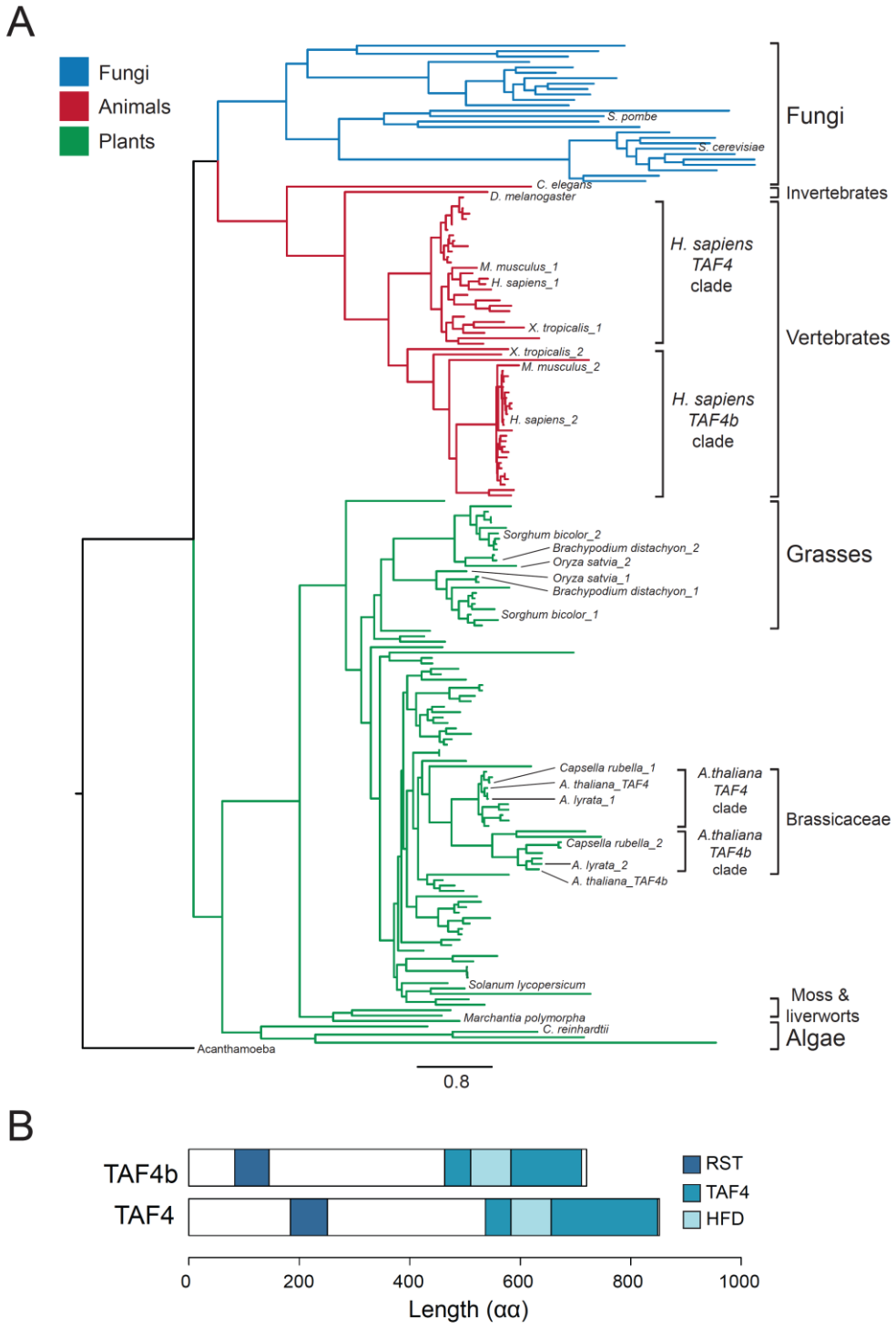

Figure S4. Phylogenetic analysis of eukaryotic TAF4 homologs. *Related to Figure 2*. (A) Phylogenetic tree of TAF4 orthologs identified by BLAST searches in eukaryotic genomes. The phylogenetic tree was constructed using a multiple sequence alignment of full length amino acid sequences and RaxML. The tree was rooted using an amoeba sequence (Acanthamoeba). Monophyletic fungi, animal and plant clades are indicated in blue, red and green, respectively. Annotations for species of interest are also indicated. (B) Comparison of *Arabidopsis thaliana* TAF4b (712 αα) and TAF4 (852 αα) protein structure, highlighting the relative positions of the RST domain, TAF4 domain and HFD. The location of each domain was determined using annotated protein databases, with the exception of the HFD of TAF4 which was determined by alignment to TAF4b.

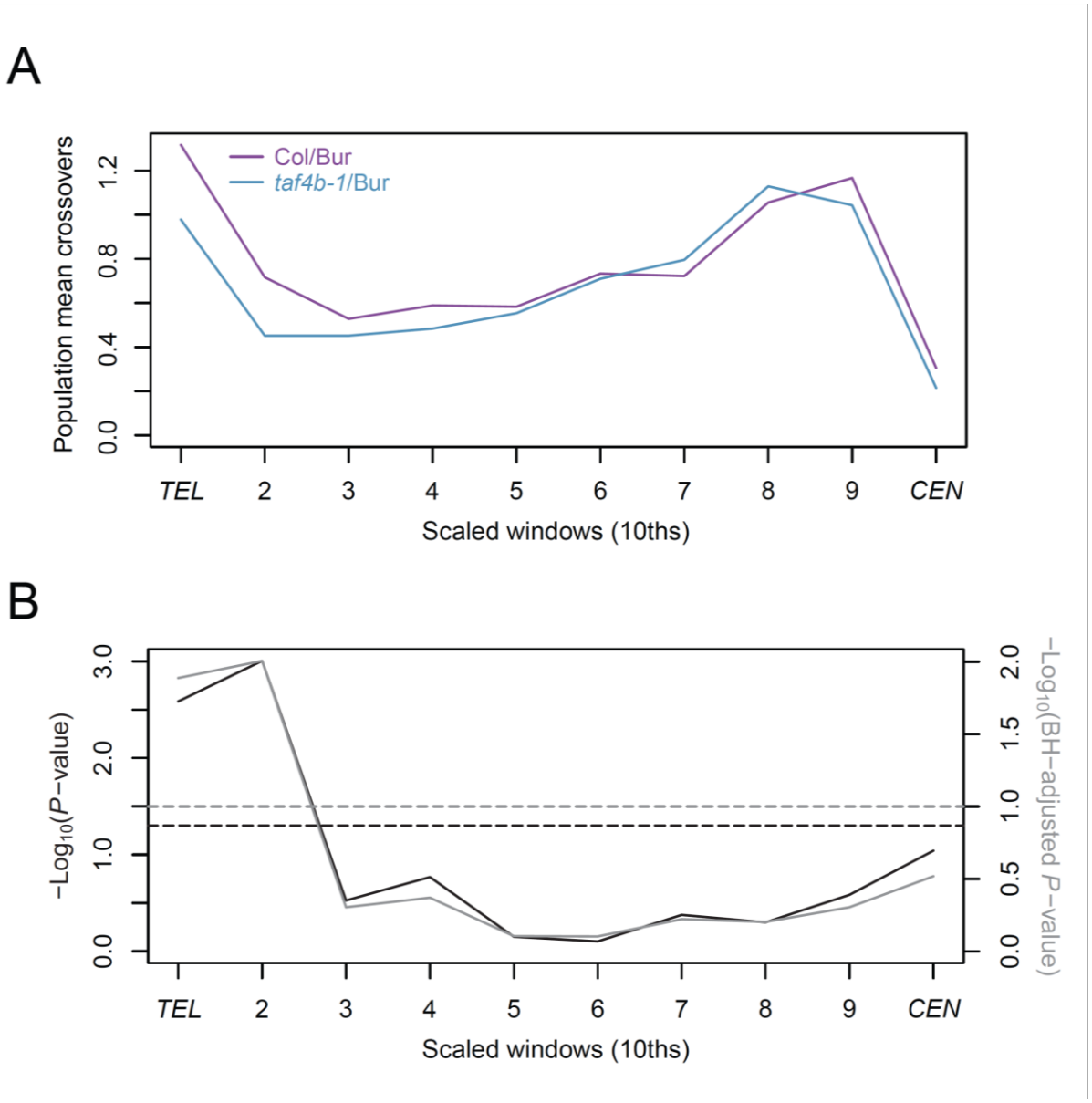

Figure S5. Testing the significance of crossover changes along telomere to centromere axes in *taf4b-1*/Bur and Col/Bur. ***Related to Figure 4.*** (A) Crossover frequency in 10 scaled windows along the proportional length of all chromosome arms from telomeres (*TEL*) to centromeres (*CEN*) in Col/Bur (purple) and *taf4b-1*/Bur (blue) F_2 populations. (B) *P*-values (black) and Benjamini-Hochberg (BH) multiple-testing-corrected *P*-values (grey) derived using a Poisson model to compare crossover counts in each scaled window, summed across all chromosome arms, between Col/Bur and *taf4b-1*/Bur populations. Horizontal dashed lines correspond to an unadjusted *P*-value threshold of $-\log_{10}(0.05)$ (black) and a BH multiple-testing-corrected *P*-value threshold of $-\log_{10}(0.1)$ (grey).

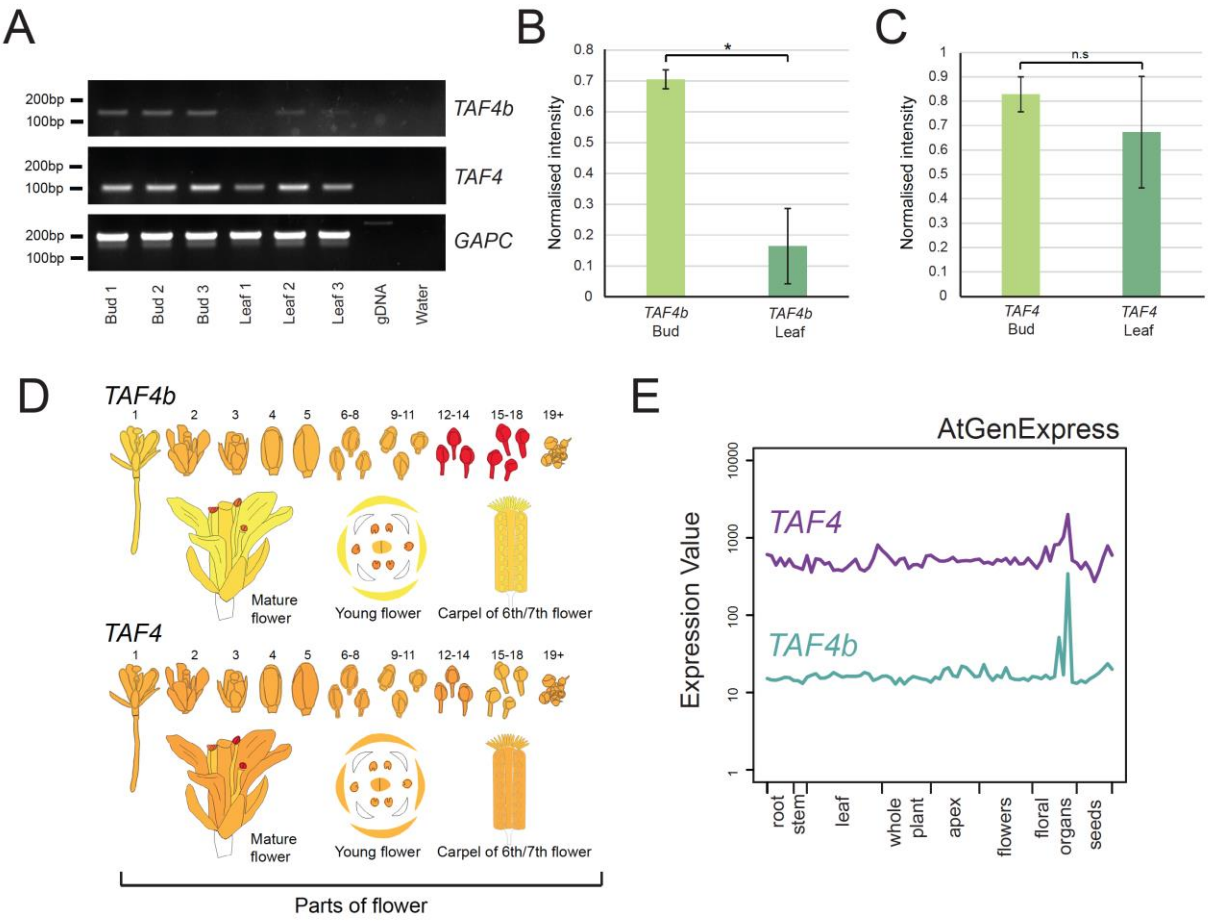

Figure S6. Expression analysis of *TAF4* and *TAF4b*. *Related to Figure 5*. (A) Ethidium bromide stained gels showing RT-PCR amplification products from cDNA of 3 bud replicates and 3 leaf replicates using primers for *TAF4b* (upper), *TAF4* (middle), and *GAPC* (lower). Amplifications from genomic DNA and water controls are also shown. (B) Pixel quantification of *TAF4b* RT-PCR bands from bud and leaf shown in A, normalised by *GAPC* for each equivalent sample. Significance was assessed using Student's *t* test (*=$P \leq 0.05$). Error bars represent the standard deviation. (C) As for B, but for *TAF4*. (D) Screenshots of *TAF4* and *TAF4b* expression analysis from the Bioanalytic Resource eFP browser. (E) Gene expression data from AtGenExpress for *TAF4* and *TAF4b.*

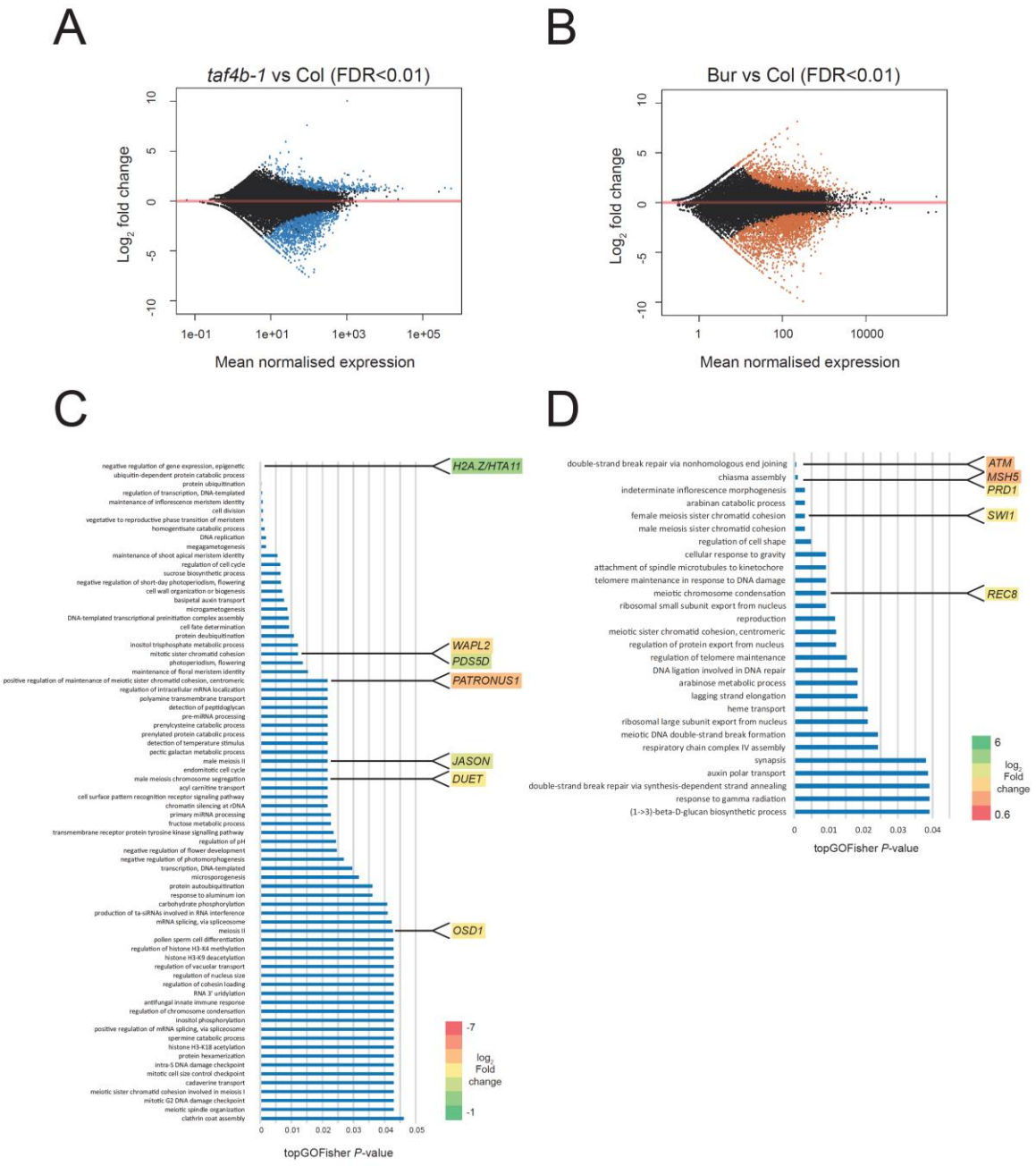

Figure S7. Identification of differentially expressed meiotic genes in Bur and *taf4b-1* compared to Col. *Related to Figure 5*. (A) MA plot displaying $\log_2$ fold change in gene expression for all genes in *taf4b-1* relative to Col, plotted against the mean of read counts normalised by library size. Differentially expressed genes at a Benjamini-Hochberg-adjusted *P*-value FDR threshold of less than 0.01 are highlighted in blue. (B) As for A, but showing differentially expressed genes in Col vs Bur in orange. (C) Significant GO terms ($P \leq 0.05$) identified in the intersecting gene set down-regulated in *taf4b-1* and up-regulated in meiocytes, ranked by topGOFisher *P*-values [S1]. Genes with functions in meiosis are highlighted adjacent to the most significant GO term category in which they appear and are shaded according to their $\log_2$ fold change in *taf4b-1* relative to Col. (D) As for C, but displaying significant GO terms ($P \leq 0.05$) identified in the intersecting gene set that were up-regulated in *taf4b-1* and up-regulated in meiocytes.

Supplemental Tables S1 to S5

Table S1. Presence of the L481* *taf4b-1* mutation in Arabidopsis accessions collected in the British Isles. ***Related to Figure 2.*** Location of accessions in the British Isles and their genotype at 9,644,611 bp on chromosome 1 are listed. A Bur allele at this position indicates the presence of the L481* *taf4b-1* mutation, whereas a Col allele indicates its absence. The first 68 accessions are part of the 1,001 Genomes Project and genotype was determined based on published sequences [S2]. The remaining accessions (69-116) were obtained from Dr. Sureshkumar Balasubramanian [S3]. Two plants per line were genotyped using the *d-taf4b-1* dCAPs marker (Table S6) to determine genotype. Lines where at least one plant was heterozygous are indicated as Col/Bur.

No.	Name	Latitude	Longitude	Location	Country	*taf4b-1* genotype
1	11C1	55.89	-3.21	Hillend	UK	Col/Col
2	Abd-0	57.15	-2.22	Aberdeen	UK	Col/Col
3	Alst-1	54.8	-2.43	Alston	UK	Col/Col
4	Ba-1	56.55	-4.8	Blackmount	UK	Col/Col
5	Boot-1	54.4	-3.27	Boot, Eskdale	UK	Col/Col
6	Bra-1	54.6	-3.2	Braithwaite	UK	Col/Col
7	Bur-0	53.03	-9.08	Clare	Ireland	Bur/Bur
8	Cal-0	53.27	-1.64	Calver	UK	Bur/Bur
9	Cal-2	53.3	-1.6	Calver	UK	Bur/Bur
10	CIBC-17	51.41	-0.64	Ascot, Berkshire	UK	Col/Col
11	CIBC-5	51.41	-0.64	Ascot, Berkshire	UK	Col/Col
12	Cnt-1	51.3	1.1	Canterbury	UK	Col/Col
13	Durh-1	54.78	-1.57	Durham	UK	Col/Col
14	Edi-0	55.95	-3.16	Edinburgh	UK	Col/Col
15	Edi-1	55.97	-3.22	North Edinburgh	UK	Col/Col
16	Ema-1	51.3	0.5	East Malling	UK	Col/Col
17	For-2	56.6	-4.1	Fortingdale	UK	Col/Col
18	Gol-2	57.97	-3.97	Golspie, Scotland	UK	Col/Col
19	HR-10	51.41	-0.64	HR Ascot	UK	Col/Col
20	HR-5	51.41	-0.64	HR Ascot	UK	Col/Col
21	Kent	51.15	0.4	Kent	UK	Col/Col
22	Kil-0	56	-4.4	Killean	UK	Col/Col
23	Lan-0	55.67	-3.78	Lanark	UK	Col/Col
24	Mc-1	54.6	-2.3	Mickell's Fell	UK	Col/Col
25	NFA-10	51.41	-0.64	Ascot	UK	Col/Col
26	NFA-8	51.41	-0.64	Ascot	UK	Col/Col
27	Ragl-1	54.35	-3.42	Ravensglas	UK	Col/Col
28	Set-1	54.1	-2.3	Settle	UK	Col/Col
29	Sq-1	51.41	-0.64	Ascot	UK	Col/Col
30	Sq-8	51.41	-0.64	Ascot	UK	Col/Col
31	Su-0	53.65	-3.01	Southport	UK	Col/Col
32	Ty-1	56.4	-5.2	Taynuilt	UK	Col/Col
33	UKID107	52.9	-3.1	Chirk	UK	Col/Col

34	UKID11	57	-3.4	Braemar	UK	Col/Col
35	UKID116	56.73	-5.98	Ardtoe	UK	Col/Col
36	UKID63	54.1	-1.5	Ripon	UK	Col/Col
37	UKID71	52.9	-1.3	Stanton-by-Dale	UK	Col/Col
38	UKID74	51	-3.1	Taunton	UK	Col/Col
39	UKID93	53.1	-3.3	Ruthin	UK	Col/Col
40	UKID96	57.4	-5.5	Lochcarron	UK	Col/Col
41	UKNW06-003	54.5	-3	Grasmere	UK	Col/Col
42	UKNW06-102	54.4	-3	Outgate	UK	Col/Col
43	UKNW06-233	54.6	-3.3	High Lorton	UK	Col/Col
44	UKNW06-403	54.7	-3.4	Cockermouth	UK	Col/Col
45	UKNW06-481	54.4	-2.9	Windemere	UK	Col/Col
46	UKNW06-488	54.4	-2.9	Windemere	UK	Col/Col
47	UKSE06-118	51.3	0.5	East Malling	UK	Col/Col
48	UKSE06-252	51.3	0.5	East Malling	UK	Col/Col
49	UKSE06-325	52.2	-1.7	West Malling	UK	Col/Col
50	UKSE06-362	51.3	0.4	Wateringbury	UK	Col/Col
51	UKSE06-432	51.2	0.3	Tonbridge Castle	UK	Col/Col
52	UKSE06-470	51.2	0.4	Paddock Wood	UK	Col/Col
53	UKSE06-491	51.2	0.3	Sissinghurst	UK	Col/Col
54	UKSE06-500	51.1	0.6	Sissinghurst	UK	Col/Col
55	UKSE06-533	51.3	1.1	Canterbury	UK	Col/Col
56	UKSE06-541	51.3	1.1	Canterbury	UK	Col/Col
57	UKSE06-639	51.1	0.4	Scotney Castle	UK	Col/Col
58	UKSW06-179	50.4	-4.9	St Columb	UK	Col/Col
59	UKSW06-207	50.4	-4.9	Indian Queen	UK	Col/Col
60	UKSW06-226	50.4	-4.9	St Dennis	UK	Col/Col
61	UKSW06-240	50.4	-4.9	St Dennis	UK	Col/Col
62	UKSW06-257	50.3	-4.9	St Stephens	UK	Col/Col
63	UKSW06-285	50.3	-4.9	St Stephens	UK	Col/Col
64	UKSW06-302	50.3	-4.8	St Austel	UK	Col/Col
65	UKSW06-341	50.4	-4.7	Lostwitheil	UK	Col/Col
66	UKSW06-360	50.5	-4.5	Liskeard	UK	Col/Col
67	Ullapool-8	57.9	-5.15	Ullapool, Scotland	UK	Col/Col
68	Vind-1	54.99	-2.37	Vindolanda	UK	Col/Col
69	At12	53.11	-9.13	Clare	Ireland	Col/Col
70	At24	53.28	-9.06	Galway	Ireland	Col/Col
71	At32	53.4	-9.92	Galway	Ireland	Col/Col
72	At34	53.4	-9.92	Galway	Ireland	Col/Col
73	At50-57	53.56	-9.89	Galway	Ireland	Col/Col
74	At69	53.56	-9.89	Galway	Ireland	Col/Col
75	At75-76	53.55	-9.95	Galway	Ireland	Col/Col
76	At77-79	53.52	-9.45	Galway	Ireland	Col/Col
77	At80-86	53.52	-9.45	Galway	Ireland	Col/Col
78	At100	53.48	-9.13	Galway	Ireland	Col/Col

79	At109-135	52.91	-9.06	Clare	Ireland	Bur/Bur
80	At112	52.91	-9.06	Clare	Ireland	Col/Col
81	At136-140	52.91	-9.07	Clare	Ireland	Col/Col
82	At143	52.91	-9.09	Clare	Ireland	Col/Col
83	At158	52.91	-9.09	Clare	Ireland	Col/Col
84	At161-162	53.27	-9.06	Galway	Ireland	Col/Col
85	At164-170	53.27	-9.05	Galway	Ireland	Col/Col
86	At208-217	52.36	-7.58	Waterford	Ireland	Col/Col
87	At249	52.37	-7.93	Tipperary	Ireland	Bur/Bur
88	At308	52.27	-7.1	Waterford	Ireland	Col/Col
89	At313-314	53.13	-8.96	Galway	Ireland	Col/Col
90	At317	53.13	-8.96	Galway	Ireland	Col/Col
91	At339-348	53.09	-8.99	Clare	Ireland	Bur/Bur
92	At359	53.28	-9.06	Galway	Ireland	Col/Col
93	At361	52.93	-8.44	Clare	Ireland	Col/Col
94	At365	53.04	-9.08	Clare	Ireland	Col/Bur
95	At369	53.06	-9.08	Clare	Ireland	Col/Col
96	At370	53.13	-8.96	Clare	Ireland	Col/Col
97	At376	53.95	-9.32	Mayo	Ireland	Col/Col
98	At379	53.12	-9.07	Clare	Ireland	Col/Col
99	At383	53.27	-8.92	Galway	Ireland	Col/Col
100	At386	53.04	-9.08	Clare	Ireland	Col/Col
101	At394-395	53.43	-9.32	Galway	Ireland	Col/Col
102	At396	53.44	-9.31	Galway	Ireland	Col/Col
103	At400-404	53.32	-9.74	Galway	Ireland	Col/Col
104	At405	53.25	-9.28	Galway	Ireland	Col/Col
105	At407-408	53.27	-9.21	Galway	Ireland	Col/Col
106	At409-412	53.28	-9.14	Galway	Ireland	Col/Col
107	At413-414	53.43	-9.32	Galway	Ireland	Col/Col
108	At434	56.3	-4.33	Callander, Scotland	UK	Col/Bur
109	At444-448	53.3	-8.74	Galway	Ireland	Col/Col
110	At454-459	53.73	-7.13	Meath, Galway	Ireland	Col/Col
111	At463-465	53.33	-8.22	West Meath, Galway	Ireland	Col/Col
112	At467-468	53.69	-7.6	Longford	Ireland	Col/Col
113	At477-478	52.88	-8.6	Clare	Ireland	Col/Col
114	At494	52.87	-8.62	Clare	Ireland	Col/Col
115	At510	53.41	-9.01	Galway	Ireland	Col/Col
116	At533	53.15	-9.08	Clare	Ireland	Bur/Bur

Table S2. Seeds per silique counts in *taf4b-1*, *taf4b-2* and Col. *Related to Figure 3.* Seed quantity in 10 siliques per plant (5 siliques above and the 5 siliques below the midpoint of the primary stem), for 8 plants per genotype. *P*-values were obtained by performing Student's *t* tests comparing mean seeds per silique in Col wild type to *taf4b-1* and *taf4b-2*.

Genotype	Plant	Seed per silique											*P*
		1	2	3	4	5	6	7	8	9	10	Mean	
Col	1	53	55	63	63	65	63	61	72	64	67	62.6	
	2	65	66	61	61	59	64	60	64	61	57	61.8	
	3	60	61	60	58	60	63	63	58	66	-	61.0	
	4	55	57	58	55	-	-	-	-	-	-	56.3	
	5	63	62	57	63	63	64	52	64	61	57	60.6	
	6	64	61	59	65	58	61	58	59	61	63	60.9	
	7	64	61	58	63	67	65	66	69	69	61	64.3	
	8	60	58	61	61	60	59	59	54	66	66	60.4	n.d
taf4b-1	1	60	69	67	61	58	65	59	65	67	64	63.5	
	2	58	65	64	56	66	65	59	57	63	61	61.4	
	3	64	53	45	57	50	62	51	57	62	63	56.4	
	4	63	68	58	59	65	70	65	61	63	61	63.3	
	5	61	62	64	61	65	58	63	64	45	60	60.3	
	6	45	64	50	58	62	64	54	52	63	60	57.2	
	7	64	60	66	62	57	61	53	56	60	48	58.7	
	8	62	66	62	65	66	67	61	61	68	55	63.3	0.718
taf4b-2	1	61	64	67	65	61	67	62	62	61	63	63.3	
	2	61	61	63	61	63	59	57	61	61	64	61.1	
	3	67	65	66	59	62	65	69	67	61	60	64.1	
	4	64	64	66	61	61	68	63	65	63	65	64.0	
	5	59	55	65	61	61	62	60	46	59	61	58.9	
	6	68	64	61	67	65	65	69	64	58	61	64.2	
	7	57	61	64	61	63	65	56	62	62	62	61.3	
	8	62	57	57	64	67	61	64	60	64	59	61.5	0.234

Table S3. MLH1 foci counts in Col, *taf4b-1* and Bur. *Related to Figure 3.* Frequency of diakinesis meiocytes with the indicated quantity of MLH1 foci in Col, *taf4b-1* and Bur. *P*-values were obtained by performing Mann-Whitney-Wilcoxon tests comparing MLH1 foci counts in Col to both *taf4b-1* and Bur MLH1 foci counts.

No. of foci	Frequency of meiocytes		
	Col	*taf4b-1*	Bur
6	0	6	2
7	0	5	3
8	1	9	6
9	3	4	11
10	5	6	6
11	6	1	0
12	4	1	1
13	1	1	1
14	1	0	0
15	2	0	0
Total	23	33	30
P	n.d.	3.17×10^{-6}	1.36×10^{-5}

Table S4. Total crossovers identified by GBS in Col/Bur and *taf4b-1*/Bur F_2 populations. ***Related to Figure 4.*** Total crossover (CO) counts per chromosome, and as an average per F_2 individual, are displayed for Col/Bur and *taf4b-1*/Bur F_2 populations.

	Col/Bur (*n*=180)		*taf4b-1*/Bur (*n*=186)	
	Total CO	CO/F_2	Total CO	CO/F_2
Chr 1	334	1.86	319	1.72
Chr 2	223	1.24	203	1.09
Chr 3	259	1.44	247	1.33
Chr 4	251	1.39	222	1.19
Chr 5	322	1.79	276	1.48
Total	1,389	7.72	1,267	6.81

Table S5. Significantly enriched GO terms in genes down-regulated or up-regulated in *taf4b-1* meiocytes relative to Col, and significantly enriched in Col meiocytes relative to Col leaves. *Related to Figure 5.* For each significantly enriched GO term (*P*≤0.05), the number of genes annotated to this term in the *A. thaliana* genome (Annotated), the number annotated in the gene set (Observed) and the number expected if there was no significant enrichment (Expected) is displayed. The *P*-values were obtained using topGO, coupled with the Fisher's exact test statistic. Genes of biological interest are displayed for their relevant GO term.

(A) Down-regulated

GO ID	GO term	Annotated	Observed	Expected	topGO Fisher (*P*)	Included genes of interest
GO:0045814	negative regulation of gene expression, epigenetic	71	7	1.54	0.00019	*DRM1, H2A.Z*
GO:0006511	ubiquitin-dependent protein catabolic process	392	21	8.52	0.00021	
GO:0016567	protein ubiquitination	544	29	11.82	0.00038	
GO:0006355	regulation of transcription, DNA-templated	2367	76	51.42	0.00064	
GO:0010077	maintenance of inflorescence meristem identity	9	3	0.2	0.00078	
GO:0051301	cell division	363	16	7.89	0.00086	
GO:0010228	vegetative to reproductive phase transition of meristem	207	16	4.5	0.00089	
GO:1902000	homogentisate catabolic process	3	2	0.07	0.00139	
GO:0006260	DNA replication	141	9	3.06	0.00184	
GO:0009561	megagametogenesis	74	6	1.61	0.00186	
GO:0010492	maintenance of shoot apical meristem identity	17	3	0.37	0.00552	
GO:0051726	regulation of cell cycle	219	15	4.76	0.00642	
GO:0005986	sucrose biosynthetic process	18	3	0.39	0.00652	
GO:0048577	negative regulation of short-day photoperiodism, flowering	6	2	0.13	0.00667	
GO:0071554	cell wall organization or biogenesis	709	12	15.4	0.00707	
GO:0010540	basipetal auxin transport	19	3	0.41	0.00762	
GO:0055046	microgametogenesis	56	6	1.22	0.00872	
GO:0070897	DNA-templated transcriptional preinitiation complex assembly	21	3	0.46	0.00918	
GO:0001709	cell fate determination	7	2	0.15	0.0092	
GO:0016579	protein deubiquitination	40	4	0.87	0.01084	
GO:0007064	mitotic sister chromatid cohesion	8	2	0.17	0.01209	*WAPL2, PDS5D*
GO:0032957	inositol trisphosphate metabolic process	8	2	0.17	0.01209	
GO:0048573	photoperiodism, flowering	114	8	2.48	0.0137	
GO:0010076	maintenance of floral meristem identity	9	2	0.2	0.01532	
GO:0000183	chromatin silencing at rDNA	1	1	0.02	0.02172	
GO:0002752	cell surface pattern recognition receptor signalling pathway	1	1	0.02	0.02172	
GO:0006844	acyl carnitine transport	1	1	0.02	0.02172	
GO:0007060	male meiosis chromosome segregation	1	1	0.02	0.02172	*DUET*
GO:0007113	endomitotic cell cycle	1	1	0.02	0.02172	
GO:0007142	male meiosis II	1	1	0.02	0.02172	*JASON*

GO:0010401	pectic galactan metabolic process	1	1	0.02	0.02172	
GO:0016048	detection of temperature stimulus	1	1	0.02	0.02172	
GO:0030327	prenylated protein catabolic process	1	1	0.02	0.02172	
GO:0030328	prenylcysteine catabolic process	1	1	0.02	0.02172	
GO:0031054	pre-miRNA processing	1	1	0.02	0.02172	
GO:0032499	detection of peptidoglycan	1	1	0.02	0.02172	
GO:1902047	polyamine transmembrane transport	1	1	0.02	0.02172	
GO:1904580	regulation of intracellular mRNA localization	1	1	0.02	0.02172	
GO:2000711	positive regulation of maintenance of meiotic sister chromatid cohesion, centromeric	1	1	0.02	0.02172	*PATRONUS 1*
GO:0006000	fructose metabolic process	11	2	0.24	0.02275	
GO:0031053	primary miRNA processing	11	2	0.24	0.02275	
GO:0007169	transmembrane receptor protein tyrosine kinase signalling pathway	130	7	2.82	0.02361	
GO:0006885	regulation of pH	51	4	1.11	0.02444	
GO:0009910	negative regulation of flower development	51	4	1.11	0.02463	
GO:0010100	negative regulation of photomorphogenesis	12	2	0.26	0.02691	
GO:0006351	transcription, DNA-templated	2476	82	53.79	0.02958	
GO:0009556	microsporogenesis	32	3	0.7	0.03172	
GO:0010044	response to aluminum ion	14	2	0.3	0.03607	
GO:0051865	protein autoubiquitination	14	2	0.3	0.03607	
GO:0046835	carbohydrate phosphorylation	17	3	0.37	0.04089	
GO:0010267	production of ta-siRNAs involved in RNA interference	15	2	0.33	0.04103	
GO:0000398	mRNA splicing, via spliceosome	125	7	2.72	0.0423	
GO:0007135	meiosis II	16	4	0.35	0.04276	*JASON, WAPL2, OSD1, PATRONUS 1*
GO:0048235	pollen sperm cell differentiation	36	3	0.78	0.04287	
GO:0051569	regulation of histone H3-K4 methylation	7	2	0.15	0.0429	
GO:0000212	meiotic spindle organization	2	1	0.04	0.04297	
GO:0007095	mitotic G2 DNA damage checkpoint	2	1	0.04	0.04297	
GO:0010789	meiotic sister chromatid cohesion involved in meiosis I	2	1	0.04	0.04297	*WAPL2*
GO:0015839	cadaverine transport	2	1	0.04	0.04297	
GO:0031567	mitotic cell size control checkpoint	2	1	0.04	0.04297	
GO:0031573	intra-S DNA damage checkpoint	2	1	0.04	0.04297	
GO:0034214	protein hexamerization	2	1	0.04	0.04297	
GO:0043971	histone H3-K18 acetylation	2	1	0.04	0.04297	
GO:0046208	spermine catabolic process	2	1	0.04	0.04297	
GO:0048026	positive regulation of mRNA splicing, via spliceosome	2	1	0.04	0.04297	
GO:0052746	inositol phosphorylation	2	1	0.04	0.04297	
GO:0060623	regulation of chromosome condensation	2	1	0.04	0.04297	
GO:0061760	antifungal innate immune response	2	1	0.04	0.04297	

GO:0071076	RNA 3' uridylation	2	1	0.04	0.04297	
GO:0071922	regulation of cohesin loading	2	1	0.04	0.04297	
GO:0097298	regulation of nucleus size	2	1	0.04	0.04297	
GO:1903335	regulation of vacuolar transport	2	1	0.04	0.04297	
GO:1990619	histone H3-K9 deacetylation	2	1	0.04	0.04297	
GO:0048268	clathrin coat assembly	16	2	0.35	0.04623	
(B) Up-regulated						
GO ID	GO term	Annotated	Observed	Expected	topGO Fisher (*P*)	Included genes of interest
GO:0006303	double-strand break repair via nonhomologous end joining	12	2	0.04	0.0006	*ATM*
GO:0051026	chiasma assembly	16	2	0.05	0.0011	*MSH5, PRD1*
GO:0007065	male meiosis sister chromatid cohesion	1	1	0	0.0031	*SWI1*
GO:0007066	female meiosis sister chromatid cohesion	1	1	0	0.0031	*SWI1*
GO:0031222	arabinan catabolic process	1	1	0	0.0031	
GO:0048283	indeterminate inflorescence morphogenesis	1	1	0	0.0031	
GO:0008360	regulation of cell shape	34	2	0.1	0.0049	
GO:0000056	ribosomal small subunit export from nucleus	3	1	0.01	0.0092	
GO:0010032	meiotic chromosome condensation	3	1	0.01	0.0092	*REC8*
GO:0043247	telomere maintenance in response to DNA damage	3	1	0.01	0.0092	
GO:0051455	attachment of spindle microtubules to kinetochore	3	1	0.01	0.0092	
GO:0071258	cellular response to gravity	3	1	0.01	0.0092	
GO:0000003	reproduction	1808	9	5.56	0.0118	
GO:0046825	regulation of protein export from nucleus	4	1	0.01	0.0122	
GO:0051754	meiotic sister chromatid cohesion, centromeric	4	1	0.01	0.0122	*REC8*
GO:0032204	regulation of telomere maintenance	5	1	0.02	0.0153	
GO:0006273	lagging strand elongation	6	1	0.02	0.0183	
GO:0019566	arabinose metabolic process	6	1	0.02	0.0183	
GO:0051103	DNA ligation involved in DNA repair	6	1	0.02	0.0183	
GO:0000055	ribosomal large subunit export from nucleus	7	1	0.02	0.0213	
GO:0015886	heme transport	7	1	0.02	0.0213	
GO:0008535	respiratory chain complex IV assembly	8	1	0.02	0.0243	
GO:0042138	meiotic DNA double-strand break formation	8	1	0.02	0.0243	*PRD1*
GO:0007129	synapsis	29	3	0.09	0.0382	*MSH5, ATM, PRD1*
GO:0009926	auxin polar transport	101	2	0.31	0.0387	
GO:0006075	(1->3)-beta-D-glucan biosynthetic process	13	1	0.04	0.0392	
GO:0010332	response to gamma radiation	13	1	0.04	0.0392	*ATM*
GO:0045003	double-strand break repair via synthesis-dependent strand annealing	13	1	0.04	0.0392	*ATM*

Supplemental References:

S1. Alexa, A., and Rahnenfuhrer, J. (2016). topGO: Enrichment Analysis for Gene Ontology. R Package. version 2.26.0.

S2. The 1001 Genomes Consortium, Alonso-Blanco, C., Andrade, J., Becker, C., Bemm, F., Bergelson, J., Borgwardt, K. M. M., Cao, J., Chae, E., Dezwaan, T. M. M., et al. (2016). 1,135 Genomes Reveal the Global Pattern of Polymorphism in Arabidopsis thaliana. Cell *166*, 481–491.

S3. Tabib, A., Vishwanathan, S., Seleznev, A., McKeown, P. C., Downing, T., Dent, C., Sanchez-Bermejo, E., Colling, L., Spillane, C., and Balasubramanian, S. (2016). A Polynucleotide Repeat Expansion Causing Temperature-Sensitivity Persists in Wild Irish Accessions of Arabidopsis thaliana. Front. Plant Sci. *7*, 1311.

A) Col-*420* ×Bur F_2 mapping population. ***Related to Figure 1.***

FTL	Genotype	Green alone	Red alone	Both	None	Total	cM
420	Col-*420* ×Bur F_2	59	79	1,479	437	2,054	6.96
420	Col-*420* ×Bur F_2	69	55	1,336	379	1,839	6.99
420	Col-*420* ×Bur F_2	46	66	1,216	310	1,638	7.09
420	Col-*420* ×Bur F_2	50	43	940	266	1,299	7.44
420	Col-*420* ×Bur F_2	33	40	693	197	963	7.89
420	Col-*420* ×Bur F_2	35	49	779	211	1,074	8.15
420	Col-*420* ×Bur F_2	44	50	863	242	1,199	8.17
420	Col-*420* ×Bur F_2	63	69	1,174	327	1,633	8.44
420	Col-*420* ×Bur F_2	66	63	1,124	336	1,589	8.48
420	Col-*420* ×Bur F_2	60	65	1,099	298	1,522	8.58
420	Col-*420* ×Bur F_2	70	65	1,121	314	1,570	9.00
420	Col-*420* ×Bur F_2	57	64	1,018	262	1,401	9.05
420	Col-*420* ×Bur F_2	12	17	232	74	335	9.07
420	Col-*420* ×Bur F_2	35	59	751	219	1,064	9.26
420	Col-*420* ×Bur F_2	59	82	1,105	325	1,571	9.42
420	Col-*420* ×Bur F_2	68	80	1,160	336	1,644	9.45
420	Col-*420* ×Bur F_2	95	105	1,551	466	2,217	9.47
420	Col-*420* ×Bur F_2	42	45	660	214	961	9.50
420	Col-*420* ×Bur F_2	34	39	589	141	803	9.55
420	Col-*420* ×Bur F_2	72	72	1,088	352	1,584	9.55
420	Col-*420* ×Bur F_2	84	95	1,380	381	1,940	9.70
420	Col-*420* ×Bur F_2	79	96	1,298	397	1,870	9.84
420	Col-*420* ×Bur F_2	80	102	1,384	353	1,919	9.98
420	Col-*420* ×Bur F_2	56	67	905	262	1,290	10.04
420	Col-*420* ×Bur F_2	55	89	1,072	286	1,502	10.10
420	Col-*420* ×Bur F_2	95	127	1,617	462	2,301	10.16
420	Col-*420* ×Bur F_2	74	79	1,129	303	1,585	10.17
420	Col-*420* ×Bur F_2	80	88	1,222	339	1,729	10.24
420	Col-*420* ×Bur F_2	96	92	1,315	382	1,885	10.53
420	Col-*420* ×Bur F_2	88	96	1,269	357	1,810	10.74
420	Col-*420* ×Bur F_2	71	87	1,077	315	1,550	10.77
420	Col-*420* ×Bur F_2	119	93	1,452	387	2,051	10.93
420	Col-*420* ×Bur F_2	64	90	999	300	1,453	11.23
420	Col-*420* ×Bur F_2	106	107	1,399	370	1,982	11.40
420	Col-*420* ×Bur F_2	100	111	1,388	343	1,942	11.53
420	Col-*420* ×Bur F_2	103	133	1,497	427	2,160	11.60
420	Col-*420* ×Bur F_2	94	103	1,293	308	1,798	11.63
420	Col-*420* ×Bur F_2	61	88	922	266	1,337	11.85
420	Col-*420* ×Bur F_2	58	72	843	191	1,164	11.87
420	Col-*420* ×Bur F_2	98	96	1,166	376	1,736	11.88
420	Col-*420* ×Bur F_2	81	71	947	250	1,349	11.99
420	Col-*420* ×Bur F_2	61	59	734	210	1,064	12.00
420	Col-*420* ×Bur F_2	142	113	1,521	449	2,225	12.21
420	Col-*420* ×Bur F_2	79	74	935	241	1,329	12.26

420	Col-*420*×Bur F_2	102	102	1,191	325	1,720	12.66
420	Col-*420*×Bur F_2	106	80	1,100	280	1,566	12.68
420	Col-*420*×Bur F_2	117	120	1,401	349	1,987	12.74
420	Col-*420*×Bur F_2	84	131	1,249	337	1,801	12.75
420	Col-*420*×Bur F_2	115	126	1,382	375	1,998	12.89
420	Col-*420*×Bur F_2	68	88	866	265	1,287	12.96
420	Col-*420*×Bur F_2	80	106	1,065	259	1,510	13.19
420	Col-*420*×Bur F_2	132	157	1,599	450	2,338	13.24
420	Col-*420*×Bur F_2	72	73	820	200	1,165	13.34
420	Col-*420*×Bur F_2	92	94	999	279	1,464	13.63
420	Col-*420*×Bur F_2	114	142	1,397	361	2,014	13.64
420	Col-*420*×Bur F_2	75	63	744	202	1,084	13.66
420	Col-*420*×Bur F_2	130	116	1,337	348	1,931	13.67
420	Col-*420*×Bur F_2	109	116	1,217	323	1,765	13.68
420	Col-*420*×Bur F_2	115	129	1,321	340	1,905	13.75
420	Col-*420*×Bur F_2	150	114	1,409	371	2,044	13.88
420	Col-*420*×Bur F_2	111	117	1,248	288	1,764	13.89
420	Col-*420*×Bur F_2	112	120	1,293	269	1,794	13.90
420	Col-*420*×Bur F_2	123	133	1,378	341	1,975	13.93
420	Col-*420*×Bur F_2	91	100	997	270	1,458	14.09
420	Col-*420*×Bur F_2	53	73	629	202	957	14.17
420	Col-*420*×Bur F_2	83	95	922	249	1,349	14.20
420	Col-*420*×Bur F_2	84	93	915	247	1,339	14.23
420	Col-*420*×Bur F_2	49	50	502	146	747	14.27
420	Col-*420*×Bur F_2	142	175	1,631	439	2,387	14.30
420	Col-*420*×Bur F_2	88	89	917	229	1,323	14.42
420	Col-*420*×Bur F_2	102	103	1,052	274	1,531	14.43
420	Col-*420*×Bur F_2	104	128	1,193	303	1,728	14.47
420	Col-*420*×Bur F_2	52	78	646	192	968	14.48
420	Col-*420*×Bur F_2	112	148	1,316	350	1,926	14.56
420	Col-*420*×Bur F_2	136	153	1,439	412	2,140	14.57
420	Col-*420*×Bur F_2	108	140	1,241	336	1,825	14.66
420	Col-*420*×Bur F_2	140	135	1,390	340	2,005	14.81
420	Col-*420*×Bur F_2	137	110	1,211	337	1,795	14.87
420	Col-*420*×Bur F_2	103	106	1,074	229	1,512	14.94
420	Col-*420*×Bur F_2	127	151	1,377	346	2,001	15.02
420	Col-*420*×Bur F_2	72	93	827	195	1,187	15.03
420	Col-*420*×Bur F_2	129	152	1,357	356	1,994	15.26
420	Col-*420*×Bur F_2	144	155	1,409	402	2,110	15.35
420	Col-*420*×Bur F_2	121	154	1,335	327	1,937	15.38
420	Col-*420*×Bur F_2	109	105	1,030	263	1,507	15.38
420	Col-*420*×Bur F_2	120	108	1,045	322	1,595	15.50
420	Col-*420*×Bur F_2	142	151	1,392	351	2,036	15.61
420	Col-*420*×Bur F_2	125	167	1,384	352	2,028	15.62
420	Col-*420*×Bur F_2	149	155	1,437	369	2,110	15.63
420	Col-*420*×Bur F_2	119	134	1,182	317	1,752	15.67
420	Col-*420*×Bur F_2	123	120	1,160	272	1,675	15.75
420	Col-*420*×Bur F_2	133	124	1,220	287	1,764	15.82

420	Col-*420*×Bur F_2	123	134	1,182	313	1,752	15.94
420	Col-*420*×Bur F_2	102	100	931	239	1,372	16.00
420	Col-*420*×Bur F_2	99	137	1,067	292	1,595	16.09
420	Col-*420*×Bur F_2	163	143	1,408	354	2,068	16.09
420	Col-*420*×Bur F_2	133	126	1,186	303	1,748	16.12
420	Col-*420*×Bur F_2	130	121	1,133	299	1,683	16.23
420	Col-*420*×Bur F_2	163	156	1,448	371	2,138	16.24
420	Col-*420*×Bur F_2	107	99	945	219	1,370	16.38
420	Col-*420*×Bur F_2	117	106	988	272	1,483	16.38
420	Col-*420*×Bur F_2	125	119	1,094	279	1,617	16.44
420	Col-*420*×Bur F_2	78	90	732	211	1,111	16.48
420	Col-*420*×Bur F_2	146	193	1,510	381	2,230	16.58
420	Col-*420*×Bur F_2	113	128	1,102	238	1,581	16.63
420	Col-*420*×Bur F_2	140	166	1,343	350	1,999	16.70
420	Col-*420*×Bur F_2	124	133	1,137	284	1,678	16.71
420	Col-*420*×Bur F_2	84	118	889	226	1,317	16.74
420	Col-*420*×Bur F_2	132	127	1,108	283	1,650	17.17
420	Col-*420*×Bur F_2	152	152	1,326	286	1,916	17.38
420	Col-*420*×Bur F_2	69	60	555	125	809	17.47
420	Col-*420*×Bur F_2	71	116	745	235	1,167	17.57
420	Col-*420*×Bur F_2	133	122	1,074	255	1,584	17.66
420	Col-*420*×Bur F_2	122	138	1,121	232	1,613	17.68
420	Col-*420*×Bur F_2	108	140	1,082	199	1,529	17.80
420	Col-*420*×Bur F_2	128	130	1,040	284	1,582	17.91
420	Col-*420*×Bur F_2	147	176	1,327	327	1,977	17.95
420	Col-*420*×Bur F_2	147	163	1,250	331	1,891	18.02
420	Col-*420*×Bur F_2	161	159	1,277	353	1,950	18.04
420	Col-*420*×Bur F_2	172	166	1,388	333	2,059	18.04
420	Col-*420*×Bur F_2	124	127	1,074	204	1,529	18.04
420	Col-*420*×Bur F_2	176	150	1,314	338	1,978	18.12
420	Col-*420*×Bur F_2	203	136	1,384	331	2,054	18.15
420	Col-*420*×Bur F_2	137	177	1,280	308	1,902	18.16
420	Col-*420*×Bur F_2	138	124	1,063	259	1,584	18.20
420	Col-*420*×Bur F_2	116	124	974	235	1,449	18.22
420	Col-*420*×Bur F_2	123	146	1,089	263	1,621	18.26
420	Col-*420*×Bur F_2	163	165	1,314	326	1,968	18.35
420	Col-*420*×Bur F_2	170	203	1,484	373	2,230	18.42
420	Col-*420*×Bur F_2	158	173	1,341	303	1,975	18.46
420	Col-*420*×Bur F_2	85	103	748	181	1,117	18.55
420	Col-*420*×Bur F_2	88	117	819	192	1,216	18.59
420	Col-*420*×Bur F_2	119	150	1,083	240	1,592	18.63
420	Col-*420*×Bur F_2	86	101	741	163	1,091	18.93
420	Col-*420*×Bur F_2	84	101	728	162	1,075	19.02
420	Col-*420*×Bur F_2	162	171	1,299	286	1,918	19.21
420	Col-*420*×Bur F_2	178	182	1,353	312	2,025	19.72
420	Col-*420*×Bur F_2	158	178	1,247	306	1,889	19.73
420	Col-*420*×Bur F_2	137	160	1,068	286	1,651	19.99
420	Col-*420*×Bur F_2	134	142	983	274	1,533	20.00

420	Col-*420*×Bur F_2	195	169	1,355	301	2,020	20.02
420	Col-*420*×Bur F_2	111	98	746	192	1,147	20.28
420	Col-*420*×Bur F_2	230	214	1,581	404	2,429	20.35
420	Col-*420*×Bur F_2	99	98	716	164	1,077	20.37
420	Col-*420*×Bur F_2	193	166	1,278	314	1,951	20.50
420	Col-*420*×Bur F_2	196	180	1,316	338	2,030	20.66
420	Col-*420*×Bur F_2	163	168	1,179	256	1,766	21.40
420	Col-*420*×Bur F_2	197	192	1,345	281	2,015	21.65
420	Col-*420*×Bur F_2	191	175	1,240	257	1,863	22.08
420	Col-*420*×Bur F_2	86	96	597	122	901	22.80
420	Col-*420*×Bur F_2	190	157	1,017	213	1,577	25.17

B) Col-*420*/Bur F_1 hybrids. *Related to Figure 1.*

FTL	Genotype	Green alone	Red alone	Both	None	Total	cM
420	Col-*420*/Bur F_1	115	104	975	231	1,425	16.78
420	Col-*420*/Bur F_1	70	92	814	225	1,201	14.55
420	Col-*420*/Bur F_1	89	81	842	211	1,223	15.03
420	Col-*420*/Bur F_1	87	81	766	189	1,123	16.29
420	Col-*420*/Bur F_1	78	88	816	214	1,196	15.01
420	Col-*420*/Bur F_1	95	91	958	220	1,364	14.72
420	Col-*420*/Bur F_1	99	88	788	183	1,158	17.72
420	Col-*420*/Bur F_1	81	98	829	200	1,208	16.12
420	Col-*420*/Bur F_1	83	125	940	222	1,370	16.55
420	Col-*420*/Bur F_1	87	99	900	236	1,322	15.23
420	Col-*420*/Bur F_1	97	102	937	220	1,356	15.95
420	Col-*420*/Bur F_1	81	114	884	201	1,280	16.61
420	Col-*420*/Bur F_1	67	65	737	188	1,057	13.38
420	Col-*420*/Bur F_1	73	63	686	181	1,003	14.63
420	Col-*420*/Bur F_1	88	87	867	212	1,254	15.09
420	Col-*420*/Bur F_1	103	91	936	200	1,330	15.84
420	Col-*420*/Bur F_1	128	175	1,327	342	1,972	16.77
420	Col-*420*/Bur F_1	121	122	1,277	308	1,828	14.32
420	Col-*420*/Bur F_1	128	108	1,189	323	1,748	14.56
420	Col-*420*/Bur F_1	97	100	825	198	1,220	17.72
420	Col-*420*/Bur F_1	87	91	911	242	1,331	14.41
420	Col-*420*/Bur F_1	129	130	1,063	281	1,603	17.73
420	Col-*420*/Bur F_1	121	125	1,225	263	1,734	15.37

C) Col-*420* ×Bur BC_2F_2 mapping population. *Related to Figure 2.*

FTL	Genotype	Green alone	Red alone	Both	None	Total	cM
420	Col-*420* ×Bur BC_2F_2	112	108	1,571	487	2,278	10.18
420	Col-*420* ×Bur BC_2F_2	102	122	1,595	463	2,282	10.35
420	Col-*420* ×Bur BC_2F_2	96	117	1,474	467	2,154	10.43
420	Col-*420* ×Bur BC_2F_2	93	99	1,314	416	1,922	10.55
420	Col-*420* ×Bur BC_2F_2	105	113	1,511	449	2,178	10.57
420	Col-*420* ×Bur BC_2F_2	93	108	1,356	413	1,970	10.78
420	Col-*420* ×Bur BC_2F_2	115	123	1,615	467	2,320	10.85
420	Col-*420* ×Bur BC_2F_2	109	114	1,449	453	2,125	11.11
420	Col-*420* ×Bur BC_2F_2	121	130	1,643	489	2,383	11.16
420	Col-*420* ×Bur BC_2F_2	135	129	1,716	524	2,504	11.17
420	Col-*420* ×Bur BC_2F_2	109	123	1,536	432	2,200	11.17
420	Col-*420* ×Bur BC_2F_2	111	111	1,499	378	2,099	11.20
420	Col-*420* ×Bur BC_2F_2	136	110	1,620	455	2,321	11.23
420	Col-*420* ×Bur BC_2F_2	116	111	1,488	418	2,133	11.28
420	Col-*420* ×Bur BC_2F_2	114	135	1,622	458	2,329	11.33
420	Col-*420* ×Bur BC_2F_2	124	124	1,576	474	2,298	11.45
420	Col-*420* ×Bur BC_2F_2	116	134	1,597	468	2,315	11.46
420	Col-*420* ×Bur BC_2F_2	111	126	1,481	447	2,165	11.62
420	Col-*420* ×Bur BC_2F_2	125	122	1,554	450	2,251	11.65
420	Col-*420* ×Bur BC_2F_2	123	124	1,550	451	2,248	11.67
420	Col-*420* ×Bur BC_2F_2	112	125	1,512	401	2,150	11.71
420	Col-*420* ×Bur BC_2F_2	124	119	1,508	449	2,200	11.73
420	Col-*420* ×Bur BC_2F_2	129	125	1,577	444	2,275	11.87
420	Col-*420* ×Bur BC_2F_2	106	122	1,326	388	1,942	12.52
420	Col-*420* ×Bur BC_2F_2	118	114	1,341	381	1,954	12.68
420	Col-*420* ×Bur BC_2F_2	142	124	1,463	413	2,142	13.30
420	Col-*420* ×Bur BC_2F_2	146	132	1,518	410	2,206	13.52
420	Col-*420* ×Bur BC_2F_2	161	145	1,643	473	2,422	13.55
420	Col-*420* ×Bur BC_2F_2	148	164	1,659	489	2,460	13.61
420	Col-*420* ×Bur BC_2F_2	148	156	1,560	404	2,268	14.45
420	Col-*420* ×Bur BC_2F_2	128	152	1,416	382	2,078	14.53
420	Col-*420* ×Bur BC_2F_2	144	144	1,436	398	2,122	14.64
420	Col-*420* ×Bur BC_2F_2	159	128	1,424	403	2,114	14.65
420	Col-*420* ×Bur BC_2F_2	161	174	1,675	457	2,467	14.65
420	Col-*420* ×Bur BC_2F_2	167	143	1,536	407	2,253	14.86
420	Col-*420* ×Bur BC_2F_2	158	148	1,509	389	2,204	15.01
420	Col-*420* ×Bur BC_2F_2	138	151	1,413	377	2,079	15.03
420	Col-*420* ×Bur BC_2F_2	150	148	1,457	380	2,135	15.10
420	Col-*420* ×Bur BC_2F_2	158	145	1,472	375	2,150	15.26
420	Col-*420* ×Bur BC_2F_2	161	169	1,604	402	2,336	15.30
420	Col-*420* ×Bur BC_2F_2	146	137	1,367	350	2,000	15.32
420	Col-*420* ×Bur BC_2F_2	160	163	1,543	413	2,279	15.35
420	Col-*420* ×Bur BC_2F_2	145	148	1,398	376	2,067	15.35
420	Col-*420* ×Bur BC_2F_2	163	155	1,514	397	2,229	15.46

420	Col-*420* ×Bur BC_2F_2	167	170	1,611	405	2,353	15.53
420	Col-*420* ×Bur BC_2F_2	154	176	1,534	421	2,285	15.67
420	Col-*420* ×Bur BC_2F_2	157	175	1,555	410	2,297	15.68
420	Col-*420* ×Bur BC_2F_2	183	154	1,586	408	2,331	15.69
420	Col-*420* ×Bur BC_2F_2	168	161	1,521	416	2,266	15.76
420	Col-*420* ×Bur BC_2F_2	151	207	1,683	422	2,463	15.78
420	Col-*420* ×Bur BC_2F_2	168	176	1,587	432	2,363	15.81
420	Col-*420* ×Bur BC_2F_2	159	177	1,590	382	2,308	15.81
420	Col-*420* ×Bur BC_2F_2	152	145	1,393	343	2,033	15.87
420	Col-*420* ×Bur BC_2F_2	157	167	1,498	392	2,214	15.90
420	Col-*420* ×Bur BC_2F_2	169	156	1,522	373	2,220	15.90
420	Col-*420* ×Bur BC_2F_2	166	172	1,567	399	2,304	15.94
420	Col-*420* ×Bur BC_2F_2	172	164	1,556	391	2,283	16.00
420	Col-*420* ×Bur BC_2F_2	190	168	1,654	419	2,431	16.01
420	Col-*420* ×Bur BC_2F_2	170	155	1,491	386	2,202	16.05
420	Col-*420* ×Bur BC_2F_2	139	158	1,362	351	2,010	16.07
420	Col-*420* ×Bur BC_2F_2	173	149	1,429	425	2,176	16.09
420	Col-*420* ×Bur BC_2F_2	163	160	1,472	384	2,179	16.12
420	Col-*420* ×Bur BC_2F_2	177	145	1,470	380	2,172	16.13
420	Col-*420* ×Bur BC_2F_2	150	141	1,345	326	1,962	16.13
420	Col-*420* ×Bur BC_2F_2	163	175	1,514	422	2,274	16.17
420	Col-*420* ×Bur BC_2F_2	168	180	1,582	411	2,341	16.17
420	Col-*420* ×Bur BC_2F_2	179	168	1,561	426	2,334	16.18
420	Col-*420* ×Bur BC_2F_2	161	150	1,415	359	2,085	16.23
420	Col-*420* ×Bur BC_2F_2	158	176	1,512	383	2,229	16.32
420	Col-*420* ×Bur BC_2F_2	162	167	1,503	361	2,193	16.34
420	Col-*420* ×Bur BC_2F_2	159	178	1,520	385	2,242	16.37
420	Col-*420* ×Bur BC_2F_2	157	159	1,406	375	2,097	16.42
420	Col-*420* ×Bur BC_2F_2	165	159	1,452	374	2,150	16.42
420	Col-*420* ×Bur BC_2F_2	168	173	1,512	406	2,259	16.45
420	Col-*420* ×Bur BC_2F_2	165	159	1,419	400	2,143	16.48
420	Col-*420* ×Bur BC_2F_2	171	157	1,438	381	2,147	16.67
420	Col-*420* ×Bur BC_2F_2	169	166	1,481	368	2,184	16.74
420	Col-*420* ×Bur BC_2F_2	185	173	1,570	403	2,331	16.76
420	Col-*420* ×Bur BC_2F_2	180	183	1,591	409	2,363	16.77
420	Col-*420* ×Bur BC_2F_2	167	176	1,504	383	2,230	16.79
420	Col-*420* ×Bur BC_2F_2	163	167	1,459	356	2,145	16.79
420	Col-*420* ×Bur BC_2F_2	163	182	1,469	426	2,240	16.82
420	Col-*420* ×Bur BC_2F_2	187	169	1,564	390	2,310	16.83
420	Col-*420* ×Bur BC_2F_2	182	162	1,501	387	2,232	16.83
420	Col-*420* ×Bur BC_2F_2	184	187	1,639	388	2,398	16.90
420	Col-*420* ×Bur BC_2F_2	173	179	1,542	381	2,275	16.90
420	Col-*420* ×Bur BC_2F_2	163	188	1,492	422	2,265	16.93
420	Col-*420* ×Bur BC_2F_2	187	189	1,602	441	2,419	16.99
420	Col-*420* ×Bur BC_2F_2	152	154	1,295	367	1,968	16.99
420	Col-*420* ×Bur BC_2F_2	164	174	1,462	373	2,173	17.00
420	Col-*420* ×Bur BC_2F_2	153	166	1,393	337	2,049	17.02
420	Col-*420* ×Bur BC_2F_2	172	171	1,472	387	2,202	17.03

420	Col-*420* ×Bur BC_2F_2	183	196	1,638	411	2,428	17.07
420	Col-*420* ×Bur BC_2F_2	192	183	1,607	419	2,401	17.08
420	Col-*420* ×Bur BC_2F_2	179	191	1,591	407	2,368	17.08
420	Col-*420* ×Bur BC_2F_2	165	169	1,441	362	2,137	17.09
420	Col-*420* ×Bur BC_2F_2	170	182	1,500	396	2,248	17.12
420	Col-*420* ×Bur BC_2F_2	129	144	1,139	331	1,743	17.13
420	Col-*420* ×Bur BC_2F_2	186	186	1,585	418	2,375	17.13
420	Col-*420* ×Bur BC_2F_2	148	152	1,304	307	1,911	17.17
420	Col-*420* ×Bur BC_2F_2	175	178	1,496	398	2,247	17.19
420	Col-*420* ×Bur BC_2F_2	183	166	1,490	382	2,221	17.19
420	Col-*420* ×Bur BC_2F_2	180	188	1,546	427	2,341	17.20
420	Col-*420* ×Bur BC_2F_2	167	179	1,473	381	2,200	17.21
420	Col-*420* ×Bur BC_2F_2	180	178	1,512	401	2,271	17.25
420	Col-*420* ×Bur BC_2F_2	172	201	1,595	393	2,361	17.29
420	Col-*420* ×Bur BC_2F_2	151	157	1,311	330	1,949	17.30
420	Col-*420* ×Bur BC_2F_2	177	216	1,680	412	2,485	17.31
420	Col-*420* ×Bur BC_2F_2	190	198	1,630	432	2,450	17.34
420	Col-*420* ×Bur BC_2F_2	151	188	1,430	365	2,134	17.40
420	Col-*420* ×Bur BC_2F_2	185	155	1,430	369	2,139	17.41
420	Col-*420* ×Bur BC_2F_2	172	166	1,405	379	2,122	17.45
420	Col-*420* ×Bur BC_2F_2	172	194	1,516	414	2,296	17.47
420	Col-*420* ×Bur BC_2F_2	156	178	1,391	370	2,095	17.47
420	Col-*420* ×Bur BC_2F_2	176	167	1,445	363	2,151	17.47
420	Col-*420* ×Bur BC_2F_2	181	171	1,443	412	2,207	17.48
420	Col-*420* ×Bur BC_2F_2	195	147	1,435	362	2,139	17.52
420	Col-*420* ×Bur BC_2F_2	180	171	1,469	375	2,195	17.53
420	Col-*420* ×Bur BC_2F_2	181	172	1,467	387	2,207	17.53
420	Col-*420* ×Bur BC_2F_2	152	178	1,366	364	2,060	17.56
420	Col-*420* ×Bur BC_2F_2	155	179	1,411	332	2,077	17.64
420	Col-*420* ×Bur BC_2F_2	211	174	1,620	380	2,385	17.71
420	Col-*420* ×Bur BC_2F_2	186	177	1,501	380	2,244	17.75
420	Col-*420* ×Bur BC_2F_2	174	182	1,471	371	2,198	17.78
420	Col-*420* ×Bur BC_2F_2	190	174	1,488	389	2,241	17.83
420	Col-*420* ×Bur BC_2F_2	172	206	1,538	402	2,318	17.91
420	Col-*420* ×Bur BC_2F_2	187	192	1,563	373	2,315	17.99
420	Col-*420* ×Bur BC_2F_2	184	203	1,580	389	2,356	18.06
420	Col-*420* ×Bur BC_2F_2	189	184	1,493	398	2,264	18.12
420	Col-*420* ×Bur BC_2F_2	212	180	1,567	417	2,376	18.14
420	Col-*420* ×Bur BC_2F_2	184	211	1,560	430	2,385	18.22
420	Col-*420* ×Bur BC_2F_2	182	192	1,500	377	2,251	18.29
420	Col-*420* ×Bur BC_2F_2	188	198	1,535	396	2,317	18.34
420	Col-*420* ×Bur BC_2F_2	174	213	1,525	405	2,317	18.39
420	Col-*420* ×Bur BC_2F_2	187	192	1,497	378	2,254	18.53
420	Col-*420* ×Bur BC_2F_2	187	182	1,432	386	2,187	18.60
420	Col-*420* ×Bur BC_2F_2	198	196	1,553	381	2,328	18.67
420	Col-*420* ×Bur BC_2F_2	215	202	1,581	454	2,452	18.77
420	Col-*420* ×Bur BC_2F_2	193	189	1,480	384	2,246	18.77
420	Col-*420* ×Bur BC_2F_2	187	206	1,537	378	2,308	18.79

420	Col-*420* ×Bur BC_2F_2	188	200	1,487	392	2,267	18.90
420	Col-*420* ×Bur BC_2F_2	165	165	1,267	325	1,922	18.97
420	Col-*420* ×Bur BC_2F_2	211	193	1,513	430	2,347	19.02
420	Col-*420* ×Bur BC_2F_2	204	190	1,497	392	2,283	19.08
420	Col-*420* ×Bur BC_2F_2	163	198	1,341	386	2,088	19.12
420	Col-*420* ×Bur BC_2F_2	164	187	1,340	338	2,029	19.13
420	Col-*420* ×Bur BC_2F_2	177	183	1,355	364	2,079	19.15
420	Col-*420* ×Bur BC_2F_2	172	183	1,306	376	2,037	19.29
420	Col-*420* ×Bur BC_2F_2	171	189	1,346	357	2,063	19.32
420	Col-*420* ×Bur BC_2F_2	182	201	1,427	382	2,192	19.34
420	Col-*420* ×Bur BC_2F_2	203	171	1,403	355	2,132	19.43
420	Col-*420* ×Bur BC_2F_2	205	200	1,434	395	2,234	20.16

D) Transformation of *rQTL1a*^{Bur} with candidate genes. *Related to Figure 2.*

FTL	Genotype (Plant + construct)	Green alone	Red alone	Both	None	Total	cM
420	*rQTL1a*^{Bur}+Empty	117	109	1,461	448	2,135	11.21
420	*rQTL1a*^{Bur}+Empty	138	118	1,597	429	2,282	11.93
420	*rQTL1a*^{Bur}+Empty	118	137	1,635	480	2,370	11.41
420	*rQTL1a*^{Bur}+Empty	117	129	1,464	443	2,153	12.17
420	*rQTL1a*^{Bur}+Empty	142	133	1,584	479	2,338	12.55
420	*rQTL1a*^{Bur}+Empty	117	108	1,574	437	2,236	10.63
420	*rQTL1a*^{Bur}+Empty	123	127	1,653	446	2,349	11.28
420	*rQTL1a*^{Bur}+Empty	130	135	1,619	474	2,358	11.95
420	*rQTL1a*^{Bur}+Empty	116	107	1,655	443	2,321	10.12
420	*rQTL1a*^{Bur}+Empty	127	106	1,562	447	2,242	11.00
420	*rQTL1a*^{Bur}+Empty	136	119	1,578	437	2,270	11.95
420	*rQTL1a*^{Bur}+Empty	131	151	1,526	399	2,207	13.72
420	*rQTL1a*^{Bur}+Empty	129	154	1,580	476	2,339	12.94
420	*rQTL1a*^{Bur}+Empty	113	120	1,585	493	2,311	10.65
420	*rQTL1a*^{Bur}+Empty	152	136	1,642	480	2,410	12.76
420	*rQTL1a*^{Bur}+Empty	126	112	1,638	470	2,346	10.72
420	*rQTL1a*^{Bur}+Empty	112	121	1,564	459	2,256	10.92
420	*rQTL1a*^{Bur}+Empty	130	105	1,555	452	2,242	11.10
420	*rQTL1a*^{Bur}+Empty	129	127	1,620	433	2,309	11.78
420	*rQTL1a*^{Bur}+Empty	131	135	1,651	460	2,377	11.90
420	*rQTL1a*^{Bur}+Empty	132	127	1,723	492	2,474	11.08
420	*rQTL1a*^{Bur}+Empty	120	117	1,688	477	2,402	10.41
420	*rQTL1a*^{Bur}+Empty	140	131	1,578	479	2,328	12.41
420	*rQTL1a*^{Bur}+Empty	116	145	1,740	511	2,512	10.99
420	*rQTL1a*^{Bur}+TAF4b	202	178	1,468	360	2,208	19.02
420	*rQTL1a*^{Bur}+TAF4b	221	183	1,450	361	2,215	20.30
420	*rQTL1a*^{Bur}+TAF4b	197	185	1,626	433	2,441	17.11
420	*rQTL1a*^{Bur}+TAF4b	171	152	1,248	290	1,861	19.20
420	*rQTL1a*^{Bur}+TAF4b	166	166	1,514	388	2,234	16.17
420	*rQTL1a*^{Bur}+TAF4b	187	189	1,550	364	2,290	18.05
420	*rQTL1a*^{Bur}+TAF4b	162	171	1,436	407	2,176	16.70
420	*rQTL1a*^{Bur}+TAF4b	176	185	1,564	373	2,298	17.19
420	*rQTL1a*^{Bur}+TAF4b	207	186	1,542	372	2,307	18.80
420	*rQTL1a*^{Bur}+TAF4b	195	217	1,325	258	1,995	23.39
420	*rQTL1a*^{Bur}+TAF4b	195	217	1,565	431	2,408	18.89
420	*rQTL1a*^{Bur}+TAF4b	200	220	1,576	355	2,351	19.83
420	*rQTL1a*^{Bur}+TAF4b	179	199	1,549	387	2,314	17.95
420	*rQTL1a*^{Bur}+TAF4b	196	179	1,626	364	2,365	17.36
420	*rQTL1a*^{Bur}+TAF4b	196	186	1,608	428	2,418	17.29
420	*rQTL1a*^{Bur}+TAF4b	198	163	1,005	218	1,584	26.23
420	*rQTL1a*^{Bur}+TAF4b	187	195	1,248	292	1,922	22.38
420	*rQTL1a*^{Bur}+TAF4b	180	187	1,420	377	2,164	18.71

420	*rQTL1a* ^{Bur}+TAF4b	207	196	1,553	393	2,349	18.95
420	*rQTL1a* ^{Bur}+TAF4b	199	158	1,581	391	2,329	16.73
420	*rQTL1a* ^{Bur}+At1g27695	113	105	1,558	482	2,258	10.17
420	*rQTL1a* ^{Bur}+At1g27695	54	80	943	287	1,364	10.36
420	*rQTL1a* ^{Bur}+At1g27695	105	97	1,629	485	2,316	9.14
420	*rQTL1a* ^{Bur}+At1g27695	98	135	1,522	440	2,195	11.25
420	*rQTL1a* ^{Bur}+At1g27695	121	129	1,568	490	2,308	11.49
420	*rQTL1a* ^{Bur}+At1g27695	118	112	1,546	487	2,263	10.74
420	*rQTL1a* ^{Bur}+At1g27695	125	128	1,646	503	2,402	11.16
420	*rQTL1a* ^{Bur}+At1g27695	110	132	1,565	481	2,288	11.20
420	*rQTL1a* ^{Bur}+At1g27695	97	137	1,538	455	2,227	11.13
420	*rQTL1a* ^{Bur}+At1g27695	136	131	1,483	426	2,176	13.13
420	*rQTL1a* ^{Bur}+At1g27700	116	149	1,657	458	2,380	11.83
420	*rQTL1a* ^{Bur}+At1g27700	132	124	1,438	389	2,083	13.16
420	*rQTL1a* ^{Bur}+At1g27700	107	105	1,444	425	2,081	10.77
420	*rQTL1a* ^{Bur}+At1g27710	141	110	1,681	513	2,445	10.86
420	*rQTL1a* ^{Bur}+At1g27710	96	97	1,602	483	2,278	8.87
420	*rQTL1a* ^{Bur}+At1g27710	121	122	1,662	497	2,402	10.69
420	*rQTL1a* ^{Bur}+At1g27710	94	114	1,598	508	2,314	9.43
420	*rQTL1a* ^{Bur}+At1g27710	139	126	1,480	430	2,175	13.03
420	*rQTL1a* ^{Bur}+At1g27710	165	132	1,569	408	2,274	14.05
420	*rQTL1a* ^{Bur}+At1g27710	183	167	1,200	264	1,814	21.63
420	*rQTL1a* ^{Bur}+At1g27710	105	115	1,386	402	2,008	11.63
420	*rQTL1a* ^{Bur}+At1g27710	121	119	1,595	470	2,305	11.02
420	*rQTL1a* ^{Bur}+At1g27710	131	119	1,539	404	2,193	12.14
420	*rQTL1a* ^{Bur}+At1g27710	129	114	1,527	420	2,190	11.79
420	*rQTL1a* ^{Bur}+At1g27730	108	133	1,678	500	2,419	10.52
420	*rQTL1a* ^{Bur}+At1g27730	128	107	1,694	466	2,395	10.35
420	*rQTL1a* ^{Bur}	164	162	1,613	466	2,405	14.62
420	*rQTL1a* ^{Bur}	149	136	1,482	434	2,201	13.92
420	*rQTL1a* ^{Bur}	121	125	1,470	451	2,167	12.08
420	*rQTL1a* ^{Bur}	134	121	1,529	430	2,214	12.27
420	*rQTL1a* ^{Bur}	132	129	1,460	401	2,122	13.17
420	*rQTL1a* ^{Bur}	144	150	1,496	430	2,220	14.26
420	*rQTL1a* ^{Bur}	144	149	1,616	433	2,342	13.41
420	*rQTL1a* ^{Bur}	135	154	1,520	418	2,227	13.95
420	*rQTL1a* ^{Bur}	141	131	1,529	427	2,228	13.06
420	*rQTL1a* ^{Bur}	122	132	1,504	422	2,180	12.42
420	Col-*420*	168	178	1,465	373	2,184	17.35
420	Col-*420*	207	200	1,383	359	2,149	21.18
420	Col-*420*	184	195	1,474	350	2,203	19.01
420	Col-*420*	199	182	1,414	378	2,173	19.42
420	Col-*420*	197	184	1,396	388	2,165	19.50
420	Col-*420*	189	198	1,534	388	2,309	18.47
420	Col-*420*	192	189	1,440	408	2,229	18.87
420	Col-*420*	202	192	1,322	313	2,029	21.79
420	Col-*420*	164	198	1,390	332	2,084	19.22

420	Col-*420*	162	199	1,347	345	2,053	19.48
420	Col-*420*	198	183	1,456	384	2,221	18.95

E) taf4b-2* ×Col-*420* F_2. *Related to Figure 2.

FTL	Genotype	Green alone	Red alone	Both	None	Total	cM
420	+/+	202	237	1,808	479	2,726	17.66
420	+/+	206	177	1,681	461	2,525	16.54
420	+/+	190	248	1,823	477	2,738	17.53
420	+/+	216	196	1,802	468	2,682	16.77
420	+/+	190	189	1,668	440	2,487	16.62
420	+/+	214	212	1,734	453	2,613	17.91
420	+/+	241	249	1,885	480	2,855	18.96
420	+/+	216	213	1,714	405	2,548	18.56
420	*taf4b-2*/+	223	229	1,801	433	2,686	18.55
420	*taf4b-2*/+	205	192	1,785	500	2,682	16.10
420	*taf4b-2*/+	244	177	1,797	453	2,671	17.25
420	*taf4b-2*/+	225	231	1,795	517	2,768	18.11
420	*taf4b-2*/+	227	240	1,965	506	2,938	17.41
420	*taf4b-2*/+	228	213	1,922	477	2,840	16.97
420	*taf4b-2*/+	239	237	1,896	477	2,849	18.40
420	*taf4b-2*/+	209	240	1,812	426	2,687	18.40
420	*taf4b-2*/+	215	184	1,714	445	2,558	17.05
420	*taf4b-2*	155	142	1,798	491	2,586	12.23
420	*taf4b-2*	154	133	1,813	503	2,603	11.71
420	*taf4b-2*	173	174	1,811	552	2,710	13.75
420	*taf4b-2*	190	175	1,857	519	2,741	14.35
420	*taf4b-2*	155	174	1,869	501	2,699	13.04
420	*taf4b-2*	189	162	1,865	491	2,707	13.94

F) taf4b-1* ×Col-FTL F_2. *Related to Figure 3.

FTL	Genotype	Green alone	Red alone	Both	None	Total	cM
1.18	+/+	146	172	1,317	396	2,031	17.12
1.18	+/+	159	125	1,350	352	1,986	15.50
1.18	+/+	163	189	1,552	423	2,327	16.49
1.18	*taf4b-1*/+	136	135	1,380	406	2,057	14.18
1.18	*taf4b-1*/+	143	147	1,274	321	1,885	16.79
1.18	*taf4b-1*/+	167	155	1,578	414	2,314	15.05
1.18	*taf4b-1*/+	144	159	1,489	375	2,167	15.13
1.18	*taf4b-1*/+	151	153	1,510	452	2,266	14.46
1.18	*taf4b-1*/+	131	152	1,398	396	2,077	14.71
1.18	*taf4b-1*/+	139	155	1,488	376	2,158	14.70
1.18	*taf4b-1*/+	132	145	1,445	373	2,095	14.24
1.18	*taf4b-1*/+	148	152	1,492	402	2,194	14.76
1.18	*taf4b-1*	109	125	1,350	380	1,964	12.72
1.18	*taf4b-1*	124	113	1,359	397	1,993	12.70
1.18	*taf4b-1*	85	109	1,330	362	1,886	10.88
1.13	+/+	226	208	1,466	330	2,230	21.85
1.13	+/+	224	262	1,445	314	2,245	24.70
1.13	+/+	193	163	1,308	318	1,982	19.95
1.13	+/+	239	214	1,407	344	2,204	23.26
1.13	+/+	219	204	1,434	360	2,217	21.36
1.13	+/+	218	236	1,477	326	2,257	22.69
1.13	+/+	216	218	1,383	346	2,163	22.62
1.13	*taf4b-1*/+	230	188	1,383	345	2,146	21.87
1.13	*taf4b-1*/+	259	229	1,541	345	2,374	23.26
1.13	*taf4b-1*/+	229	229	1,481	379	2,318	22.23
1.13	*taf4b-1*/+	223	211	1,491	314	2,239	21.75
1.13	*taf4b-1*/+	260	232	1,522	371	2,385	23.36
1.13	*taf4b-1*/+	215	220	1,426	347	2,208	22.16
1.13	*taf4b-1*	192	183	1,476	353	2,204	18.78
1.13	*taf4b-1*	205	201	1,412	379	2,197	20.60
1.13	*taf4b-1*	173	181	1,452	353	2,159	18.02
1.13	*taf4b-1*	215	192	1,509	398	2,314	19.49
1.13	*taf4b-1*	198	208	1,440	359	2,205	20.52
1.13	*taf4b-1*	196	163	1,470	363	2,192	18.00
1.13	*taf4b-1*	193	179	1,435	360	2,167	18.96
2.2	+/+	175	166	1,062	272	1,675	23.00
2.2	+/+	217	212	1,529	357	2,315	20.67
2.2	+/+	182	223	1,265	305	1,975	23.20
2.2	+/+	213	215	1,539	377	2,344	20.32
2.2	+/+	206	247	1,578	383	2,414	20.96
2.2	+/+	241	217	1,529	334	2,321	22.20
2.2	*taf4b-1*/+	187	195	1,271	298	1,951	22.00

2.2	*taf4b-1/+*	240	219	1,540	349	2,348	21.96
2.2	*taf4b-1/+*	244	209	1,517	346	2,316	21.97
2.2	*taf4b-1/+*	213	240	1,521	339	2,313	22.01
2.2	*taf4b-1/+*	138	132	989	240	1,499	20.02
2.2	*taf4b-1/+*	194	210	1,457	317	2,178	20.69
2.2	*taf4b-1/+*	217	221	1,552	390	2,380	20.51
2.2	*taf4b-1*	196	176	1,282	311	1,965	21.17
2.2	*taf4b-1*	162	167	1,205	334	1,868	19.52
2.2	*taf4b-1*	137	147	1,195	311	1,790	17.38
2.2	*taf4b-1*	176	137	1,331	356	2,000	17.11
2.2	*taf4b-1*	199	202	1,459	379	2,239	19.89
2.2	*taf4b-1*	184	207	1,495	371	2,257	19.16
2.2	*taf4b-1*	226	197	1,566	384	2,373	19.78
2.2	*taf4b-1*	211	192	1,517	360	2,280	19.60
2.2	*taf4b-1*	192	195	1,560	378	2,325	18.32
3.15	+/+	252	256	1,488	329	2,325	24.97
3.15	+/+	202	166	1,239	288	1,895	21.79
3.15	+/+	239	247	1,485	347	2,318	23.80
3.15	+/+	243	222	1,497	373	2,335	22.43
3.15	+/+	242	190	1,334	357	2,123	22.99
3.15	+/+	230	183	1,409	341	2,163	21.38
3.15	+/+	163	155	995	228	1,541	23.37
3.15	+/+	227	211	1,387	307	2,132	23.25
3.15	*taf4b-1/+*	223	222	1,560	363	2,368	21.00
3.15	*taf4b-1/+*	196	201	1,460	381	2,238	19.67
3.15	*taf4b-1/+*	237	241	1,561	383	2,422	22.20
3.15	*taf4b-1/+*	208	181	1,389	370	2,148	20.14
3.15	*taf4b-1*	159	173	1,580	391	2,303	15.64
3.15	*taf4b-1*	199	191	1,536	382	2,308	18.63
3.15	*taf4b-1*	187	180	1,265	312	1,944	21.11
3.15	*taf4b-1*	198	196	1,567	387	2,348	18.49
3.15	*taf4b-1*	195	182	1,562	402	2,341	17.66
5.1	+/+	186	233	1,501	390	2,310	20.17
5.1	+/+	206	207	1,517	358	2,288	20.06
5.1	+/+	201	167	1,397	354	2,119	19.21
5.1	+/+	223	245	1,477	366	2,311	22.87
5.1	+/+	89	77	626	165	957	19.19
5.1	+/+	192	193	1,458	364	2,207	19.31
5.1	+/+	202	204	1,421	347	2,174	20.85
5.1	*taf4b-1/+*	140	144	1,213	308	1,805	17.22
5.1	*taf4b-1/+*	196	192	1,549	367	2,304	18.56
5.1	*taf4b-1/+*	206	170	1,548	399	2,323	17.76
5.1	*taf4b-1/+*	193	213	1,420	336	2,162	20.98
5.1	*taf4b-1/+*	166	187	1,338	326	2,017	19.38
5.1	*taf4b-1/+*	210	185	1,441	372	2,208	19.86
5.1	*taf4b-1/+*	167	169	1,278	353	1,967	18.86
5.1	*taf4b-1/+*	180	168	1,408	402	2,158	17.69

5.1	*taf4b-1/+*	189	189	1,395	338	2,111	19.88
5.1	*taf4b-1*	132	145	1,587	449	2,313	12.79
5.1	*taf4b-1*	140	139	1,425	388	2,092	14.37
5.1	*taf4b-1*	158	129	1,547	407	2,241	13.75
5.1	*taf4b-1*	172	147	1,485	399	2,203	15.72
5.1	*taf4b-1*	147	148	1,513	391	2,199	14.46
5.1	*taf4b-1*	123	106	954	258	1,441	17.41
5.2	+/+	95	87	956	249	1,387	14.12
5.2	+/+	171	143	1,405	390	2,109	16.20
5.2	+/+	154	162	1,408	390	2,114	16.27
5.2	+/+	134	148	1,512	369	2,163	14.02
5.2	+/+	125	128	1,313	358	1,924	14.15
5.2	+/+	146	166	1,617	457	2,386	14.07
5.2	+/+	148	167	1,549	409	2,273	14.98
5.2	+/+	151	119	1,406	395	2,071	14.02
5.2	+/+	130	125	1,461	411	2,127	12.81
5.2	+/+	144	161	1,522	426	2,253	14.60
5.2	*taf4b-1/+*	135	147	1,462	409	2,153	14.09
5.2	*taf4b-1/+*	153	130	1,464	387	2,134	14.28
5.2	*taf4b-1/+*	161	156	1,472	427	2,216	15.51
5.2	*taf4b-1/+*	155	162	1,602	418	2,337	14.64
5.2	*taf4b-1/+*	127	94	1,121	298	1,640	14.53
5.2	*taf4b-1/+*	127	125	1,381	390	2,023	13.35
5.2	*taf4b-1/+*	142	167	1,535	450	2,294	14.52
5.2	*taf4b-1/+*	174	143	1,517	408	2,242	15.31
5.2	*taf4b-1/+*	153	145	1,670	443	2,411	13.24
5.2	*taf4b-1/+*	144	130	1,631	464	2,369	12.33
5.2	*taf4b-1/+*	160	142	1,577	409	2,288	14.21
5.2	*taf4b-1*	132	122	1,525	419	2,198	12.31
5.2	*taf4b-1*	103	102	1,398	411	2,014	10.76
5.2	*taf4b-1*	117	124	1,555	390	2,186	11.71
5.2	*taf4b-1*	119	99	1,206	357	1,781	13.10
5.2	*taf4b-1*	119	115	1,578	428	2,240	11.06
5.2	*taf4b-1*	124	133	1,472	354	2,083	13.21
5.1	+/+	114	117	775	184	1,190	21.78
5.1	+/+	192	220	1,474	366	2,252	20.37
5.1	+/+	190	197	1,508	369	2,264	18.87
5.1	+/+	171	157	1,294	376	1,998	18.04
5.1	+/+	213	172	1,389	349	2,123	20.17
5.1	+/+	206	158	1,478	390	2,232	17.91
5.1	+/+	205	193	1,376	342	2,116	21.02
5.1	*taf4b-1/+*	201	200	1,617	390	2,408	18.33
5.1	*taf4b-1/+*	213	195	1,509	369	2,286	19.81
5.1	*taf4b-1/+*	198	206	1,461	378	2,243	20.01
5.1	*taf4b-1/+*	99	99	781	219	1,198	18.18
5.1	*taf4b-1/+*	189	187	1,457	343	2,176	19.10
5.1	*taf4b-1/+*	201	225	1,582	384	2,392	19.76

5.1	*taf4b-1/+*	185	191	1,515	342	2,233	18.56
5.1	*taf4b-1/+*	209	198	1,479	366	2,252	20.09
5.1	*taf4b-1*	194	184	1,524	371	2,273	18.31
5.1	*taf4b-1*	189	181	1,537	374	2,281	17.81
5.1	*taf4b-1*	172	202	1,502	380	2,256	18.24
5.1	*taf4b-1*	193	153	1,516	423	2,285	16.50
5.1	*taf4b-1*	195	168	1,467	365	2,195	18.19
5.1	*taf4b-1*	208	161	1,434	340	2,143	19.03
5.1	*taf4b-1*	189	165	1,486	376	2,216	17.51
5.1	*taf4b-1*	182	164	1,405	343	2,094	18.18
5.18	+/+	116	118	1,586	427	2,247	11.02
5.18	+/+	106	107	1,566	472	2,251	9.96
5.18	+/+	91	105	1,535	423	2,154	9.56
5.18	+/+	105	127	1,556	453	2,241	10.95
5.18	+/+	109	92	1,595	483	2,279	9.25
5.18	*taf4b-1/+*	104	103	1,561	463	2,231	9.75
5.18	*taf4b-1/+*	86	116	1,557	428	2,187	9.71
5.18	*taf4b-1/+*	128	103	1,561	449	2,241	10.90
5.18	*taf4b-1/+*	98	108	1,448	443	2,097	10.36
5.18	*taf4b-1/+*	97	82	1,529	437	2,145	8.73
5.18	*taf4b-1/+*	107	115	1,492	413	2,127	11.05
5.18	*taf4b-1/+*	114	96	1,549	479	2,238	9.87
5.18	*taf4b-1/+*	93	109	1,497	429	2,128	9.99
5.18	*taf4b-1*	128	111	1,634	463	2,336	10.82
5.18	*taf4b-1*	91	90	1,579	468	2,228	8.48
5.18	*taf4b-1*	99	76	1,636	467	2,278	8.00
5.18	*taf4b-1*	83	82	1,562	525	2,252	7.62
5.18	*taf4b-1*	100	74	1,563	459	2,196	8.27
5.18	*taf4b-1*	93	86	1,534	463	2,176	8.60
5.18	*taf4b-1*	70	97	1,588	453	2,208	7.87

G) Col/Bur and *taf4b-1* /Bur F_1 hybrids. *Related to Figure 4.*

FTL	Genotype	Green alone	Red alone	Both	None	Total	cM
420	Col/Bur	124	122	1,334	368	1,948	13.55
420	Col/Bur	113	128	1,316	334	1,891	13.68
420	Col/Bur	124	121	1,313	343	1,901	13.85
420	Col/Bur	132	136	1,429	342	2,039	14.14
420	Col/Bur	128	149	1,401	363	2,041	14.64
420	Col/Bur	130	160	1,366	352	2,008	15.67
420	Col/Bur	119	173	1,348	306	1,946	16.34
420	Col/Bur	135	165	1,321	319	1,940	16.89
420	*taf4b-1* /Bur	81	85	1,453	404	2,023	8.57
420	*taf4b-1* /Bur	82	104	1,479	412	2,077	9.40
420	*taf4b-1* /Bur	88	95	1,392	376	1,951	9.87
420	*taf4b-1* /Bur	95	99	1,445	376	2,015	10.14
420	*taf4b-1* /Bur	100	101	1,507	377	2,085	10.16
420	*taf4b-1* /Bur	94	99	1,351	343	1,887	10.81
420	*taf4b-1* /Bur	86	124	1,462	371	2,043	10.87
420	*taf4b-1* /Bur	100	140	1,550	375	2,165	11.78

Table S6

Col/Bur SSLP genotyping oligonucleotides. ***Related to Figures 1 and 2.***

Name	Sequence (5′-3′)	Col size (bp)	Bur size (bp)	Chr
1-529-F	TTCCGGTTAAATGAAAATCCTC	300	155	1
1-529-R	ACTGACAGATGGAGAGACAAGAGTT			
1-1771-F	CAATCAAGCGAGGAGCAACA	453	340	1
1-1771-R	TTCCGAGTACGCATTGCTCA			
1-4797-F	CATGTGATAGATGTGATTCCATGTT	256	182	1
1-4797-R	TGGTCACCTTGTTACAATAATACAATC			
1-6315-F	TGTGTTTGAATGTGAAGATAACGA	474	330	1
1-6315-R	GCACGAGGTTAAATGCATGG			
1-7823-F	CAACATTTTCACTTTATTTCTCATCC	250	185	1
1-7823-R	GCAAATCTTTGTTCCATAAATTCAC			
1-7963-F	CCGATGAAGGTTCCGAATAA	535	311	1
1-7963-R	TCAGCGACGTTCGTGAAATA			
1-8097-F	CGCGTAATGGGTAAGGCTAT	239	191	1
1-8097-R	GCATGGCGTAAAACTCGCTAT			
1-8547-F	GGAACCTTCCATGCATGACT	270	185	1
1-8547-R	CCTGAATATAAACCCACAAAATGA			
1-8685-F	ACACACAGAGCATCGTGGAT	246	176	1
1-8685-R	CTGTTTTCATCCGTGGAGGT			
1-9019-F	TTAAATTTCTTCGTAATTCGTATGGTT	250	188	1
1-9019-R	TTTTTGATTATTTTTGTGGGTCAA			
1-9568-F	CTTCTGCAATCAGCATCAGC	293	203	1
1-9568-R	TCCATTTCAATATGCGCAAC			
1-9807-F	TGTCACTTCTCGGTGTTTGG	595	350	1
1-9807-R	GTGCTTTGGTCCACATTTGA			
1-10655-F	TTGTGGTCCCTGGCTAATCA	230	176	1
1-10655-R	CAGTGACGAATTCCAAAACGA			
1-11282-F	TCCTTGGATTCTGGTTGTTTG	340	224	1
1-11282-R	TCGTGCCACACATAAATAGGA			
1-11965-F	CTATAAGCCCAGTAGATTGCTTCC	472	323	1
1-11965-R	TTGTCAAGTATCGCGTCTGTG			
1-12444-F	GCTTTGGACCTCTTTTGGTG	239	191	1
1-12444-R	AGCGACCAAATGATTCAACC			
1-13178-F	ACGTTGTTCTCGTTGCACAG	282	210	1
1-13178-R	TGTGATGGACTTCCCCTTACTT			
1-14122-F	GCTAGCAGTCGAGTATTCTGTCGAG	239	190	1
1-14122-R	CGTGTCCCACCATCATCAC			
1-16161-F	AAAGTGGGTGGCAGGATAGTT	208	166	1
1-16161-R	AAGGCTATCACTATTTGTCCAAAAC			
1-18237-F	AAAAAGCCGAATTGGGTTGG	621	343	1
1-18237-R	CAATATACTGTGCCTTTCGTGTCT			
1-18570-F	CGTACAGTGTTTCGTGTTCCA	162	128	1

1-18570-R	TCTCCTTTTGGCTTCTGATGA	102	123	1
1-19556-F	ATTTCGTTTTTGTCAAACCACTT	206	144	1
1-19556-R	TTGCATAGGACAAGAAAAATGTG			
1-19918-F	TCACGTTCTGTTGTCCCGTA	402	275	1
1-19918-R	TCGAAATGCAGATTTCTCTTCC			
1-20158-F	CCAAGAGCTCGTTCATGGTAT	246	193	1
1-20158-R	GGCACAAGAAGCGTTTTCTC			
1-21236-F	CAATGAGCCCTCTACGCTCT	476	340	1
1-21236-R	AAGCCCATCATATCCCAACA			
1-25036-F	GAGTTGGACCCAACGAACAC	271	193	1
1-25036-R	CGCACATCCGCATATTAGTG			
1-30355-F	TGGTTAATCTAAAGCCCAATAAAAG	258	201	1
1-30355-R	TGCGATTGAATAGTGGAGGTAG			
2-132-F	TCCAATGGGCCACAAATTAAC	229	163	2
2-132-R	TTTGTGCTTTGATTACTGCAAGTG			
2-2346-F	GGCAAATTTGGTTGGCTCTC	347	261	2
2-2346-R	TGTTTTGTGCTATTTGTGTCAACC			
2-6789-F	GCGTTTTGTATCATCAAAGGTTCC	112	82	2
2-6789-R	CGCAATTTCTCGAACTTCCTTT			
2-14407-F	CCTATGTGTCAAGAGAGATTTCCA	271	198	2
2-14407-R	AGCGTTTCTCTACTTTTAATGATTGAT			
2-18444-F	CAAGAGGGAAACACAATTAATGC	303	210	2
2-18444-R	CCCATCTCCATACACTACAAACC			
3-1031-F	ATGCCTTGGTTTCAATTTGG	419	345	3
3-1031-R	TACCCGCTCCTTGACAGTTT			
3-4049-F	GCAAATAGGAATCAGAAGTTGGA	275	236	3
3-4049-R	TTTAAAAAGGCCTCCGCTTT			
3-8495-F	AACGAAAAAGGGGGAATATGAA	177	132	3
3-8495-R	GGGCTTTAAAAAGCAAAAGCA			
3-10695-F	GAGGGATGCAAGGAGGATCA	161	122	3
3-10695-R	TTCATCACATCAACGCTCCAA			
3-17088-F	GCTCTTGAGGTTTTAGGGTTGTT	560	360	3
3-17088-R	TGCGTTCGCATGATTCAAAA			
3-21008-F	CCGACGTTGTGTTTCTATTTCC	211	174	3
3-21008-R	TGAGGGAACAAGGACCTAACCA			
4-1782-F	TGGTTGATTTCACTTGATTTTGA	147	114	4
4-1782-R	CTTCCCATCACGACTTCTCTCT			
4-6445-F	GCCCGATATGTGATGTGAAA	209	166	4
4-6445-R	TTTGGCAGTTTTTGCTGTCA			
4-10599-F	TGGGTACATCTTAAAGGGTGGA	559	369	4
4-10599-R	ATCGAGCAACACTGACCACA			
4-15631-F	CGTGATGGAACACATCAACAT	476	326	4
4-15631-R	ACAACATCGAAGGTTGAGCA			
4-18510-F	TGACGGCAGATTCAGAGAGA	215	157	4
4-18510-R	AGGGAGGACGAAGAATGAGG			

5-6680-F	GCAGAACCCAGAAACAGCAC	283	206	5
5-6680-R	TTGCCCAAACCCAGATCTAA			
5-10048-F	TCTTCAGAACTAGTCTTGGTTTTGC	508	303	5
5-10048-R	GATATGACGGGTTTGGATCG			
5-19994-F	TCTAAACCGAACTAAACCGTGAA	169	109	5
5-19994-R	CAAACCAAAACCTACTTTTTCCAA			
5-23287-F	GAGATGTTGAGAAGCAGAGGAAA	204	151	5
5-23287-R	TGGCGTGAAATACTGAAGCAA			
5-26907-F	TGTGGATCTTTATGACGTGTGC	270	200	5
5-26907-R	ACCATCTACTTCCATTCAAATAACG			

CAPS and dCAPS genotyping oligonucleotides. ***Related to Figure 2.***

Name	Sequence (5′-3′)	Col size (bp)	Bur size (bp)	Chr
c1-8036-F	CTCCAAAGTAGGGCAAAACG	118, 55	173	1
c1-8036-R	CCCTAGAACCGCTAACACCA			
c1-8622-F	ACTCCTCATCCGTTCCACAC	113, 88	201	1
c1-8622-R	TCGATTTGCGGGATTAATGT			
c1-9197-F	TGCTTCTGCTGCTACCTTGA	117, 81	198	1
c1-9197-R	GAAGATTCCGGCTTCCTTTC			
c1-9608-F	TTCTGGTGTGGGAAACAGAAC	212, 38	250	1
c1-9608-R	TCATGACTGGAGGAGAGTATGC			
c1-9630-F	AAATTCATTTCCCCCAAATAAAA	108, 89	197	1
c1-9630-R	GAGAAGATTCAGCTCCGAGAAA			
c1-9645-F	GCAACTCGTAAACATACCCTGA	248	201, 47	1
c1-9645-R	TGGCTGGTTTGTGAAAGATG			
c1-9660-F	GACCCCACTGCTTTTGACAT	190, 41	231	1
c1-9660-R	AAATTTAATGCGCCAAGGAA			
c1-10013-F	CATGTGACTTGGGTGGTGTC	192	133, 59	1
c1-10013-R	TGTGGGAGGGATGGAAGATA			
c1-10401-F	TGTTGGCGCATAAAAGTGAA	125, 91	216	1
c1-10401-R	GTTGTGTTGGCCTTCTCGAT			
d1-9634-F	AAACCTCTCTTTAGGAGCAGTGTATGTAGC	100, 30	130	1
d1-9634-R	AACGATCACGTTTAAAGTTGCTAAAACTG			
d1-9653-F	AAATTAACGATCTCATATTGTAGGGATA	107, 31	138	1
d1-9653-R	GATATTATAATAAATCCGATGTATGAGAAAG			
d-*taf4b-1* -F	CGATCGTTCTTTTTAGGACCAGAATCTGAT	138	109, 29	1
d-*taf4b-1* -R	CTCAGGGTATGTTTACGAGTTGCTACAC			

Additional oligonucleotides. ***Related to Figures 2 and 5.***

Name	Sequence (5′-3′)	Experiment
AT1G27695_*Bam* HI_F	AAAAAAGGATCCCTGAAGACTCCGGAAGCAGT	
AT1G27695_*Sma* I_R	TTTTTTCCCGGGTGATTGCAGTGGTAGTTGCAG	

AT1G27700_*Eco*RV_F	AAAAAAGATATCTCAAATGCTTCTTCTTTCCTAGC	Cloning of *rQTL1a* candidate genes
AT1G27700_*Apa*I_R	TTTTTTGGGCCCTGCAAATGTTGCTGTTCGT	
AT1G27710_*Xba*I_F	AAAAAATCTAGATGCTTTAGCAGATTCAGATGGA	
AT1G27710_*Eco*RV_R	TTTTTTGATATCTTCTGTTGCTGGTTATTCTTGTG	
AT1G27720_*Xba*I_F	AAAAAATCTAGATGCTTTAGCAGATTCAGATGGA	
AT1G27720_*Apa*I_R	TTTTTTGGGCCCGCACTGGACAAAGGGTAAGC	
AT1G27730_*Sma*I_F	AAAAAACCCGGGTTCGGTAACTGGGCTTGTTC	
AT1G27730_*Apa*I_R	TTTTTTGGGCCCTGAAGAGTGGACCCAAACATT	
SALK_025468_LP	CTCTGCAGTGGAATTTTCTGC	Genotyping *taf4b-2*
SALK_025468_RP	CCCAAAGAACTCATCCTTTCC	
SALK_BP	ATTTTGCCGATTTCGGAAC	
TAF4B_F1	TCTGATTCGAGATATTGAAGGAAGT	
TAF4B_R1	ACAGTCTTTTCCACCCAAGGA	
TAF4B_F2	TGGTGGTACACAATTTGGGAAG	
TAF4B_R2	CATCTGAGGCTCCTTTTCCA	RT-PCR
TAF4_F	TCTGGTACTGGTGGTCGAAG	
TAF4_R	CTCTCTTTCGAGGACCGCAA	
GAPC_RTF	CGAGAAAGCTGCTACCTACGAT	
GAPC_RTR	GTTGTCGTACCATGACACCAAT	

Coordinates (bp)
528,997
1,771,064
4,796,903
6,315,210
7,822,623
7,963,346
8,097,721
8,546,722
8,686,154
9,018,718
9,567,731
9,806,927
10,655,860
11,282,116
11,964,554
12,444,277
13,177,859
14,122,817
16,161,636
18,237,140
18,569,811

18,569,611

19,555,786

19,917,692

20,158,440

21,236,506

25,035,796

30,354,927

132,652

2,346,993

6,789,815

14,406,955

18,443,819

1,031,549

4,049,059

8,495,131

10,695,968

17,088,210

21,008,127

1,782,446

6,445,150

10,599,330

15,631,355

18,510,483

6,680,077

10,048,066

19,994,907

23,287,613

26,907,352

Coordinates (bp)	Enzyme
8,036,376	*Eco* RI
8,622,092	*Sac* I
9,196,642	*Xho* I
9,607,633	*Psi* I
9,629,971	*Mfe* I
9,644,742	*Eco* RV
9,659,666	*Xho* I
10,012,987	*Xho* I
10,401,022	*Eco* RV
9,634,487	*Alu* I
9,652,842	*Hin* dIII
9,644,611	*Mbo* I